ON THE PHOSPHORUS DIFFUSION IN SILICON IN OXIDISING AND CHLORO - OXIDISING AMBIENT

A Thesis Submitted
In Partial Fulfilment of the Requirements
for the Degree of
DOCTOR OF PHILOSOPHY

by

A. K. GUPTA

to the

DEPARTMENT OF ELECTRICAL ENGINEERING

INDIAN INSTITUTE OF TECHNOLOGY, KANPUR

OCTOBER 1984

CERTIFICATE

Certified that this work entitled 'On the Phosphorus Diffusion in Silicon in Oxidising and Chloro-oxidising Ambients' by Sri A.K. Gupta has been carried out under my supervision and has not been submitted elsewhere for a degree.

October, 1984

M. S. Tyagi

Dr. M.S. Tyagi
Professor
Department of Electrical Engineering
Indian Institute of Technology
Kanpur.

ACKNOWLEDGEMENTS

CONTENTS

LIST OF TABLES

LIST OF FIGURES

LIST OF SYMBOLS

$C_1(x,t)$ Depth distribution of phosphorus conc. in PSG at time 't' (cm^{-3})

$C_2(z,t)$ Depth distribution of phosphorus conc. in silicon at time 't' (cm^{-3})

C_o Phophorus conc. at PSG surface (cm^{-3})

D_1 Diffusion coefficient of phosphorus in PSG $(cm^2 \ sec^{-1}$

D_2 Diffusion coefficient of phosphorus in silicon $(cm^2 \ sec^{-1})$

B Parabolic growth constant for thermal PSG/SiO_2, $(cm^2 \ sec^{-1})$

X_o PSG thickness, $X_o(t) = \sqrt{Bt}$ (cm.)

r Silicon to SiO_2 volume ratio

K Rate limitation constant of phosphorus at PSG-Si interface $(cm.sec^{-1})$

α $\alpha = K/D_2$

$h_n(x)$ $h_n(x) = (i)^{3n} \cdot H_n(ix)$ where $i = \sqrt{-1}$ and $H_n(ix)$ is nth Hermite polynomial of argument ix.

$i^n.erfc(x)$ An integral of complementary error function, defined

$$i^n \ erfc(x) = \int_x^\infty i^{n-1} \ erfc(u) \ du$$

a_n, A_n Constant coefficients

δ $\delta = \sqrt{B}/2\sqrt{D_2}$

C_B Background impurity conc. (cm^{-3})

β $\beta = 1/erfc(r\sqrt{B}/2\sqrt{D_2})$

σ_s Sheet conductivity (ohm^{-1}) of diffused layer

$\sigma(x)$ Conductivity variation with depth $(ohm^{-1} \ cm^{-1})$

ρ_s — Sheet resistivity of diffused layer (ohm)

$\mu[n(x)]$ — Mobility of electrons as a function of electron conc. $(cm^2 \ V^{-1} \ sec^{-1})$

$n(x)$ — Electron concentration $(cm^{-3}.)$

D_i — Diffusion coefficient of phosphorus in silicon in inert ambient $(cm^2.sec^{-1})$

D_{ox} — Diffusion coefficient of phosphorus in silicon in oxidising ambient

D_{2I} — Diffusion coefficient of phosphorus for interstitialcy mechanism

D_{2V} — Diffusion coefficient of phosphorus for vacancy mechanism

C_I — Self-interstitial conc. (cm^{-3}) in silicon

C_I^{eq} — Thermal equilibrium self-interstitial conc. in silicon (cm^{-3})

C_V — Vacancy concentration in silicon (cm^{-3})

C_V^{eq} — Thermal equilibrium vacancy conc. in silicon (cm^{-3})

k_I — Annihilation velocity of self-interstitials at silicon surface $(cm.sec^{-1})$

G — Diffusivity enhancement factor

C_{Cl} — Concentration of chlorine at PSG-Si interface (cm^{-3})

$D_{ox,Cl}$ — Diffusion coefficient of phosphorus in chloro-oxidising ambient

m — Segregation coefficient of phosphorus in PSG-Si system

m_I — Segregation coefficient of self-interstitials in PSG-Si system

SYNOPSIS

ON THE PHOSPHORUS DIFFUSION IN SILICON IN OXIDISING AND CHLORO-OXIDISING AMBIENTS

by
A.K. GUPTA
DEPARTMENT OF ELECTRICAL ENGINEERING
INDIAN INSTITUTE OF TECHNOLOGY, KANPUR
October, 1984

The performance of a silicon device/I.C. is dominantly influenced by the impurity distribution in the active regions of the device. These impurities are introduced into silicon by diffusion/ion implantation. In the device/I.C. fabrication process sequence, this impurity deposition is invariably followed by other high temperature processes such as drive-in, oxidation etc. The deposited impurities redistribute themselve during these processes and the final impurity distribution is rather a complicated function of the initial distribution and the parameters such as ambient, temperature etc., of the later processes. To accurately relate the process parameters with the device performance, therefore, a precise knowledge of the effect of process parameters on the impurity diffusion is essential. The recent years have seen considerable activity in this area, primarily motivated by two factors. (i) As the I.C. complexity increases, the computer aided design methods are to be used, in order to reduce the time required for the development of a new product. This in turn needs

accurate mathematical models for process variable-impurity profile relationship, besides the models for devices/circuits. (ii) It is recognised that the process-profile relationship is still not adequately known and remains a major limiting factor in our capability to accurately relate the process variables with device/circuit performance.

The objective of this work is to study the effect of oxygen and chlorine (in diffusion ambient) on the diffusion of phosphorus in silicon. It is now well established that the thermal oxidation of silicon causes an injection of excess self-interstitials into the bulk silicon, which cause an enhancement in impurity diffusion coefficient. The study of this oxidation enhanced diffusion (OED) has been reported by several workers [1-3], who estimated OED by evaluating the redistribution of impurities, deposited by ion implantion/CVD, during oxidation. The extraction of the diffusion coefficient in these experiments is tedius and the finer details of the experimental profile vis-a-vis its theoretical counterpart are likely to be overlooke due to the approximations made for initial distribution. The effect of chlorine on phosphorus diffusion has been reported in detail only by Nabeta et al. [4]. Their experimental results, however, cover only a narrow range of temperature and have been questioned due to the high surface concentrations ($> 10^{20}$ cm^{-3}) involved in the experiment [5]. In the present work, the effect of ambient has been studied by carrying out constant source

diffusion using PH_3 in different ambients, under intrinsic diffusion conditions. This experimental situation is amenable to simple mathematical analysis. In addition, the large segregation coefficient of phosphorus in SiO_2-Si system, allows the diffusions to be carried out in strongly oxidising ambient, thus permitting the observation of OED of nearly the same magnitude as observed during oxidation in dry O_2.

A mathematical model for impurity diffusion in oxidising ambient from a constant source is presented. The diffusion equations in dopant silicate glass (DSG) and silicon are solved for impurity distribution in the two mediums. A reaction rate limited flux boundary condition, instead of that of thermodynamic equilibrium, has been assumed at the interface. The general solution for impurity distribution in silicon is found to be a series, which converges reasonably fast only for small diffusion lengths. For extreme cases such as negligible DSG growth or large values of reaction rate constant/diffusion time, the model yields solutions, identical to those reported by Smits [6] and Grove [7].

Phosphorus was diffused in <111> and <100> silicon, using PH_3 source (1000 ppm PH_3 in Ar) at various temperatures in the range $950^{\circ}C$-$1250^{\circ}C$, in three different ambients; (i) 95.5 V% N_2 1.5 V% O_2 + 3.0 V% (PH_3+Ar), (ii) 90.1 V% O_2 + 9.9 V% (PH_3+Ar) and (iii) 94.5 V% O_2 + 0.5 V% (PH_3+Ar) + 5.0 V% N_2 bubbled

through TCE at room temperature. The impurity distribution in each sample was determined from sheet resistivity measurements made after successive removal of silicon by anodic oxidation. The diffusion parameters were then calculated by comparing the experimental profile with the appropriate theoretical profile derived in the model.

In agreement with the theoretical predictions for diffusion in oxidising ambient, the surface impurity concentration is observed to be a strong function of the ratios of the PSG thickness to impurity diffusion lengths in PSG and silicon respectively. For identical diffusion ambients, the oxidation rate is seen to cause the surface impurity concentration to vary by two orders of magnitude. On the basis of the model predictions and the experimental results, it is concluded that the desirable process features for low concentration phosphorus diffusion are high temperature and strongly oxidising ambient.

In strongly oxidising ambient, the observed OED is in good agreement with the data reported by Antoniadis et al. [3], for OED during dry O_2 oxidation. In the present work the surface impurity concentration was of the order of 10^{18} cm^{-3}. At these concentrations, the OED was observed to be independent of crystal orientation and diffusion time. Various models proposed for the kinetics of excess-self interstitials generated during oxidation, are examined in the light of the observations of this work coupled with the observations on other oxidation related

phenomena, such as growth of oxidation induced stacking faults (OSF), reported in literature. It is shown that only the model proposed by Hu [8], satisfactorily explains all the experimental observations reported so far on OED and OSF growth in silicon. It is suggested that the surface regrowth process in Hu's model depends upon the impurity type (through its segregation property in SiO_2-Si system) and concentration at the interface.

The presence of chlorine in diffusion ambient is observed to cause a reduction in diffusion coefficient at all the temperatures. This effect is significantly larger on <111> than on <100> silicon and decreases with temperature, becoming negligible at 950°C. The reduction in diffusion coefficient is consistent with the observation of retarded growth of OSF in Cl_2-O_2 ambient [9], reported in literature and is a pointer to the fact that the presence of chlorine in the oxidation/diffusion ambient reduces the net generation of excess self interstitials at the interface. The experimental data of this work have been correlated with the reported segregation properties of chlorine in SiO_2-Si system, during chlorine-oxidation [10-11] and it is confirmed that the chlorine containing interface acts as a sink for self-interstitials. Hu's model is extended to take into account the effect of chlorine on diffusion coefficient.

The last but important observation is the reduction o.
diffusion coefficient in chloro-oxidising ambient below its
value in inert ambient (by about 35% at $1250^{\circ}C$) in <111>
silicon at high temperatures (>$1150^{\circ}C$). It is argued to be
a direct evidence to the fact that in inert ambient,phosphorus
diffusion proceeds via partial/pure interstitialcy mechanism,
thus ruling out the possibility of a pure vacancy mechanism.

References

[1] K. Taniguchi et al., J. Electrochem. Soc., 127, p 2243 (1980).

[2] A.M. Lin et al., J. Electrochem. Soc., 128, p. 1131 (1981).

[3] D.A. Antoniadis et al., App. Phys. Lett., 33, p. 1030 (1978).

[4] Y. Nabeta et al., J. Electrochem. Soc., p 1416 (1976).

[5] R.B. Fair, J. Electrochem. Soc., 128, p 1360 (1981).

[6] F.M. Smits, R.C. Miller, Phy. Rev., 104, p. 1242 (1956).

[7] A.S. Grore et al., J. App. Phys., 35, p. 2695 (1964).

[8] S.M. Hu, App. Phys. Lett., 43, p. 449 (1983).

[9] C.L. Claeys et al., in 'Semiconductor Characterization Techniques', ed. B.A. Barnes, G.A. Rozgonyi, The Electrochem. Soc., p. 366 (1977).

[10] B.E. Deal et al., J. Electrochem. Soc., 125, p. 2024 (1978).

[11] J.W. Rouse et al., J. Electrochem. Soc., 131, p. 887 (1984).

CHAPTER 1

INTRODUCTION

1.1 IMPURITY DIFFUSION AND DIFFUSED PROFILES IN SILICON TECHNOLOGY

The terminal parameters of a silicon device/I.C. are dominantly influenced by the impurity distribution in the active region of the device. These impurities are introduced into silicon by thermal diffusion/ion implantation, the latter becoming increasingly popular because of the higher control it permits in the impurity deposition process.

The deposition is only one of the several high temperature processes used in the fabrication of integrated circuits, others being drive-in, oxidation and dielectric deposition etc. In the fabrication process sequence, the deposition is often followed by one or more high temperature processes. The deposited impurities redistribute themselves via thermal diffusion during these subsequent process steps, the extent of redistribution being a function of the process ambients and the temperatures. The situation is further complicated by the facts that (i) bipolar device processing, in certain conditions, involves the simultaneous diffusion of donor and acceptor impurities, which significantly interact with each other during diffusion (ii) the diffusion is a strong function of impurity concentration, especially at high concentration values, and (iii) the

impurity diffusion is influenced by the lattice strain that
may be caused by the deposited or grown surface films or
due to the misfit of impurity atoms in the silicon lattice
[1,2]. The impurity distribution ultimately obtained in the
device is the net result of all the process variables mentioned
i.e., temperature, impurity concentration, lattice strain,
ambient etc.

A wealth of experimental information is available in
literature on various aspects of dopant impurity diffusion in
silicon [1]. The basic question of the diffusion mechanism
of dopant impurities in silicon, however, is still not answered
uniquely. This has been and continues to be, a major limita-
tion in developing the mathematical models for diffusion in
silicon, which may be used to predict impurity profiles for a
given set of process variables.

The last seven years have witnessed a renewed interest in
understanding and mathematically modelling the dopant impurity
diffusion in silicon [1-7]. Efforts made in this direction are
specifically aimed at developing comprehensive mathematical
models, consistent with the experimental results, to accurately
relate the process variables with the resultant impurity pro-
file. The reasons for this renewed interest in the area are :
(i) The trial and error method, hitherto used successfully, to
obtain the desired impurity distribution, becomes costlier and
more time consuming as the IC complexity increases, (ii) To

shorten the time required for the development of a new product, the computer aided design methods are to be used. This, in turn, necessitates the availability of accurate mathematical models, (iii) It is now well recognised that the reason for our limited capability of accurately relating the process variables with the device/circuit performance lies in inadequate process-profile models rather than device/circuit models [1].

The objective of this work is to study the effect of process ambient, i.e., presence of oxygen and chlorine, on the diffusion of phosphorus in silicon. Various phenomenological models proposed to formulate the effects of oxidation have also been examined. As will be seen in Chapter IV, the effect of chlorine on phosphorus diffusion also yields direct evidence about the diffusion mechanism of phosphorus in silicon as suggested by Gosele and Frank [5]. The following section gives a brief review of the earlier work done in the area.

1.2 PHOSPHORUS DIFFUSION IN OXYGEN AND OXY-CHLORO AMBIENTS

1.2.1 Oxidising Ambient

The effect of the presence of O_2 in diffusion ambient was first reported by Nicholas [9] who observed larger junction depths in p-silicon samples diffused in partially oxidising ambient as compared to the same in samples diffused in an inert ambient. In his experiments, the surface impurity concentratio

was high ($> 10^{20}$ cm^{-3}) and high concentration effects, naturally, were also present. Later, Ghoshtagore [10] carried out on elaborate set of experiments, diffusing phosphorus under intrinsic diffusion conditions and confirmed that the present of O_2 in diffusion ambient enhances the phosphorus diffusion coefficient in silicon.

A systematic and quantitative evaluation of oxidation enhanced diffusion (OED) of phosphorus was reported by Masetti et al. [11-12]. His main observations were : (i) The phosphorus OED in silicon is proportional to oxidation rate at a particular temperature. (ii) The proportionality constant is less for the case of (O_2 + steam) oxidation than for oxidation in dry O_2. (iii) The OED is temperature dependent and increases with decreasing temperature. The surface concentration in his experiments, however, were of the order of 5×10^{19} cm^{-3} and the high concentration effects may be expected to have contributed to the estimated diffusion coefficient values. Subsequently, Taniguchi et al. [13] carried out more detailed study of OED of phosphorus (as also of boron) in <100> silicon. He reported that (i) at a particular temperature OED depends only on the oxidation rate and is independent of oxidising agent as reported by Masetti et al., (ii) the OED is affected by impurity concentration for values greater than approximately the intrinsic carrier concentration. (iii) The OED has a finite range in silicon, estimated to be about

25 μm from the oxidising surface. This was an important observation as it indicated that the defect species i.e. self-interstitials responsible for OED were able to penetrate only upto a certain depth. In both these experiments, the OED was studied by observing the redistribution of phosphorus, deposited by CVD, during oxidation. For estimation of diffusion coefficient, the initial distribution was approximated with an ideal distribution, i.e., erfc or Gaussian distribution. Antoniadis et al. [14] and Lin et al. [15] reported more accurate estimates of OED of phosphorus. They studied, redistribution of low dose ion implanted phosphorus. For estimating the diffusion coefficients, the diffusion equation in silicon was numerically solved using the measured (rather than approximated) initial impurity distribution. The studies on orientation dependence of phosphorus OED have not been reported in literature, although quite a few reports on the orientation dependence of boron OED are available [6]. Oxidation retarded diffusion (ORD) has also been reported by Francis Dobson [17]. This effect has been observed at high temperatures ($> 1150^{\circ}$C) and long oxidation/diffusion times. It may be pointed out that for short durations ($\leq$ 1 hrs) OED is observed even at these temperatures.

As indicated in Sec. 1.1 the modelling of OED would require the knowledge of phosphorus diffusion mechanism in silicon. Although the point defects responsible for diffusion

in inert ambient are still not uniquely identified, the same responsible for the OED have been determined to be self-interstitials which are generated during oxidation at the SiO_2-Si interface and diffuse into the bulk silicon subsequently [5,6]. This information is derived from the fact that under the same conditions in which the OED is observed, the oxidation induced stacking faults (OSF's) have been found to grow [6]. These OSF's have been determined to be extrinsic type which could only grow by absorption of self-interstitials. In an inert ambient these OSF's have been observed to shrink. This indicates the presence of self-interstitials in super-saturation during oxidation. Various models have been proposed for the kinetics of these excess self-interstitials to quanti-tatively explain the OED as well as OSF growth data [19-21]. These will be discussed in detail in Chapter IV in context with a multitude of important experimental observations on OED and OSF growth. However, it may be pointed out here, that kinetics of generation, motion and annihilation of excess self-inter-stitials is still not precisely known and consequently the modelling of OED and OSF growth is in a transition stage.

1.2.2 Chloro-Oxidising Ambient

The effect of chlorine on phosphorus (and also of boron) diffusion in oxidising ambient has been reported in detail only by Nabeta et al. [22]. The chlorine was observed to cause a reduction in OED. This observation is consistent with the

observed retardation in OSF growth in chloro-oxidising ambient
[6]. The reduction in OED was observed to be constant for
HCl concentration greater than about 4% and completely countera-
cted the OED at temperatures 1100°C-1150°C. These data, how-
ever, covered only a narrow temperature range, 1000°C-1150°C
and involved high impurity concentrations, i.e., $\geq 10^{20}$cm^{-3}.
Their observations included an anamalous feature, that is, the
larger diffusion coefficient of phosphorus in <111> than in
<100> Si in oxidising ambient at 1000°C. This has been attri-
buted to the extrinsic diffusion conditions of the experiment
[18]. Further experiments to evaluate the effect of chlorine
on phosphorus diffusion, free from other effects, are obviously
called for.

1.3 THIS WORK

As mentioned in Sec. 1.2, the experimental results on OED
reported in literature, have been obtained by studying the
redistribution of phosphorus during oxidation. The extraction
of diffusion coefficient from the redistributed profiles is
rather an involved process because this experimental situation
is not amenable to analytical mathematical methods. Further-
more, the approximations made for the initial distribution or
errors in the experimentally determined initial distribution are
likely to introduce errors in the estimation of diffusion
coefficient.

An alternative method to study the effect of ambient on phosphorus diffusion is to carry out diffusion from a gaseous source, in oxidising/chloro-oxidising ambient. Mathematical analysis of this situation is very simple. Since phosphorus tends to segregate in silicon, it is possible to carry out constant source diffusion in very highly oxidising ambient ($95\%\ O_2$), thus permitting the observation of the OED of the same magnitude as may be observed under dry O_2 oxidation conditions. The simplicity of the theoretical treatment of this experimental situation permits an easy determination of diffusion parameters.

This work utilizes the above described technique to study the phosphorus diffusion in oxidising and chloro-oxidising ambient, The plan of the work is as follows :

In Chapter II, a phenomenalogical model for the diffusion in oxidising ambient is presented. The associated moving boundary problem has been solved for impurity distribution in silicon. At the PSG/Si interface the impurity concentrations in PSG and Si are assumed to approach thermodynamic equilibrium gradually rather than instantaneously.

The details of the experimental work are presented in Chapter III. A description of the experimental set up, plan of diffusion and measurements carried out on the diffused samples, is given. The procedures adopted for the determination of impurity distribution in silicon and extraction of diffusion parameters are described.

The experimental results are discussed in Chapter IV. The special features of the diffusion in oxidising ambient are pointed out. Various models proposed for OED and OSF growth have been examined in the light of the observations made in this work. The observed effects of chlorine on phosphorus diffusion are discussed and it is pointed out that the lowering of diffusion coefficient in chloro-oxidising ambient below its value in inert ambient negates a pure vacancy diffusion mechanism of phosphorus in silicon.

Lastly, Chapter V presents a brief summary of the work presented in the foregoing chapters.

CHAPTER II

DIFFUSION IN OXIDISING AMBIENT -
THEORETICAL MODEL

Mathematical formulation of the process of impurity
diffusion from a constant source, in oxidising ambient, is
exactly similar to the problem of impurity redistribution
in a homogeneously doped sample during thermal oxidation.
The solution to the latter has been proposed by Grove et al.
[1]. In their model, however, the impurity concentrations in
SiO_2 and Si at the interface, have been assumed to be in che-
mical equilibrium, right from t = o . This assumption, natura-
lly, leads to the prediction of a time-invariant impurity con-
centration at silicon surface. In case of boron redistribution
during steam oxidation, the surface concentration is reported
to be time invariant, in agreement with the prediction of
Grove's model [2]. For the case of phosphorus [3] and boron
[4] diffusion in weak oxidising ambient, however, the surface
concentration has been reported to be time-variant, approaching
a constant value for long diffusion times. This indicates that
under slow oxidation conditions, the impurity concentration at
silicon surface approaches its equilibrium value gradually
rather than instantaneously. No experimental results appear to
have been reported in between these two extreme cases. It is
however evident that in general the impurities in SiO_2 and Si

at the interface approach thermodynamic equilibrium gradually, the rate of approach to the equilibrium being a strong function of oxidation rate.

In the Section 2.1, the mathematical formulation of impurity diffusion in oxidising ambient is presented. A rate limited flux boundary condition has been assumed at the interface, to model the gradual approach to equilibrium, as first proposed by Smits and Miller [5]. In Sec. 2.2, the solution to problem posed in Sec. 2.1 is discussed.

2.1 MATHEMATICAL FORMULATION

The process of impurity diffusion during thermal oxidation is illustrated in Fig. 2.1. Using a two coordinate system, shown in the figure, the diffusion eqs. in dopant-silicate glass (henceforward referred to as SiO_2 in this chapter) and Si can be written as,

$$\frac{\partial C_1(x,t)}{\partial t} = D_1 \frac{\partial^2 C_1(x_1,t)}{\partial x^2} \; ; \quad \begin{array}{l} x \leq X_o(t) \\ t > o \end{array} \qquad (2.1)$$

and

$$\frac{\partial C_2(y,t)}{\partial t} = D_2 \frac{\partial^2 C_2(y,t)}{\partial y^2} \; ; \quad \begin{array}{l} r.X_o(t) \leq y \leq \infty \\ t \geq o \end{array} \qquad (2.2)$$

Here oxide growth has been assumed to be parabolic so that $X_o(t) = \sqrt{Bt}$. The boundary and initial conditions for the above equations for the case of diffusion from a constant dopant source are given below.
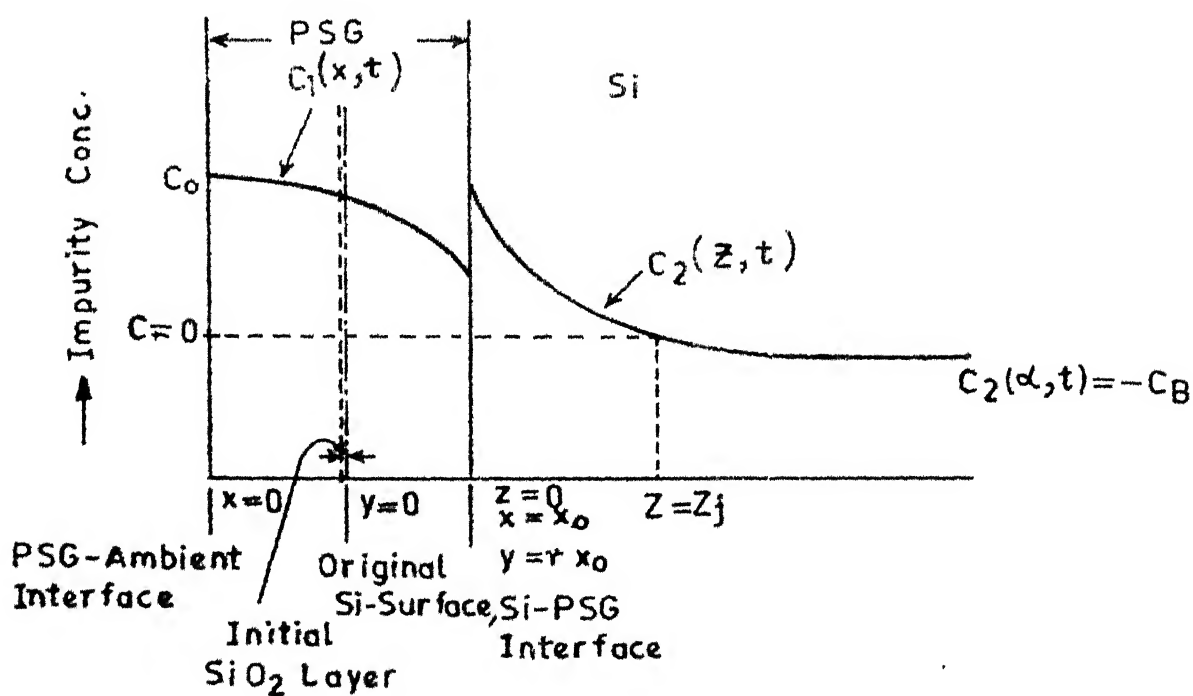
FIG. 2.1 Phosphorus Diffusion in Silicon in Oxidising Ambient.

(i)   At SiO$_2$ surface, $C_1(o,t) = C_o = $ const.   (2.3)

(ii)   Rate limitation at Si–SiO$_2$ interface :

Rate limitation at the interface is expressed as,

$$[-D_2 \frac{\partial C_2}{\partial y}]_{y=r.X_o(t)} = K[m.C_1|_{x=X_o(t)} - C_2|_{y=r.X_o(t)}]$$
(2.4)

or

$$[\frac{\partial C_2}{\partial y} - \alpha C_2]_{y=r.X_o(t)} = f(t)$$
(2.4a)

where,

$$\alpha = K/D_2$$

and $$f(t) = -m.\alpha.C_1|_{x=X_o(t)}$$

(iii) The condition of impurity conservation in Si–SiO$_2$ is given by [1],

$$[D_1 \frac{\partial C_1}{\partial x} + \frac{dX_o}{dt} C_1]_{x=X_o(t)} = [D_2 \frac{\partial C_2}{\partial y} + r.\frac{dX_o}{dt}.C_2]_{y=r.X_o(t)}$$
(2.5)

(iv) In silicon,

$$C_2(\infty,t) = -C_B$$
(2.6)

$$C_2(y,o) = -C_B$$
(2.7)

2.2   IMPURITY DISTRIBUTION IN SILICON

A general solution to eqn. (2.1), for parabolic oxide growth, may be written as [6],

$$C_1(x,t) = \sum_{n=o}^{\infty} (D_1 t)^{n/2} \left[a_n h_n \left(\frac{x}{2\sqrt{D_1 t}} \right) + A_n i^n \text{erfc} \left(\frac{x}{2\sqrt{D_1 t}} \right) \right]$$

(2.8)

The coefficients A_n may be eliminated by using eqn. (2.3). The resulting expression for $C_1(x,t)$ is, [Appendix I],

$$C_1(x,t) = a_0 + (C_0 - a_0) \text{erfc} \left(\frac{x}{2\sqrt{D_1 t}} \right) + \sum_{n=1}^{\infty} (D_1 t)^{n/2} a_n h_n \left(\frac{x}{2\sqrt{D_1 t}} \right)$$

$$- \sum_{n=2}^{2,\infty} (D_1 t)^{n/2} [n! \cdot 2^n] a_n i^n \text{erfc} \left(\frac{x}{2\sqrt{D_1 t}} \right)$$

(2.9)

From eqn. (2.9), $f(t)$ of eqn. (2.4) and L.H.S. of eqn. (2.5) may be written as,

$$f(t) = -m\alpha C_1(x_0, t)$$

$$= -m\alpha \left[a_0 + (C_0 - a_0) \text{erfc}(\delta) + \sum_{n=1}^{\infty} (D_1 t)^{n/2} a_n h_n(\delta) \right.$$

$$\left. - \sum_{n=2}^{2,\infty} (D_1 t)^{n/2} (2^n \cdot n!) a_n \cdot i^n \text{erfc}(\delta) \right] \qquad (2.10)$$

where $\delta = \sqrt{B}/(2\sqrt{D_1})$ (2.11)

and,

$$\left[D_1 \frac{\partial C_1}{\partial x} + \frac{dX_0}{dt} C_1 \right]_{x=X_0(t)} = \frac{\sqrt{D_1}}{2\sqrt{t}} \left[2\delta a_0 + (C_0 - a_0) \{ 2\delta \text{ erfc}(\delta) - \frac{2e^{-\delta^2}}{\sqrt{\pi}} \right.$$

$$+ \sum_{n=1}^{\infty} (D_1 t)^{n/2} a_n h_{n+1}(\delta) + \sum_{n=2}^{2,\infty} (D_1 t)^{n/2} a_n 2^n \cdot n! \ .$$

$$2(n+1) i^{n+1} \text{ erfc}(\delta) \qquad (2.12)$$

To determine $C_2(y,t)$, the impurity distribution in silicon, eqn. (2.2) is first transformed to (z,t) domain where $z = y-rX_o(t)$. The transformed diffusion eqn. and the related boundary and initial conditions, after substituting for $X_o(t)$, may be written as,

$$D_2 \frac{\partial^2 C_2}{\partial z^2} + \frac{r\sqrt{B}}{2\sqrt{t}} \frac{\partial C_2}{\partial z} = \frac{\partial C_2}{\partial t} \tag{2.2a}$$

$$[\frac{\partial C_2}{\partial z} - \alpha C_2]_{z=0} = -m.\alpha.C_1(X_o(t),t) = f(t) \tag{2.4b}$$

$$C_2(\infty, t) = -C_B \tag{2.6}$$

$$C_2(z,0) = -C_B \tag{2.7a}$$

The general solution to eqn. (2.2a) with boundary and initial conditions (2.4b), (2.6a) and (2.7a) is [see Appendix II]

$$C_2(z,t) = -C_B + \frac{\partial}{\partial t} \int_o^t g(z,t-\lambda).p(\lambda).d\lambda \tag{2.13}$$

where,

$$g(z,t) = \beta.[\operatorname{erfc}(\frac{z+r\sqrt{B}t}{2\sqrt{D_2}t}) - e^{\alpha(z+r\sqrt{B}t)+\alpha^2 D_2 t}.\operatorname{erfc}(\frac{z+r\sqrt{B}t}{2\sqrt{D_2}t}$$

$$+ \alpha\sqrt{D_2}t)] \tag{2.13a}$$

$$\beta = \frac{1}{\operatorname{erfc}(\frac{r\sqrt{B}}{2\sqrt{D_2}})} \tag{2.13b}$$

$$p(t) = +C_B + \frac{1}{\alpha} f(t) \approx +m\, C_1(X_o(t),t) \tag{2.13c}$$

Using eqn. (2.13), the expression for R.H.S. of eqn. (2.5) is determined (Appendix II).

$$[D_2 \frac{\partial C_2}{\partial z} + \frac{r\sqrt{B}}{2\sqrt{t}} C_2]_{z=o} = \frac{1}{2\sqrt{t}} [-r\sqrt{B} \cdot C_B + \{ C_B + m[a_o +$$

$$+ (C_o - a_o) \operatorname{erfc}(\delta)]\} \cdot \{(2D_2\sqrt{t} + \frac{r\sqrt{B}}{\alpha}) \cdot S(t) + r\sqrt{B}\}$$

$$+ \sum_{n=1}^{\infty} m D_1^{n/2} a_n h_n(\delta) \{(2D_2\sqrt{t} + \frac{r\sqrt{B}}{\alpha}) \frac{\partial}{\partial t} \int_o^t \lambda^{n/2} S(t-\lambda) d\lambda$$

$$+ r\sqrt{B} \cdot t^{n/2} \} - \sum_{n=2}^{2,\infty} m D_1^{n/2} a_n 2^n n! \ i^n \operatorname{erfc}(\delta) \{ (2D_2\sqrt{t}$$

$$+ \frac{r\sqrt{B}}{\alpha}) \frac{\partial}{\partial t} \int_o^t \lambda^{n/2} S(t-\lambda) d\lambda + r\sqrt{B} t^{n/2} \}] \qquad (2.14)$$

Now eqns. (2.12) and (2.14) may be combined in eqn. (2.5) to write the impurity conservation condition in terms of the coefficients a_n's, which are the only unknown quantities in eqn. (2.13), the equation for impurity distribution in silicon (see Appendix III for eqn. (2.5)). Because of the complicated nature of the equation, it is not possible to determine a_n's for a general case from the conservation condition. However, for some special cases it is possible to evaluate a_n's. These are considered below.

Case I : Negligible PSG Growth, $\delta \approx o$

For this case, the expression for p(t) is determined as, (see Appendix III).

$$p(t) = m C_o \qquad (2.15)$$

After substituting B = o in eqn. (2.13), the expression for impurity distribution in silicon can be written as,

$$C_2(z,t) = -C_B + mC_o\left[\text{erfc}\left(\frac{z}{2\sqrt{D_2 t}}\right) - e^{\alpha z + \alpha^2 D_2 t}\,\text{erfc}\left(\frac{z}{2\sqrt{D_2 t}} + \alpha\sqrt{D_2 t}\right)\right]$$

(2.16)

Equation (2.16) is identical to the one reported by Smits [5] for diffusion from a constant vapour source in inert ambient. It is an expected result because as $\delta \to o$, the experimental situation approaches that of diffusion in inert ambient from a constant source.

Case II : Large Value of Rate Constant/Diffusion Time, $\alpha\sqrt{D_2 t} \gg 1$

The expressions for p(t) and g(t) are derived to be, (see Appendix III)

$$p(t) = A = m[a_o + (C_o - a_o)\,\text{erfc}(\delta)]$$

$$= \frac{m[C_o(e^{-\delta^2}/\sqrt{\pi}) - (\mu.\beta/\sqrt{\pi}).e^{-r^2 B/4D_2}.\text{erf}(\delta).C_B]}{(e^{-\delta^2}/\sqrt{\pi}) + \delta.\text{erf}(\delta) + m.r.\delta.\text{erf}\phi(\delta).F(r,B,D_2)}$$

(2.17)

where, $F(r,B,D_2) = -1 + \dfrac{1}{\sqrt{\pi}(r\sqrt{B}/2\sqrt{D_2}).e^{r^2 B/4D_2}.\text{erfc}(r\sqrt{B}/2\sqrt{D_2})}$

and

$$g(t) \approx \beta\left[\text{erfc}\left(\frac{z}{2\sqrt{D_2 t}} + \frac{r\sqrt{B}}{2\sqrt{D_2}}\right) - \frac{1}{\alpha\sqrt{\pi D_2 t}}\right]$$

(2.19)

Substituting for $p(t)$ and $g(t)$ in eqn. (2.13), the expression for $C_2(z,t)$ is written as,

$$C_2(z,t) = -C_B + A[erfc(\frac{z}{2\sqrt{D_2 t}} + \frac{r\sqrt{B}}{2\sqrt{D_2}}) - \frac{1}{\alpha\sqrt{\pi D_2 t}}] \qquad (2.20)$$

In eqn. (2.20), if $\alpha \to \infty$, it is seen that,

$$C_2(z,t) = -C_B + A\ erfc(\frac{z}{2\sqrt{D_2 t}} + \frac{r\sqrt{B}}{2\sqrt{D_2}}) \qquad (2.21)$$

Equation (2.21) is exactly same as reported by Grove et al. [1] for redistribution of impurities in homogeneously doped sample. This is because as $\alpha \to \infty$, $C_1 \to (C_2/m)$ at the interface in order to maintain a finite impurity flux across the interface. The relation $C_1 = C_2/m$ essentially represents the condition of thermodynamic equilibrium at the interface, assumed in Grove's model.

Case III : $\alpha\sqrt{D_2 t} \gg \frac{r\sqrt{B}}{2\sqrt{D_2}}$

Since at the diffusion temperatures normally encountered, $r\sqrt{B} \ll 2\sqrt{D_2}$, this condition represents a practical diffusion process. The expression for $p(t)$ is derived as, (see Appendix III)

$$p(t) = A + \sum_{n=1}^{\infty} \frac{h_n(\delta)}{h_{n+1}(\delta)}\ 2m\ A\mu\beta\ n\ (-1)^n\ (\alpha\sqrt{D_2})^n\ t^{n/2}$$

$$(2.22)$$

where

$$A = m \frac{C_0(e^{-\delta^2}/\sqrt{\pi}) - r.\delta.erf(\delta)\ C_B}{(e^{-\delta^2}/\sqrt{\pi}) + \delta.erf(\delta)} \qquad (2.22a)$$

Using equations (2.22) and (2.13a), the expression for $C_2(z,t)$ can be written as,

$$C_2(z,t) = -C_B + A.g(z,t) + \sum_{n=1}^{\infty} \frac{h_n(\delta)}{h_{n+1}(\delta)}\ 2mA\mu\beta\ n\ (-1)^n\ .$$

$$(\alpha\sqrt{D_2})^n]\ \frac{\partial}{\partial t} \int_0^t \lambda^{n/2}\ g(z,t-\lambda)d\lambda \qquad (2.23)$$

It can be seen that series in eqn. (2.23) converges only for small values of $\alpha\sqrt{D_2}t$ such that $\alpha\sqrt{D_2}t < 1$. Since the value of 'α' in weak oxidising ambient is typically $6\times10^3 - 10^4$ cm^{-1} [7], this equation is useful only for small diffusion lengths (less than a micron).

The three cases considered above, do not encompass all the possible diffusion situations. Case III, however, corresponds to an important situation namely deposition process which generally involves small diffusion lengths. In the following chapters, we will be concerned with Cases I and II only.

CHAPTER   III

PHOSPHORUS DIFFUSION AND CHARACTERIZATION OF DIFFUSED
LAYERS

In the theoretical model presented in the preceding
chapter, a constant dopant source and position independent
diffusion coefficient were assumed. These assumptions impose
certain constraints on the experiment, which have been discussed
in Sec. 3.1. In Section 3.2, the details of experimental set-
up and the scheme of experimental work have been given.
Sections 3.3 and 3.4 are devoted to the characterization of PSG
and the phosphorus diffused layer in silicon, respectively. The
last section i.e. Sec. 3.5 describes the method of determination
of diffusion parameters.

3.1 EXPERIMENTAL CONSTRAINTS

In order to closely match the experimental situation with
the theoretical model proposed in Chapter II, the following
conditions should be satisfied.

(i) The partial pressure of the dopant in diffusion ambient
should remain constant with time. This requires that the
dopant should have good miscibility with the carrier/dilutent
gases (N_2,Ar,O_2 etc.). Furthermore, the deposition of dopant
impurity on the walls of diffusion tube at the cool input end
should be minimised as it would act as a time dependent second-
ary dopant source.

(ii) The dopant concentration at silicon surface should be less than the intrinsic carrier concentration at diffusion temperature. It ensures that the diffusion coefficient is impurity concentration (and therefore position) independent as assumed in the model [1].

A reasonable choice of dopant source satisfying all the above requirements is PH_3 [3]. The experimental set-up used for diffusing phosphorus using this source is described in the following section.

3.2 PHOSPHORUS DIFFUSION

3.2.1 Experimental Set-up

A schematic of the experimental set-up is shown in Fig. 3.1. The diffusion furnace used is Thermco Mini-brute type MB-71. As per manufacturer's claim, this furnace provides a flat temperature zone of 12-14" with spatial variation within $\pm$ 0.5°C, with a quartz tube of OD 3.25". The temperature in the flat zone is expected to be stable within $\pm$ 0.25°C. In the experiments reported in this work a quartz tube of 1.5" ID was used and wafer carrier was a quartz boat of 3" length. The diffusion temperature was measured using a Pt.-Pt. + 10% Rhodium thermocouple. The quartz tube was so positioned in the furnace that the gas entrance point (see Fig. 3.1) is maintained at a temperature > 500°C. This eliminated the deposition of P_2O_5 at the input end to the extent that even after 15 hours of diffusion

Gas entrance point

Furnace

Liner

Diffn. Tube

→ Exhaust

Mixer Flask

Flow meters with needle valve.

PH3+Ar
(1000 ppm PH₃)
0–100 cc./min

N₂
0–1600 cc/min

O₂
0–45 cc./min
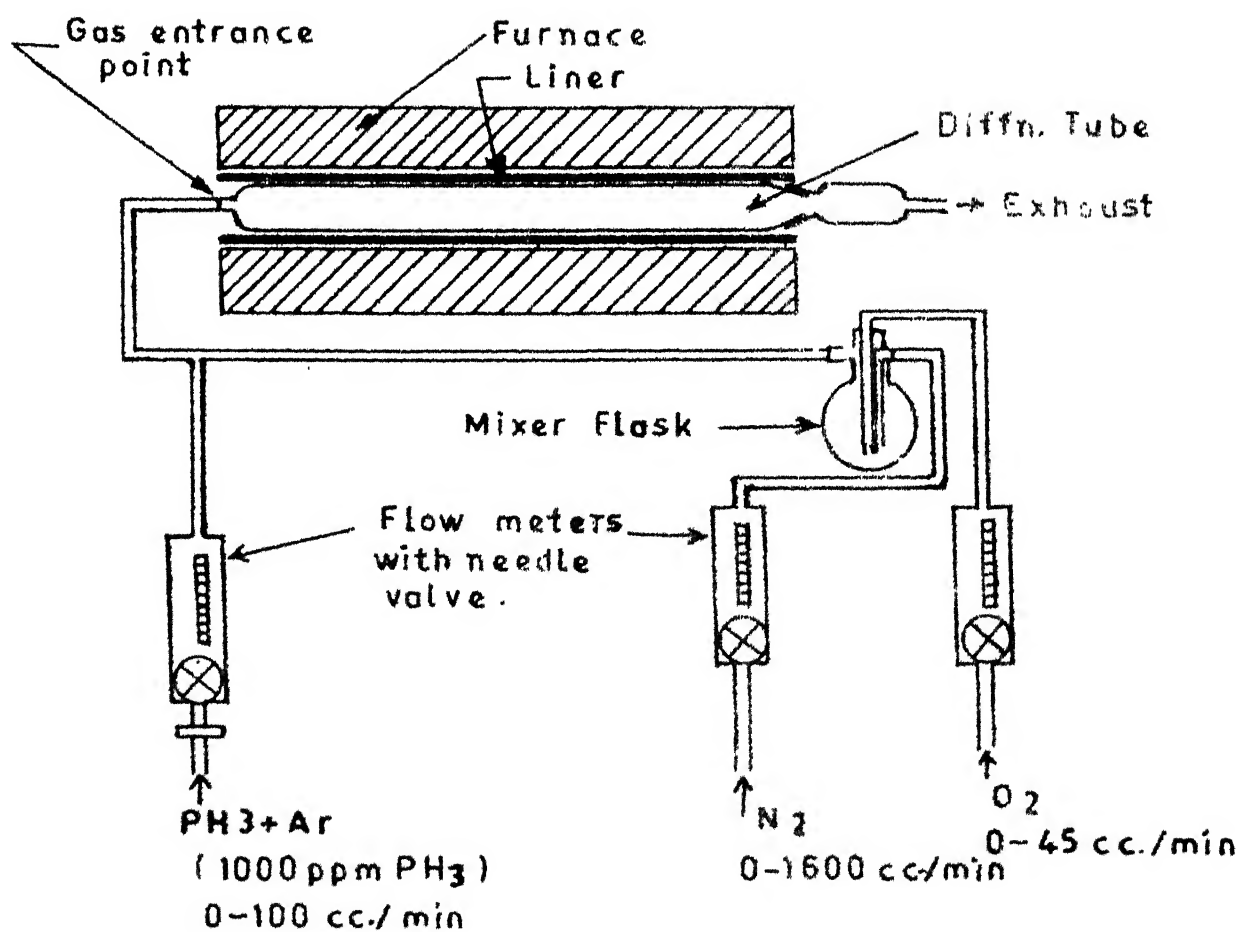
FIG.3.1   Schematic of experimental set-up
for Phosphorus diffusion using PH₃

there was no visible layer of P_2O_5. However, the P_2O_5 deposition was observed at cooler output end.

Teflon tubes were used for making gas connections. The dopant source was an electronic grade PH_3+Ar mixture supplied by Matheson/International. Other gases used in diffusion (N_2, O_2) were also of high purity, having a maximum impurity concentration of less than 6 ppm. The needle valves used to control the flow of gases were made of teflon.

The experimental set-up shown in Fig. 3.1 corresponds to the case of diffusion in inert (i.e., negligible % of O_2) ambient. For diffusion in strong oxidising ambient, the N_2, O_2 gases lines were interchanged at the input end of the respective flowmeters, N_2 flow was blocked and mixer flask was bypassed. For diffusion in chloro-oxidising ambient, the trichloroethylene (electronic grade) was filled in the mixer flask and N_2 was bubbled through it. One inlet of mixer flask (bubbler) was blocked. At the outlet of the bubbler a two way teflon valve was connected so that the TCE carrying N_2 could either be exited to atmosphere or let into the input gas line of the diffusion tube.

3.2.2 Details of Experiments

The dopant source used in the experiments was electronic grade PH_3+Ar mixture (1000 ppm PH_3 in Ar). The diffusions were carried out in three different ambients.

(i)   Strong oxidising ambient : 90.1 V% O_2 + 9.9 V% (PH_3+Ar)

(ii)   Inert ambient : 95.5 V% N_2 + 1.5 V% O_2 + 3.0 V%(PH_3+Ar)

(iii) Chloro-oxidising ambient : 94.5 V% O_2+0.5 V% (PH_3+Ar) +

5.0 V% N_2 bubbled through trichloro-
ethylene at 27°C.

The ambient compositions given above are the typical ones.
The exact ambient composition for each sample is given in
Tables 3.1 - 3.4. The pre-diffusion cleaning of silicon sam-
ples was done using hydrogen peroxide based cleaning solutions
[4]. Prior to loading the samples into the furnace, the gases
were allowed to flow through the tube at the pre-determined rate
to let the flow of respective gases stabilize. The quartz boat,
with samples horizontally placed on it, was quickly loaded into
the furnace without interrupting the gases flow.* However, the
dopant gas flow was stopped at the time of unloading.

The samples used in these investigations were squares of
12 mm x 12 mm size. Starting wafers for <111> samples were p-
silicon slices of 3" dia. and 5-10 Ω.cm resistivity. The same
for <100> samples were p-silicon wafers of 2" dia. and 4-6 Ω.cm/
22-50 Ω.cm resistivity. The starting wafers were supplied with
one side mirror polished.

---

*In case of diffusion in the inert ambient, the dopant gas was
interrupted while loading the sample.

A typical sample load for a diffusion consisted of two
<111> and two <100> samples of the type mentioned above, along
with a small size (typical dimensions 5 mm x 3 mm) p-sample,
ear marked for oxide thickness measurement. In case of diffu-
sions in inert ambient, this last sample was omitted.

Tables 3.1 - 3.4 give the details of each diffusion, such
as diffusion temperature, time and important sample specifica-
tions along with sample identification numbers. First the
diffusions were carried out in strongly oxidising ambient.
Appropriate diffusion times were chosen to allow the growth of
$2000^{o}A$ - $3000^{o}A$ PSG (see Table 3.1). The rate of PSG growth
in these diffusions was found to be only slightly lower than
the oxidation rate of silicon in dry O_2 at corresponding tem-
peratures. The second set of diffusions were done in inert
ambient for the same time interval as chosen in case of strongly
oxidising ambient at respective temperatures. The presence of
the PSG film in these cases was visually undetectable. Since
the oxidation rate of silicon is proportional to the partial
pressure of oxygen in the ambient, the PSG film thickness in
these cases is estimated to be less than $100^{o}A$. The difference
in phosphorus diffusion coefficient in above two cases, there-
fore, can be attributed to the oxidation of silicon during
diffusion in strong oxidising ambient.

The next two sets of experiments were performed to investi-
gate the effect of chlorine on phosphorus diffusion (see Tables
3.3 - 3.4). The two sets of diffusions were done in chloro-

Table 3.1 Diffusions in Strong Oxidising Ambient Long Diffusion Times

	Sample No.	Substrate specs		N$_2$	Ambient composition (vol %)		PSG thickness (µm)
		Orient	Res. (Ω cm)		O$_2$	(PH$_3$+Ar)	
Temp.: 1250°C	O1	(111)	7	–	90.1	9.9	
Time : 1=00 hrs	OA1	(100)	5	–	90.1	9.9	0.2135
Temp.: 1150°C	O3	(111)	7	–	90.1	9.9	
Time : 3=00 hrs.	OA3	(100)	5	–	90.1	9.9	0.2849
Temp.: 1050°C	O4	(111)	7	–	90.1	9.9	
Time : 6=00 hrs.	QA4	(100)	5	–	90.1	9.9	0.2833
Temp.: 950°C	O5	(111)	7	–	90.1	9.9	
Time : 15=00 hrs	OA5	(100)	5	–	90.1	9.9	0.2866

Table 3.2 Diffusions in Inert Ambient

	Sample No.	Substrate specs			Ambient composition (Vol %)		
		Orient.	Res.(Ωcm)	N_2	O_2	(PH_3+Ar)	
Temp.: 1250°C Time : 1=00 hrs.	NO1	(111)	7	95.5	1.5	3.0	
	NOA1	(100)	30	95.5	1.5	3.0	
Temp.: 1150°C Time : 3=00 hrs.	NO3	<111>	7	95.2	2.1	2.7	
Temp.: 1050°C Time : 6=00 hrs.	NO4	<111>	7	95.8	1.5	2.7	
Temp.: 1200°C Time : 1=10 hrs.	NO2	<111>	7	94.0	1.8	4.2	

Table 3.3 Diffusions in Strong Oxidising Ambient - Short Diffusion Times

| | Sample No. | Substrate Specs. | | Ambient composition | | | PSG thickness (μm) |
		Orient	Res. (Ω cm)	N₂	O₂*	(PH₃+Ar)	
Temp.: 1250°C	SO1	(111)	5	–	99.5	0.5	0.0937
Time : 0=10 hrs.	SOA1	(100)	30	–	99.5	0.5	
Temp.: 1200°C	SO2	(111)	7	–	99.5	0.5	0.0746
Time : 0=10 hrs.	SOA2	(100)	7	–	99.5	0.5	
Temp.: 1150°C	SO3	(111)	7	–	99.5	0.5	0.1002
Time : 0=25 hrs.	SOA3	(100)	5	–	99.5	0.5	
Temp.: 1050°C	SO4	(111)	7	–	99.6	0.4	0.1273
Time : 2=00 hrs.	SOA4	(100)	–	–			
Temp.: 950°C	SO5	(111)	7	–	99.6	0.4	0.1007
Time : 4=00 hrs.	SOA5	(100)	30	–	99.6	0.4	

*O₂ used was ordinary grade and is expected to contain 5% N₂ .

Table 3.4 Diffusions in chloro-oxidising Ambient

	Sample No.	Substrate specs.		Ambient Composition (Vol. %)			PSG thickness (μm)
		Orient.	Res. (Ω.cm)	N_2 (through TCE)	O_2*	PH_3+Ar	
Temp.: 1250°C	OC1	(111)	7	5.0	94.5	0.5	0.0895
Time : 0=10 hrs.	OCA1	(100)	30	5.0	94.5	0.5	
Temp.: 1200°C	OC2	(111)	7	5.0	94.5	0.4	0.0778
Time : 0=10 hrs.	OCA2	(100)	30	5.0	94.5	0.5	
Temp.: 1150°C	OC3	(111)	7	5.0	94.5	0.5	0.1137
Time : 0=25 hrs.	OCA3	(100)	7	5.0	94.5	0.5	
Temp.: 1050°C	OC4	(111)	7	5.0	94.6	0.4	0.1374
Time : 2=00 hrs.	OCA4	(100)	5	5.0	94.6	0.4	
Temp.: 950°C	OC5	(111)	7	5.0	94.6	0.4	0.1128
Time : 4=00 hrs.	OCA5	(100)	30	5.0	94.6	0.4	

*O_2 used was ordinary grade and is expected to contain upto 5% N_2.

oxidising and strong oxidising ambient respectively. The diffusion times for these experiments were selected to be equal at respective temperatures and considerably shorter than the same for the diffusions described in preceding paragraph. The effect of chlorine on phosphorus diffusion in silicon can be obtained by comparing the diffusion coefficients estimated in the two cases. Since for strong oxidising ambient case, the diffusions have been done for two different time intervals, a comparison of respective diffusion coefficients also allows the determination of time (and hence oxidation rate) dependence of OED. The shorter diffusion times of these experiments result in reduced junction depth which in turn also reduces the time taken in evaluating the impurity distribution in diffused layers.

3.3 CHARACTERIZATION OF PSG

The PSG parameters of interest are C_o and $X_o(t)$. The knowledge of $X_o(t)$ is essential for determination of D_2. As will be explained in Chapter 4 (see Sec. 4.1), the knowledge of C_o provides a way to calculate the value of D_1. The experimental determination of C_o and $X_o(t)$ is described below.

3.3.1 Estimation of C_o

Approximate value of C_o was determined from the etch rate of PSG in p-etch [5,6]. The calibration curve given in ref. [18] was used to convert etch rate of PSG in p-etch to

mole percent of P_2O_5 in PSG. The average value of etch rate of PSG was found to be 4.3 ± 0.2 A/sec. for all the cases of diffusions in strong oxidising/chloro-oxidising ambient. The corresponding concentration of P_2O_5 in PSG is 4.0 mole percent. If the density of PSG is taken to be same as that of SiO_2, thermally grown in dry O_2 (i.e., 2.25 gm/c.c), the concentration of P_2O_5 in PSG - and the value of C_0 are calculated to be 1.7×10^{21} cm^{-3} and 3.4×10^{21} cm^{-3} respectively.

It would appear that the value of C_0 determined as above, is the average value of phosphorus concentration in PSG rather than the phosphorus concentration at the PSG surface. It has been shown, however, by radiochemical analysis, that the phosphorus distribution in PSG is box type [7] and for a box type distribution, the average value of phosphorus concentration will be nearly equal to that at the surface. The above determined value of C_0 is therefore, expected to be a good approximation to true value of C_0.

3.3.2 Determination of PSG Thickness

Ellipsometry, MOS capacitance measurements and interferometry are the most commonly used methods for measuring the oxide thickness. In this work, the oxide thickness was measured using interferometry.

The basic principle of interferometry, as applied to the measurement of step height is illustrated in Fig. 3.2. The specimen is covered with a reflective coating of silver and a

Monochromatic Light

(a)
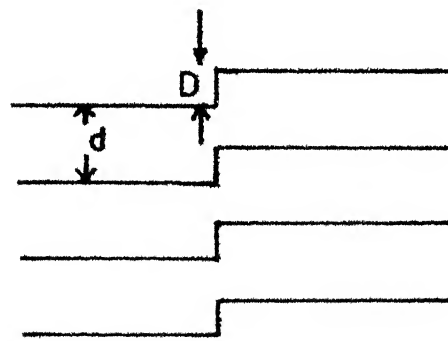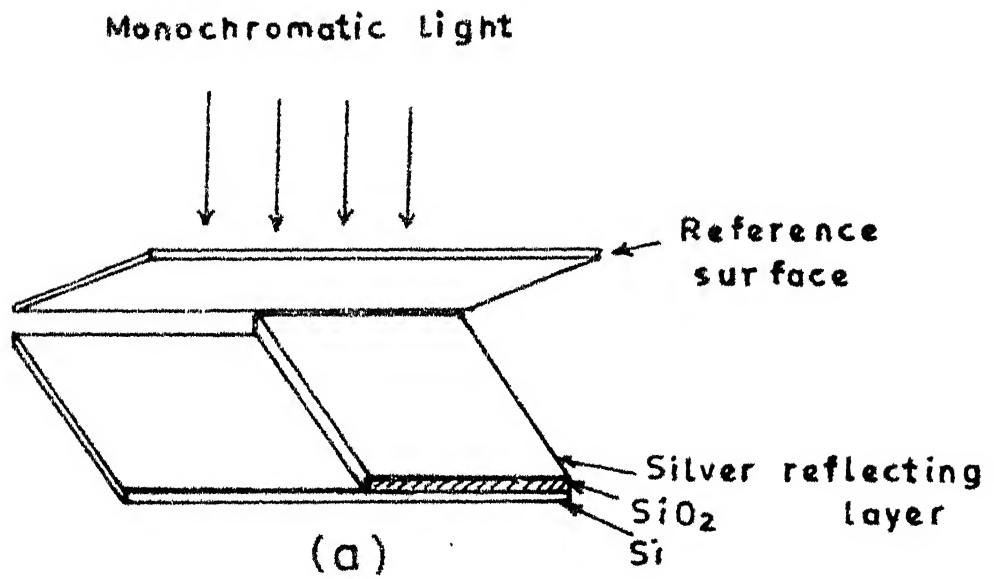
(b)

FIG.3.2 Oxide Thickness Measurement by
Interferometry (a) A typical position
of reference plane with respect to
specimen (b) Interference fringes
as seen through microscope.

partially reflecting plane is positioned over the specimen as shown in Fig. 3.2a. When a monochromatic light falls on the assembly, an interference fringe pattern, as shown in Fig. 3.2b, is created due to the path difference of the lights reflected from the reference plane and the specimen surface. These fringes are viewed through a microscope. The step height t_s is related to the fringe displacement D, the normal fringe spacing d and the wavelength of the monochromatic light λo, by the relation,

$$t_s = \frac{D}{d} \frac{\lambda o}{2}$$
(3.1)

The measurements were carried out on A scope model 960-4020 (Varian make).

3.4   Characterization of Diffused layers

Differential sheet resistance method has been used to evaluate the diffused impurity profiles. The method is applicable only to the cases in which majority carrier concentration distribution is same as impurity distribution. In case of phosphorus in silicon, the two distributions coincide for impurity concentrations $\leq 10^{20}$ cm^{-3} [1]. The impurity concentrations encountered in this work, are more than one order of magnitude lower than this limit.

3.4.1   The Differential Sheet Resistivity Method—Theory

The bulk conductivity at a depth 'x' from the surface is related to the sheet conductivity at the same depth by the equation [9]

$$\sigma_s(x) = \int_x^{x_j} \sigma(x) \, dx \qquad (3.2)$$

Differentiating eqn. (3.2) w.r.t. 'x',

$$\sigma(x) = -\frac{d\sigma_s}{dx}$$

or

$$e.\mu \{n(x)\} \cdot n(x) = -\frac{1}{\rho_s(x)} \frac{d}{dx} [\ln \rho_s(x)] \qquad (3.3)$$

Due to complicated nature of the function $\mu[n(x)]$, eqn. (3.3) can not be solved analytically for $n(x)$ and therefore has to be solved numerically [8].

It is evident from eqn. (3.3) that the sheet resistivity is required to be measured at different depths from the surface by successive removal of thin layers of silicon. The accuracy of the method, therefore, depends upon (i) accuracy of the measurement of sheet resistivity and (ii) uniform removal and accurate determination of, the thickness of silicon layer removed before each measurement.

Two methods, namely, four point probe and Vander Pauw methods have been used for measurement of sheet resistivity in this work.

(a) Four Point Probe Method

Sheet resistivity in this case is given by [8],

$$\rho_s = \frac{\pi}{\ln 2} \cdot \frac{V}{I} C(D_s/s) \cdot F(x_j/s) \qquad (3.4)$$

where I is the current flowing through the outer probes and 'V' the corresponding potential difference created between the two

inner probes by the current I, $C(D_s/s)$ and $F(x_j/s)$ are correction factors. $C(D_s/s)$ takes into account the finite lateral dimension of the sample and is a function of sample diameter 'D_s' and probe spacing 's'. $F(x_j/s)$ is the correction factor to be included when sample thickness x_j is large compared to 's'. For $x_j/s \leq 0.4$, F is unity. The values of C and F as a function of D_s/s and x_j/s are tabulated in ref. [9] and the same have been used in this work.

To measure the sheet resistivity, a four point probe having a probe spacing of 25 mils (supplied by Kulicke and Soffa) was used. For the sample shown in Fig. 3.4a, the eqn. (3.4) reduces to,

$$\rho_s = 4.1716 \frac{V}{I} \tag{3.5}$$

(b) Vander Pauw Method :

Referring to fig. (3.4b), the sheet resistivity is given by [10],

$$\rho_s = \frac{\pi}{2 \ln 2} \; (R_{12,34} + R_{23,14}) \; f(\frac{R_{12,34}}{R_{23,14}}) \tag{3.6}$$

$$R_{12,34} = \frac{V_{34}}{I_{12}}$$

$$\tag{3.6a}$$

$$R_{23,14} = \frac{V_{23}}{I_{14}}$$

where V_{34} is potential difference between terminals 3,4 when a constant current I_{12} flows between terminals 1,2 and V_{23} is the

p.d. between terminals 2,3 for current I_{14} flowing through terminals 1,4. The correction factor f is given by the transcedental equation,

$$1+\exp[\frac{2 \ln 2}{f}(\frac{R_{12,34}-R_{23,14}}{R_{12,34}+R_{23,14}})] = \exp[\frac{2 \ln 2}{f}\frac{R_{12,34}}{R_{12,34}+R_{23,14}}]$$

$$(3.7)$$

Equation (3.6) is valid if the point contacts are placed at the periphery of the sample to make current and voltage measurements. All practical contacts, however, have finite dimensions. In Fig. 3.4b, considering the heavily doped region as the contact region, the sum of the contact lengths of all the four contacts of the sample, is less than 5% of the sample periphery. For these samples, therefore, no correction needs be applied for finite contact size [10].

3.4.2 Determination of Sheet Resistivity Distribution

As mentioned in Sec. 3.2.2, the phosphorus diffused p-samples are squares of size 12 mm x 12 mm. For the measurements, the mesas of configurations shown in Fig. 3.4 were etched on these samples. The sheet resistivity measurements, each followed by removal of thin silicon layers by anodic oxidation, were done on these mesas.

(A) Sample Preparation :

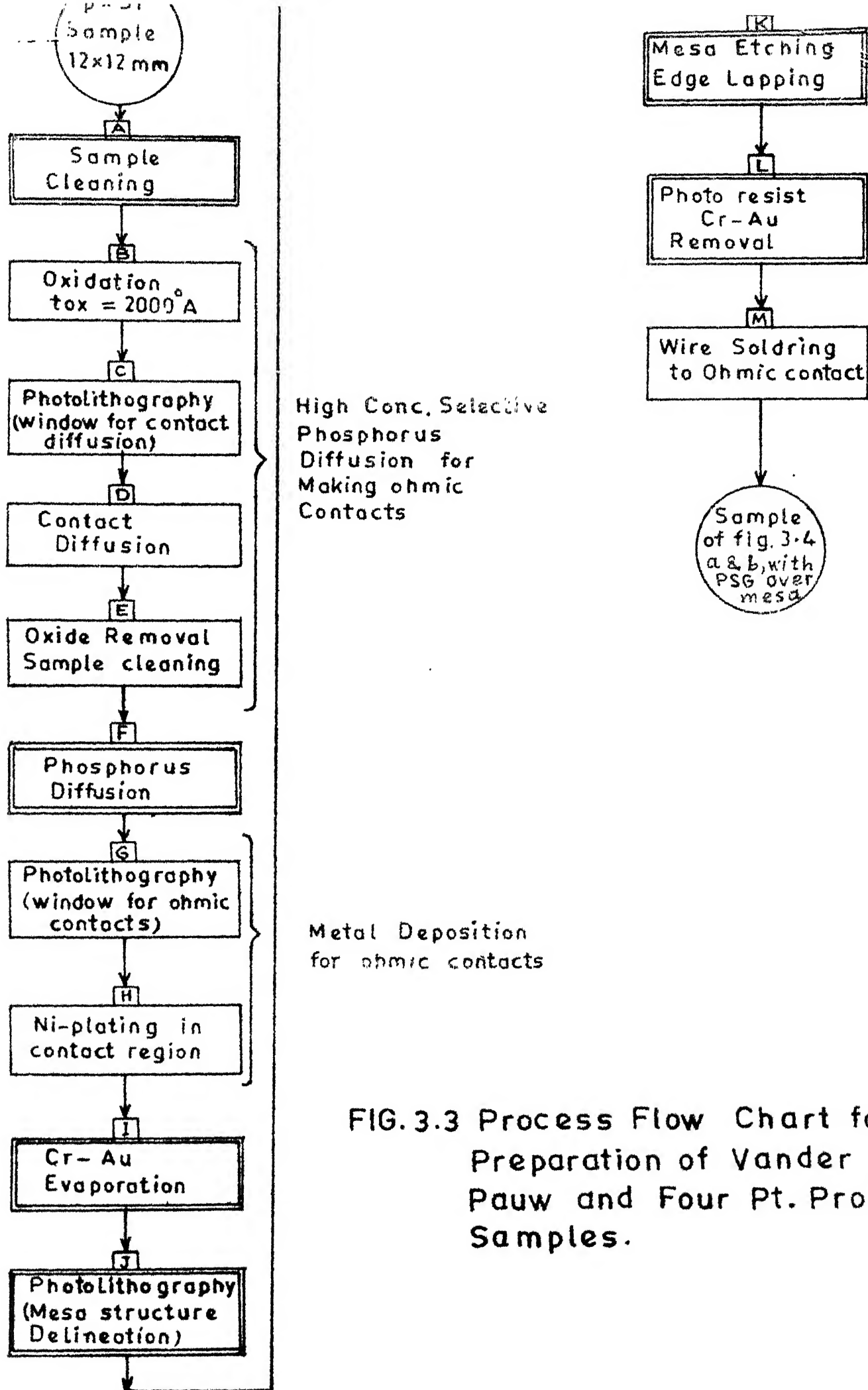The process sequence leading to the samples shown in Fig. 3.4 is given in the flow chart of Fig. 3.3. The flow chart

FIG. 3.3 Process Flow Chart for Preparation of Vander Pauw and Four Pt. Probe Samples.
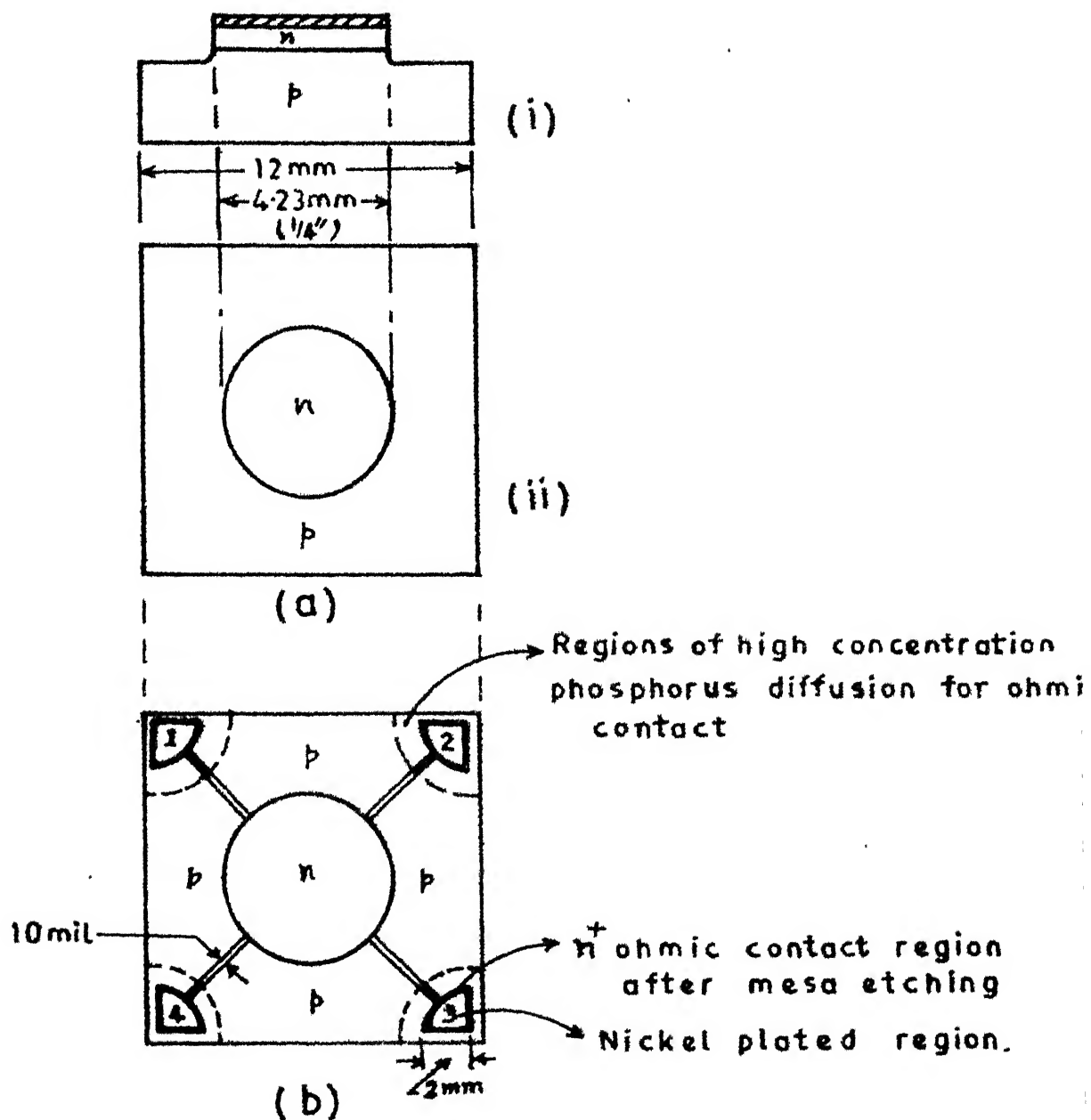
(i)

12mm
4·23mm
(¼")

(ii)

(a)

Regions of high concentration
phosphorus diffusion for ohmi
contact

10mil

n^+ ohmic contact region
after mesa etching

Nickel plated region.

2mm

(b)

FIG.3.4 (a) Four Pt. Probe Sample
(i)Elevation
(ii)Top view
(b) Vander Pauw Sample-Top view

describes the process sequence used to fabricate Vander Pauw Samples (VDP). The processes used for preparing four point probe samples (FPP) are merely a subset of VDP process sequence and have been identified by double-lining the blocks, each representing an individual process, in the flow chart. The essential details of the various processes, labelled as a,b,c,.. etc. in the flow chart, are given below.

(a) Sample cleaning was done using the hydrogen peroxide based solvents described in reference (4).

(b) The sample was then thermally oxidised in dry O_2 at $1200^{\circ}C$ for 1 hr., to grow about $2000^{\circ}A$ thick SiO_2. This oxide acts as a mask against the phosphorus diffusion during the selective high concentration phosphorus diffusion that was carried out in step (d) to form ohmic contact regions.

(c) Windows were etched in SiO_2 grown in (b), using photo-lithography, to expose the silicon surface where high concentration phosphorus diffusion was to be performed, for making ohmic contacts.

(d) High concentration phosphorus diffusion for ohmic contacts was performed using phosphosilica film (10^{20} cm^{-3}) as a source. The source was applied only to exposed silicon surface of ohmic contact region. The diffusion was done at $875^{\circ}C$ for 15 min.

(e) The masking oxide and residue of phosphosilica film were removed and sample cleaned by process (a).

(f) Now the phosphorus diffusion using PH_3 was carried out as per details given in Tables 3.1 - 3.4.

(g) The windows were etched in the PSG, grown in Step (f), to deposit metal contacts, the windows were quarter circles of 1.5 mm radius, symmetrically placed at the four corners of the sample as shown in Fig. 3.4b. The PSG on the back side of sample was preserved during window etching.

(h) The electroless nickel plating was done to deposit metal for making ohmic contacts [11]. Since the whole sample surface, except the window regions, was covered with PSG, nickel was plated only over the bare silicon surface of window region.

(i) This step consisted of Cr-Au evaporation at a pressure of 8×10^{-6} torr with sample heated to $275^{\circ}C$. This process had to be added because Cr-Au layer provides extra protection to the underlying PSG and Si surface and ensures the elimination of pin holes during mesa etching.

In case of VDP samples the nickel contacts were masked during Cr-Au evaporation. Heating of the sample to $275^{\circ}C$ improves the adhesion of nickel contact. Furthermore, since the nickel was heated in the vacuum, it did not oxidise and wires could be easily soldered to these contacts. It may be mentioned that the evaporated Cr-Au was not found suitable for making ohmic contacts presumably due to higher than desirable pressure during evaporation.

For the samples diffused in inert ambient, this step was omitted. All such samples were evaluated by four pt. probe.

(j) The photoresist pattern of the shapes shown in Fig. 3.4 were generated by photolithography. The Cr-Au from the exposed surface was removed using etchants given in Appendix IV. PSG from the exposed surface was also removed by buffered HF.

(k) Now the mesa is etched using Wright's etch [12]. This etchant was preferred because it gives a better finish of etched surface and because it has low etch rate which allows the etching to be done at room temperature without damaging the photoresist. The sample was quenched in buffered HF immediately after removal from etch bath and rinsed in DI water. The etched surface was then tested by hot probe for conductivity type.

(l) The photoresist and Cr-Au were removed from the mesa region. The phosphorus diffused mesa region at this stage is protected by PSG grown in step (f).

(m) In case of VDP samples, thin copper wires were soldered to the nickel contacts using Pb-Sn solder.

Before measurements, PSG was removed from mesa region.

(B) Sheet Resistivity Measurements

The sheet resistivity measurements were carried out using a Kithley digital multimeter (model 191) as a Voltmeter and a

Kithley digital electrometer (model 616) as an ammeter. All
the measurements were taken in the current range 1-100 μA. The
measured voltages corresponding to these currents were less
than 15 mV, thus eliminating the possibility of error caused
due to forward biasing of underlying p-n junction [13].

All the circuit connections were made using sheilded wires.
The sample was covered with a metal box during the measurement,
to ensure that the measurements are free from any error caused
by photogenerated carriers.

(C) Removal of Thin Layers of Silicon

Thin silicon layers were removed, preceding each sheet
resistivity measurements by anodic oxidation [14-17]. The
anodic oxidation cell used for the purpose is shown in
Fig. 3.5a. The electrolyte used was 0.08N solution of KNO_3
in ethylene glycol + 4% water. The advantage of keeping the
silicon sample in face up position is that the gas bubbles
released during the oxidation process move up towards the
surface of electrolyte and silicon surface is always in con-
tact with the electrolyte. This leads to uniform and repro-
ducible oxide growth. For providing the back contact to
silicon, mercury has been used as it was found to provide
good electrical contact to a lapped p-silicon surface of
resistivity upto 50 cm. Because of the hydrophobic nature
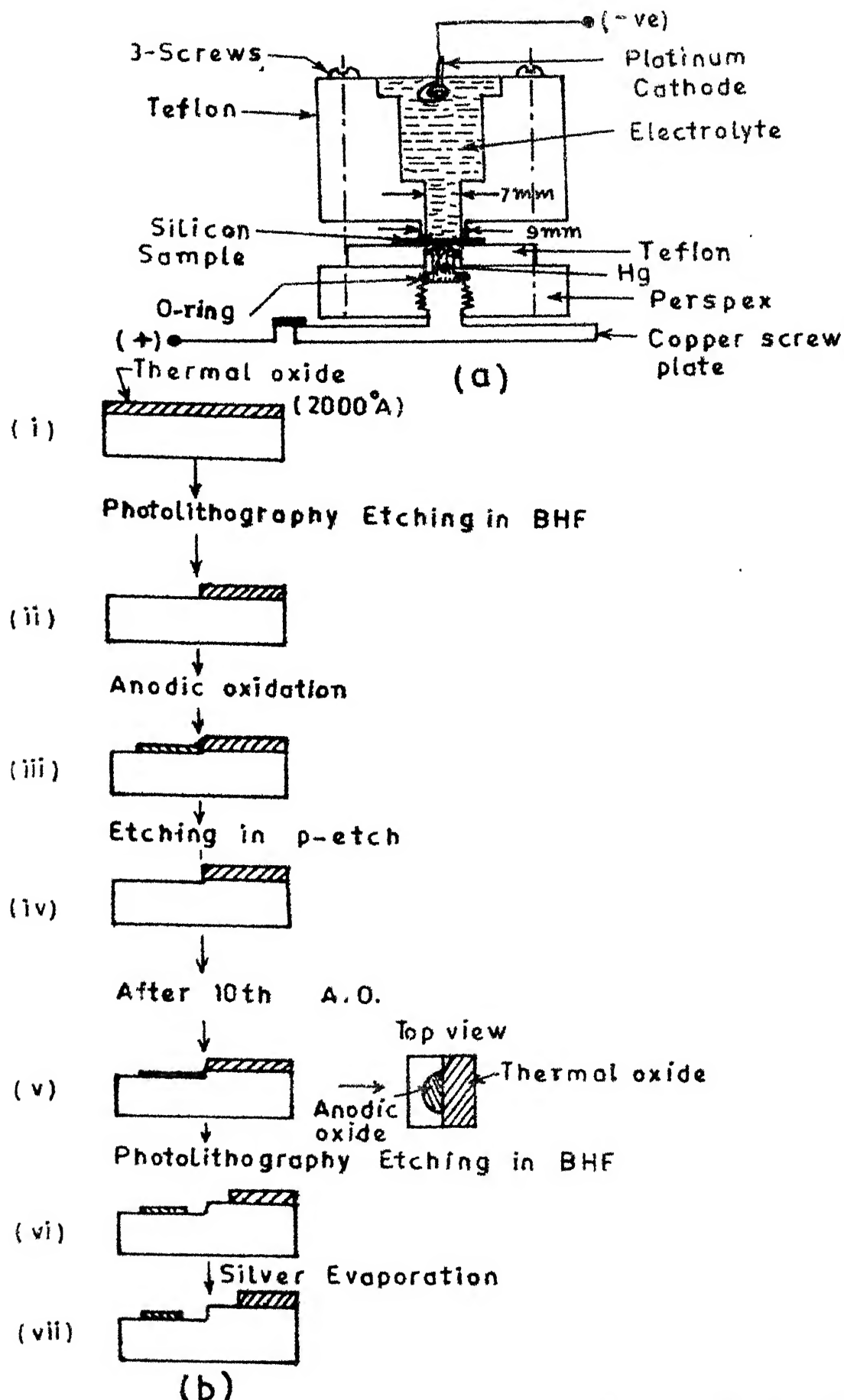of teflon and silicon surface, the electrolyte does not creep

FIG. 3.5 (a) Cross-sectional elevation of anodic oxidation cell.
(b) Process sequence used to determine the thickness of silicon removed in one standard Anodic oxidation Process.

out and anodic oxidation is strictly confined to the area
bounded by teflon structure containing the electrolyte.

In order to ensure that silicon layers of equal thickness
are removed in each oxidation step, a standard anodic oxidation
process was defined in the following manner. 'The cell voltage
is first increased so that the anode current rises to 8 mA.
As oxidation proceeds, the current decays. The cell voltage
is now gradually increased keeping the current between 6 mA –
8 mA, till the applied voltage reaches 120 V. The current is
allowed to decay to 1.2 mA. The oxidation is then terminated
by bringing the applied voltage to zero'. This standard pro-
cess was used for removal of thin silicon layers throughout
this work.

To accurately determine the thickness of silicon removed
in each standard anodic oxidation process (SAOP) the following
procedure was adopted. A phosphorus diffused p-Si (12 mm x
12 mm) sample was thermally oxidised to grow an oxide layer of
about 2600°A. The SiO_2 was then removed from half of sample
by photolithography. Now a SAOP was performed. The anodic
oxidation occurred only over the exposed Si-surface. This
anodic oxide was etched in p-etch [5] for 20 sec. Since the
etch rate of anodic oxide is about 50°A/sec as compared to
2°A/sec of thermal oxide, an etching of 20 sec in p-etch was
enough to ensure complete removal of anodic oxide while reduc-
ing the thickness of masking thermal oxide only by about 40°A.

The above process of anodic oxidation was repeated 10 times. Even at the end of 10th anodic oxidation there was enough thermal oxide to mask the underlying silicon surface from anodic oxidation. After last anodic oxidation, the sample surface appeared, as shown in Fig. 3.5b(iv). A rectangular groove of 2 mm x 5 mm was then etched in the oxide such that the boundary of anodic and thermal oxides falls in the centre of the groove. This resulted in the exposure of silicon step, height of which is equal to the silicon thickness removed in 10 SAOP's and also a step the height of which is equal to the thickness of anodic oxide grown in one SAOP. Now a silver layer of about 2000°A thickness was evaporated on the sample and the step heights measured with Varian $\overset{\circ}{A}$ Scope model 960-4020.

The above experiment was carried out on two test samples. The average silicon step height was determined to be (2440$\pm$5/$\overset{\circ}{A}$ and average anodic oxide thickness to be 543°A$\pm$15°A. The silicon removed per SAOP was thus taken to be 244°A and the ratio of the volume of silicon consumed to the volume of anodic oxide grown is determined to be 0.449, which is in agreement with the reported values of 0.38-0.45 [8,16], within experimental errors.

3.4.3 Determination of Impurity Distribution

Impurity distribution from sheet resistivity distribution

was determined using eqn. (3.3). For $\mu(n)$, the following expression was used [18],

$$\mu(n) = 55.24 + \frac{1388.57 - 55.24}{1 + (\frac{n}{1.072 \times 10^{17}})^{0.733}} \tag{3.8}$$

The measured $\rho_s(x)$ vs x data were first smoothed using cubic spline approximation. An IMSL subroutine (International Mathematical Subroutine Library) 'ICSSCU' was used for the purpose. The extent of data smoothing was adjusted to obtain a reasonably smooth impurity distribution. The value of R^2 for smoothed data was between 99.9 - 99.5*. The value of R^2 was 99.9 for inert ambient data, 99.8 for strong oxidising ambient(O/OA - samples) and 99.5 for other cases.

The slope d ρ_s/dx was determined using another IMSL sub-routine 'DCSEVU'. The impurity distribution was then determined by solving eqn. (3.3) for n(x) numerically by Newton-Raphson method.

---

*The R^2 is defined as

$$R^2 = 1 - \frac{\sum\limits_{m=1}^{n} e_m^2}{\sum\limits_{m=1}^{n} [Y_m - \overline{Y}]^2}$$

where

$\quad\quad Y_m$ = Observed value of dependent parameter

$\quad\quad \overline{Y}$ = Mean value of Y_m

$\quad\quad e_m = Y_{sm} - Y_m$

$\quad\quad Y_{sm}$ = Smoothed value of Y_m

The impurity distribution and the measured sheet resistivity distributions for different samples are plotted in Figs. 3-7 - 3.24a.

3.5 DETERMINATION OF DIFFUSION PARAMETERS

The values of diffusion parameters, i.e., A, D_2 and α, were determined in the following manner.

First the value of α was estimated from the surface concentration vs. diffusion time data plotted in Fig. 3.6. Since it has been shown that the 'α' is temperature and crystal orientation independent [18-19], the value of α was determined only at one diffusion temperature for each diffusion ambient.

It can be seen that in case of diffusion in strong oxidising ambient, the surface concentration is time-invariant. The value of α for these cases, therefore, is taken to be infinity. In inert ambient, the surface concentration varies with time. The value of α in this case is determined by using eqn. 2.16 at $x = o$. The diffusion coefficient of phosphorus in silicon at $1150^\circ C$ was taken from Ghoshtagore's data [19], for determination of α. The calculated value of 'α' for this case is 8×10^3 cm^{-1}. It is in good agreement with the value of α reported by Ghoshtagore for oxide-silicon interface [20]. It is to be expected because the inert ambient as defined in Sec.3.2
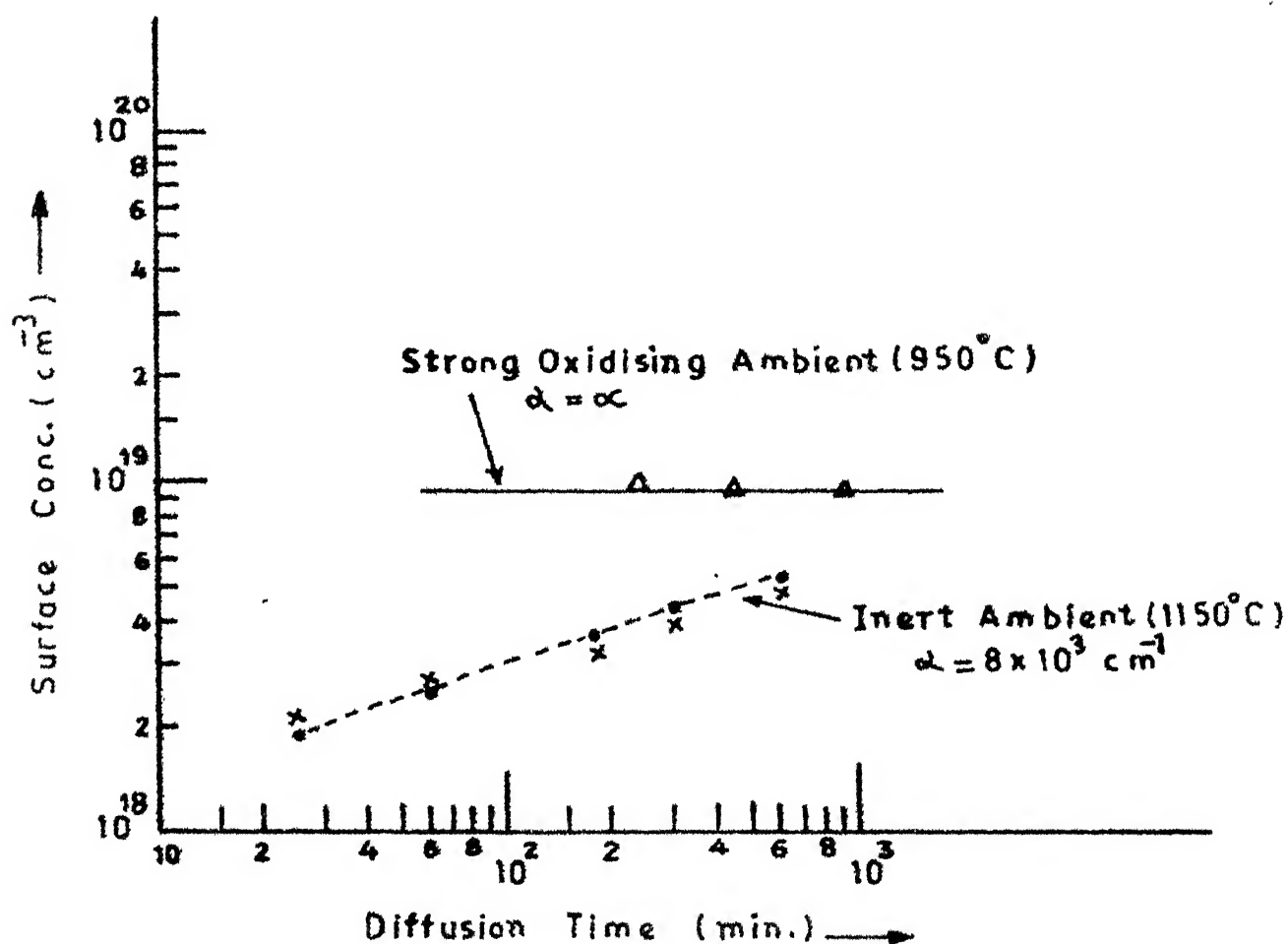
FIG.3.6 Variation of Surface Concentration with Diffusion time.
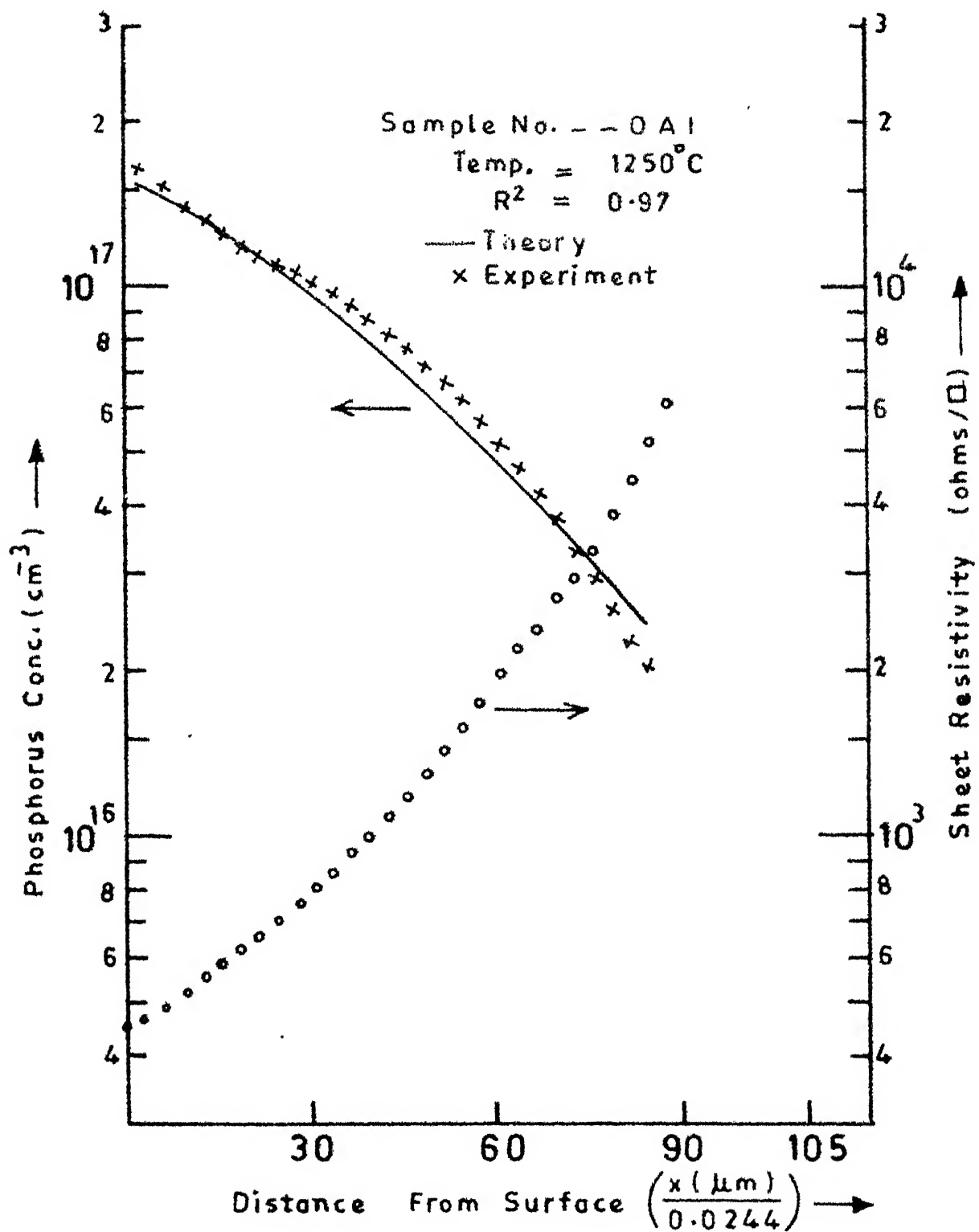
FIG. 3.7   Sheet Resistivity and Phosphorus Distribution in Silicon.

Sample No. — — O A I
Temp. = 1250°C
R^2 = 0·97
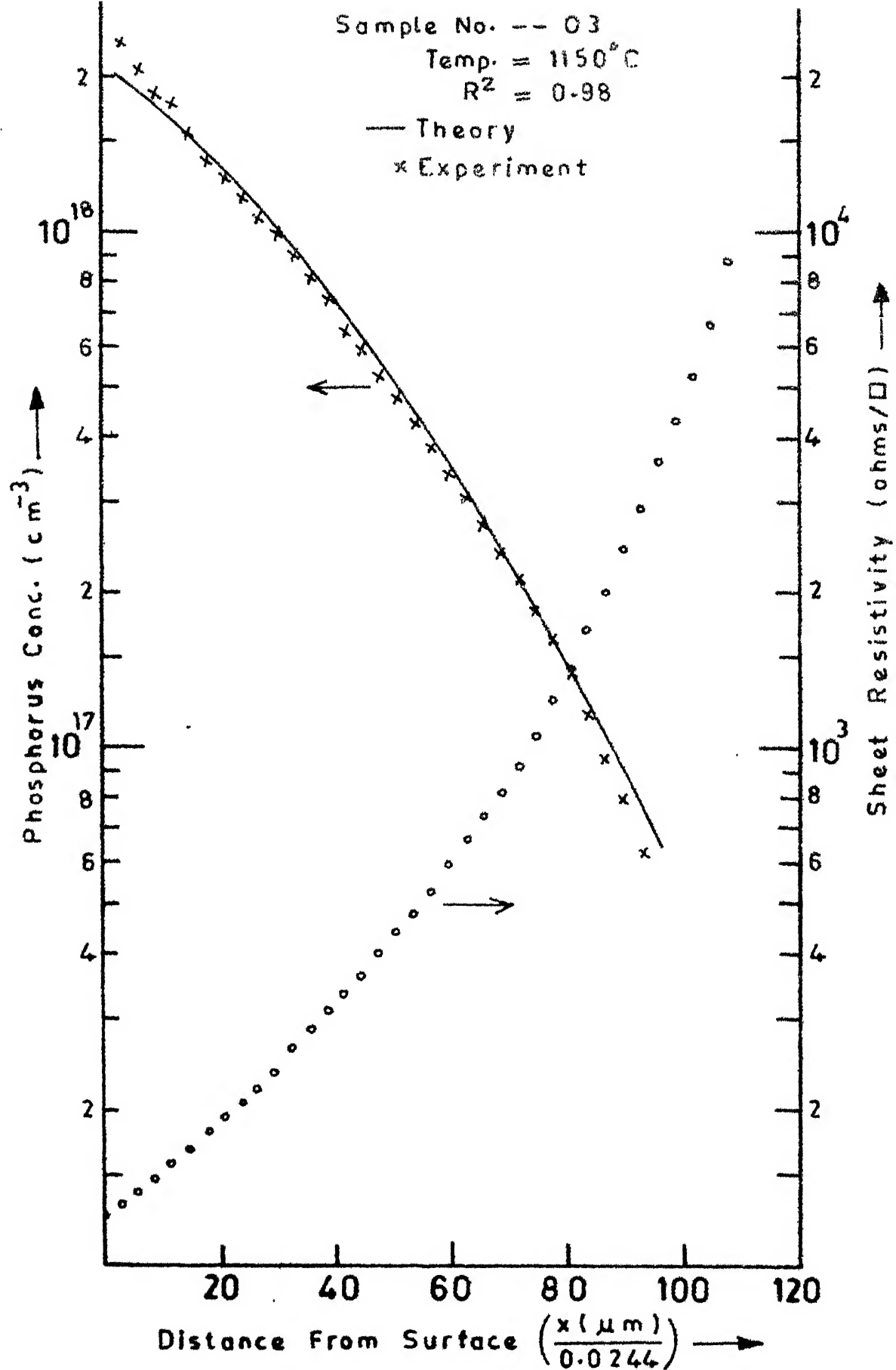—— Theory
× Experiment

FIG.3.8 Sheet Resistivity and Phosphorus
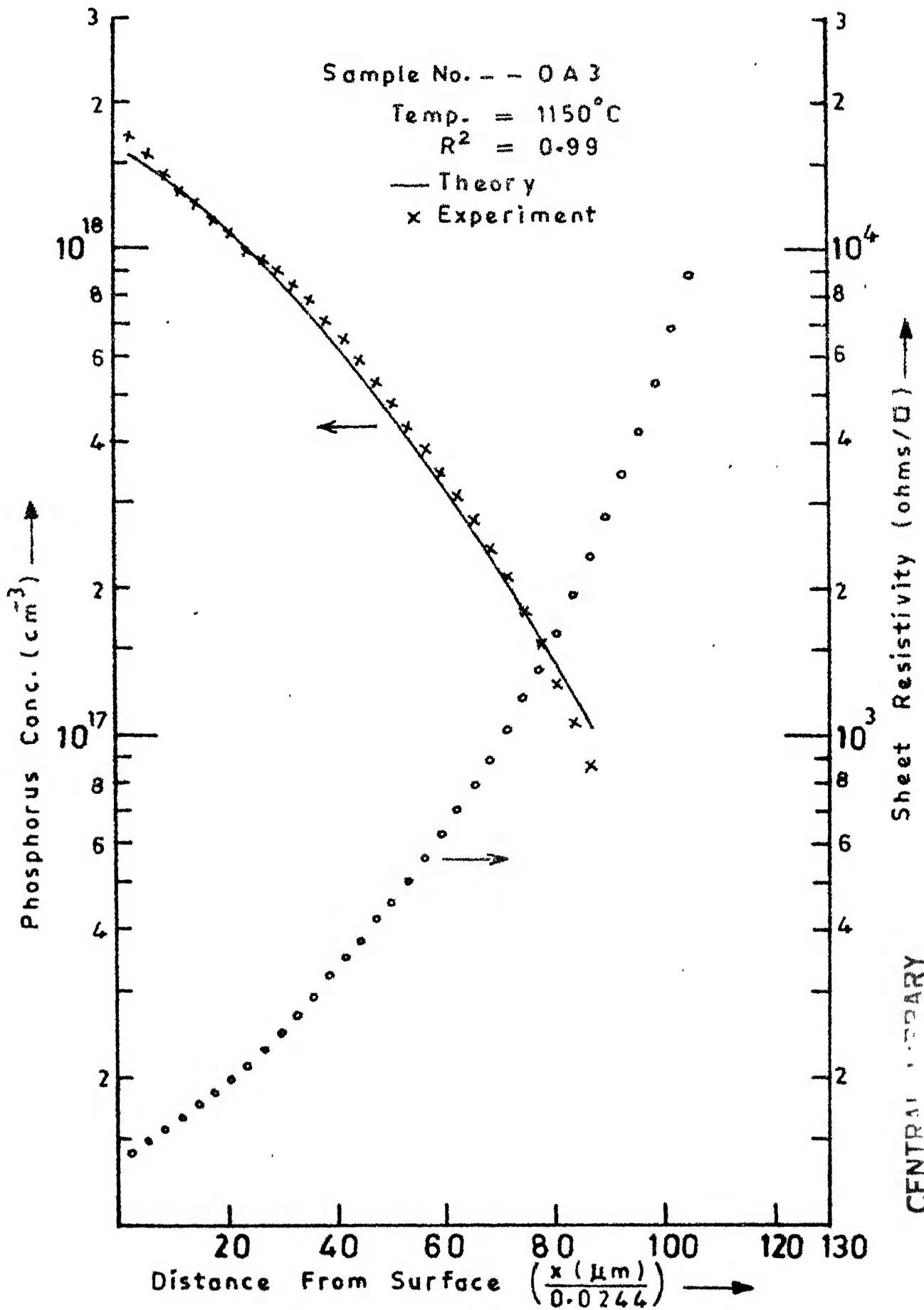Distribution in Silicon.

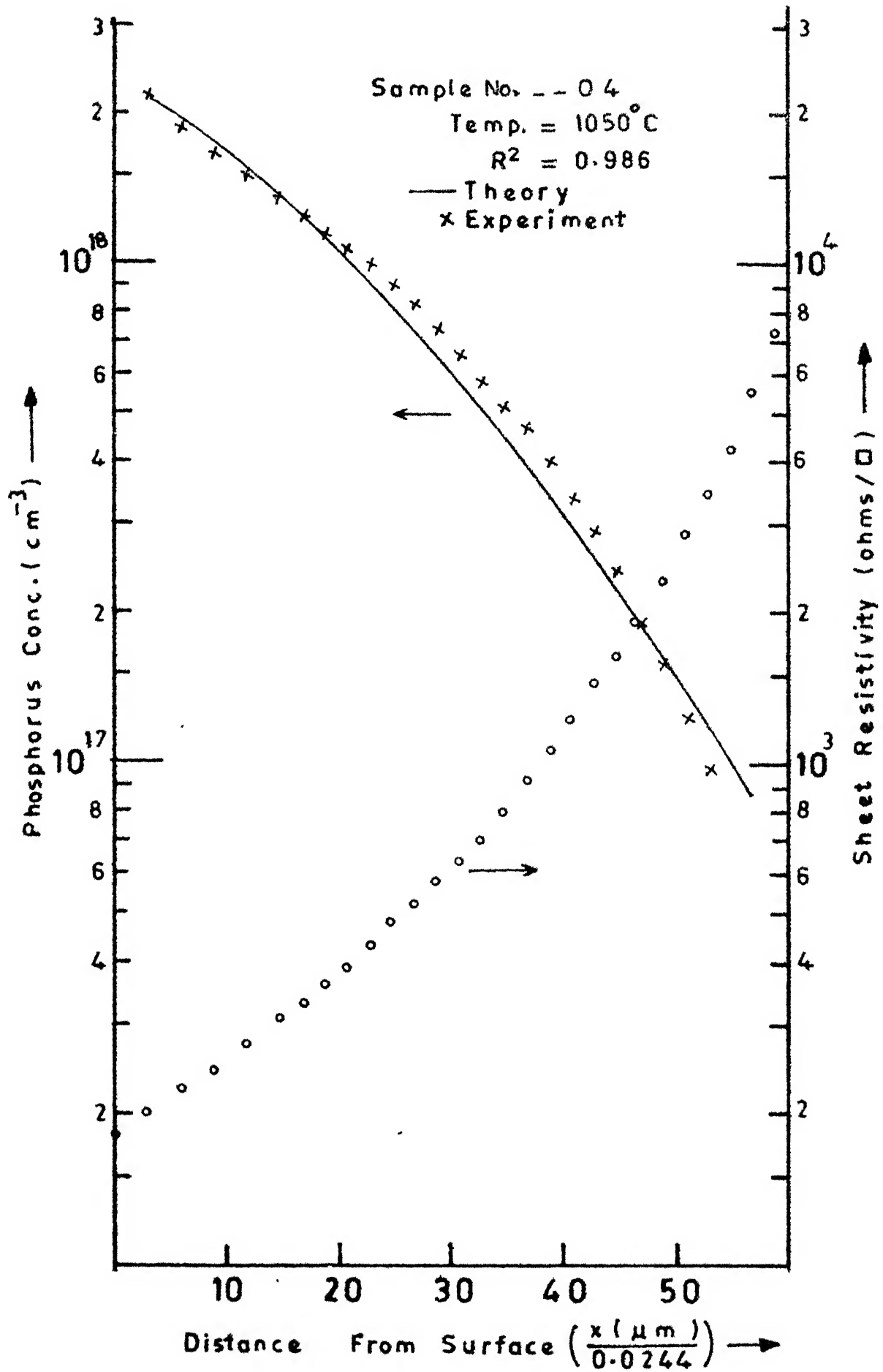FIG.3.8a Sheet Resistivity and Phosphorus Distribution in Silicon.

FIG.3.9 Sheet Resistivity and Phosphorus
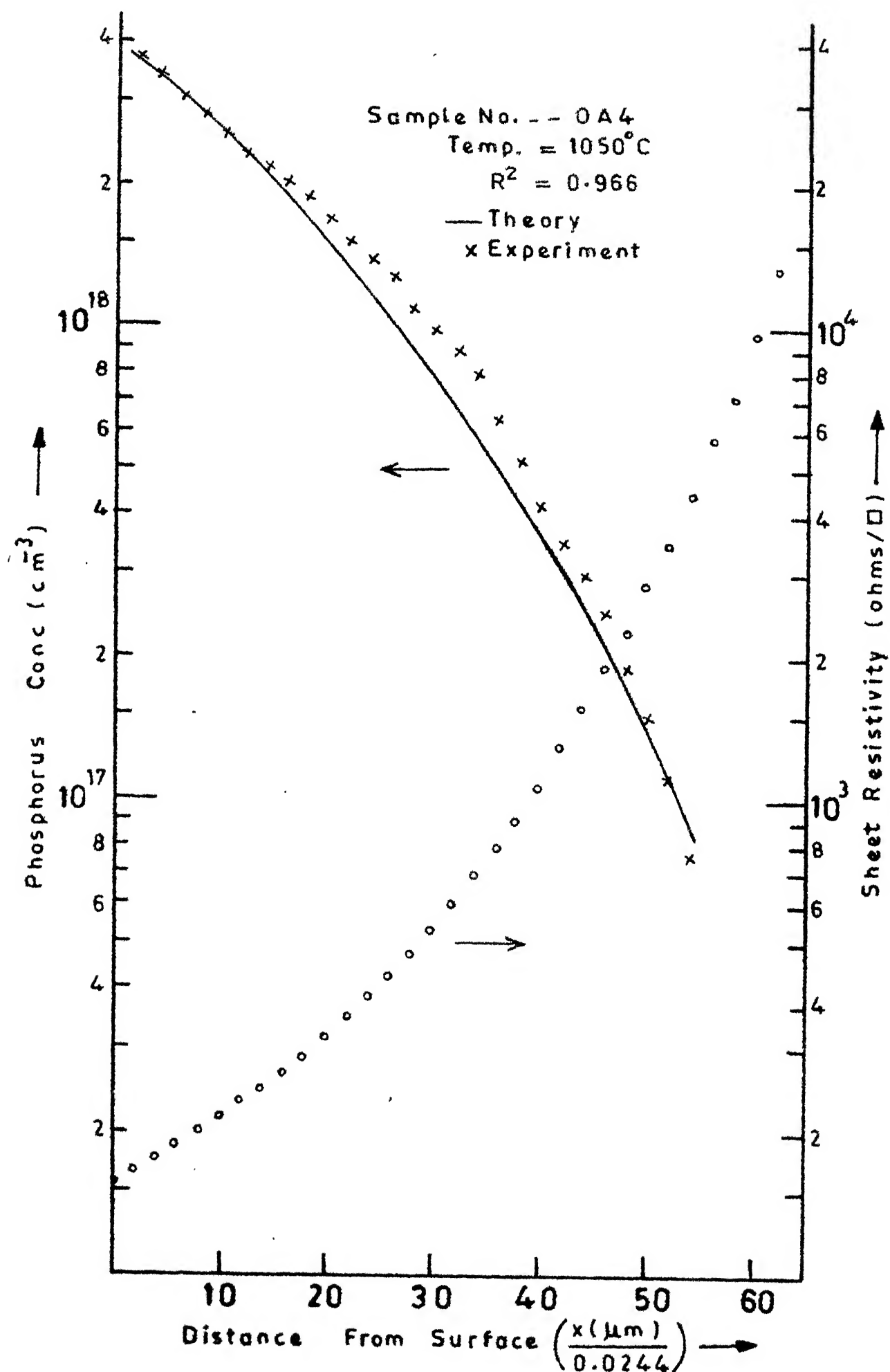Distribution in Silicon.

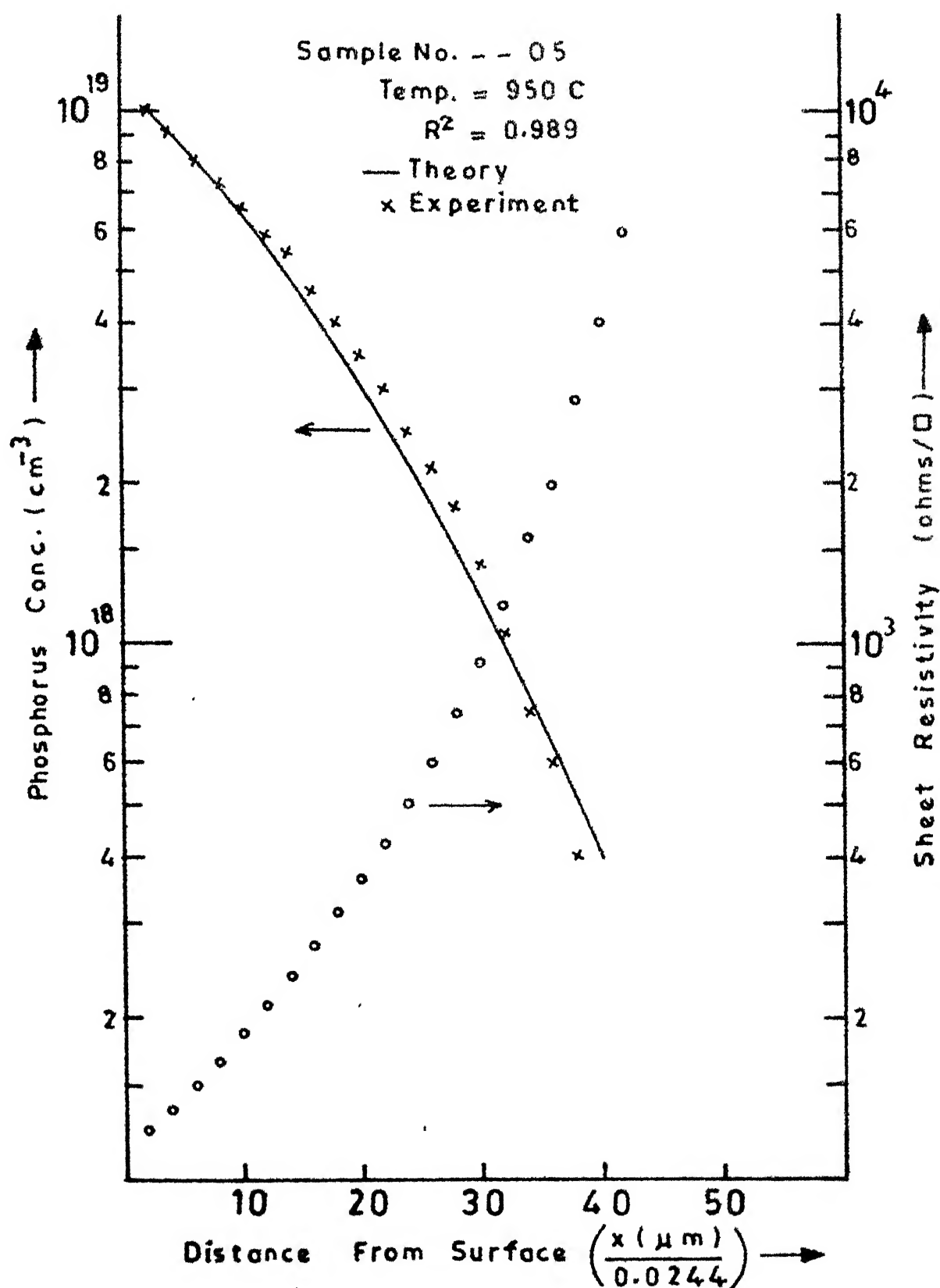FIG.3.9a Sheet Resistivity and Phosphorus Distribution in Silicon

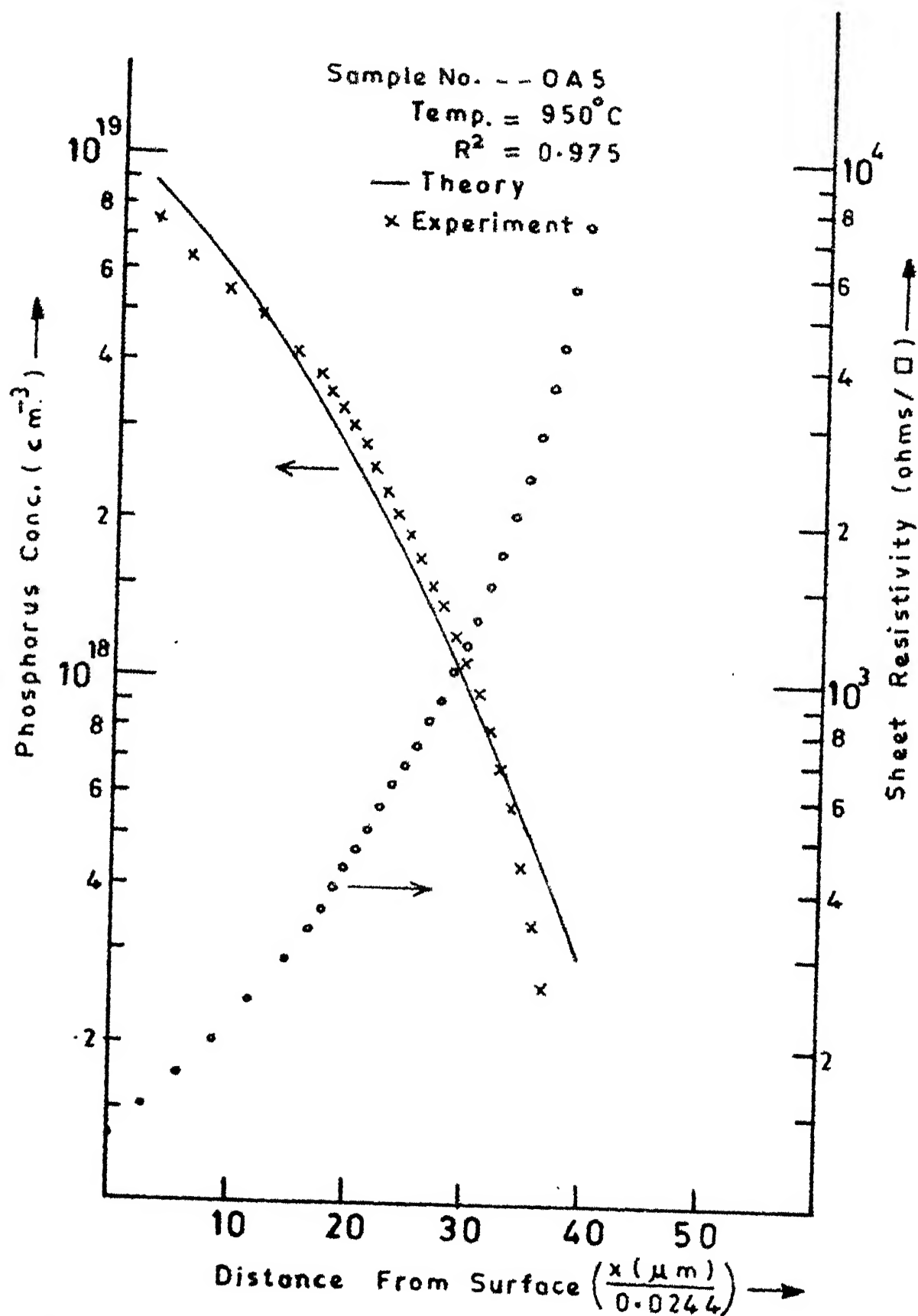FIG.3.10 Sheet Resistivity and Phosphorus Distribution in Silicon.

FIG.3.10a Sheet Resistivity and Phosphorus Distribution in Silicon.

FIG.3.11 Sheet Resistivity and Phosphorus Distribution in Silicon.

FIG.3.11 a Sheet Resistivity and Phosphorus
Distribution in Silicon.

FIG. 3.12 Sheet Resistivity and Phosphorus Distribution in Silicon.

Sample No.—NC 1
Temp. $= 1150°C$
$R^2 = 0.996$

— Theory
x Experiment

FIG. 3.13 Sheet Resistivity and Phosphorus Distribution in Silicon.

FIG. 3.14 Sheet Resistivity and Phosphorus Distribution in Silicon.

FIG. 3.15 Sheet Resistivity and Phosphorus Distribution in Silicon.

FIG. 3.15a Sheet Resistivity and Phosphorus Distribution in Silicon.
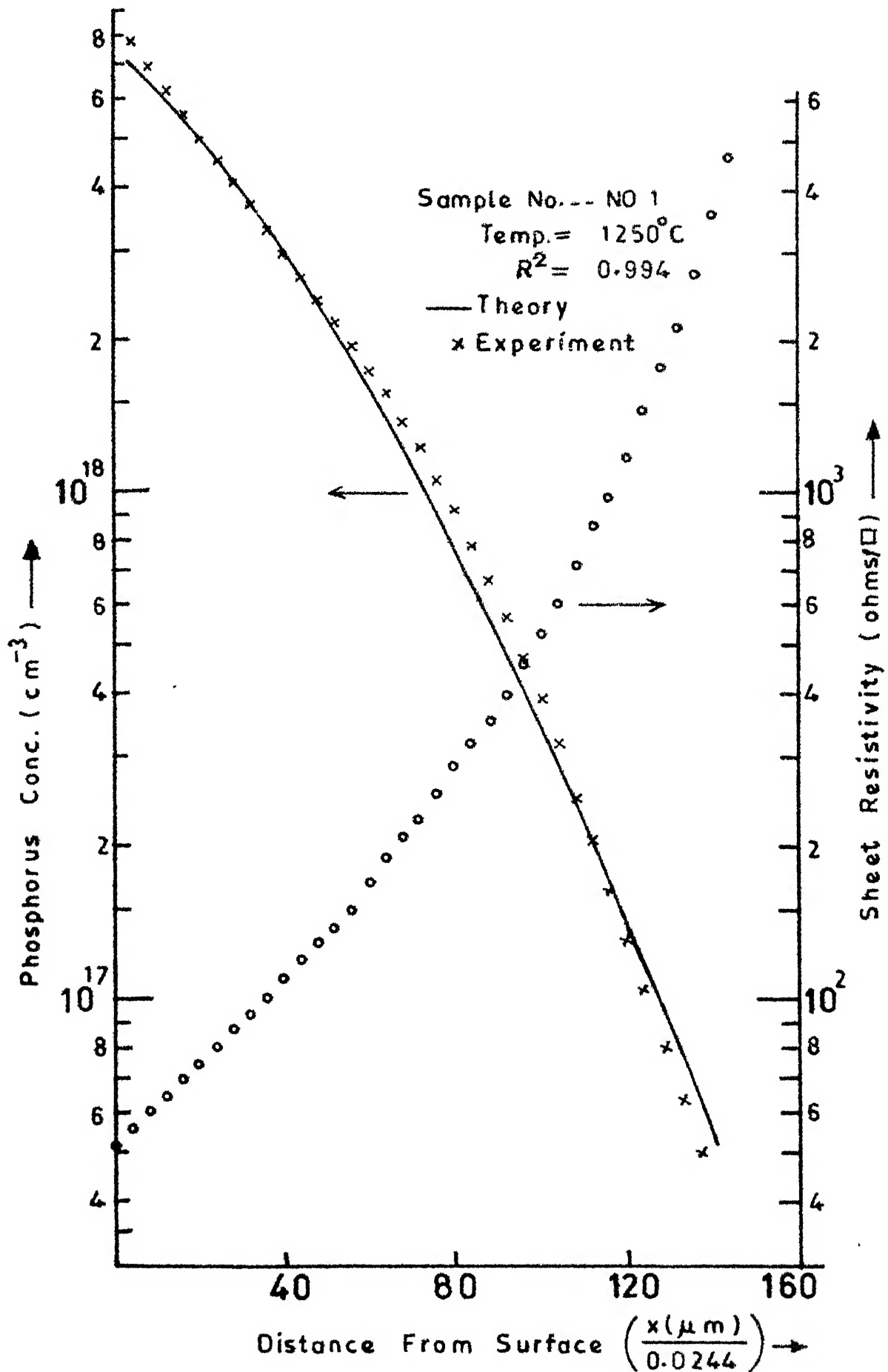
FIG. 3.16 Sheet Resistivity and Phosphorus Distribution in Silicon.

FIG. 3.16 a   Sheet Resistivity and Phosphorus
Distribution   in   Silicon.

FIG.3.17 Sheet Resistivity and Phosphorus Distribution in Silicon.

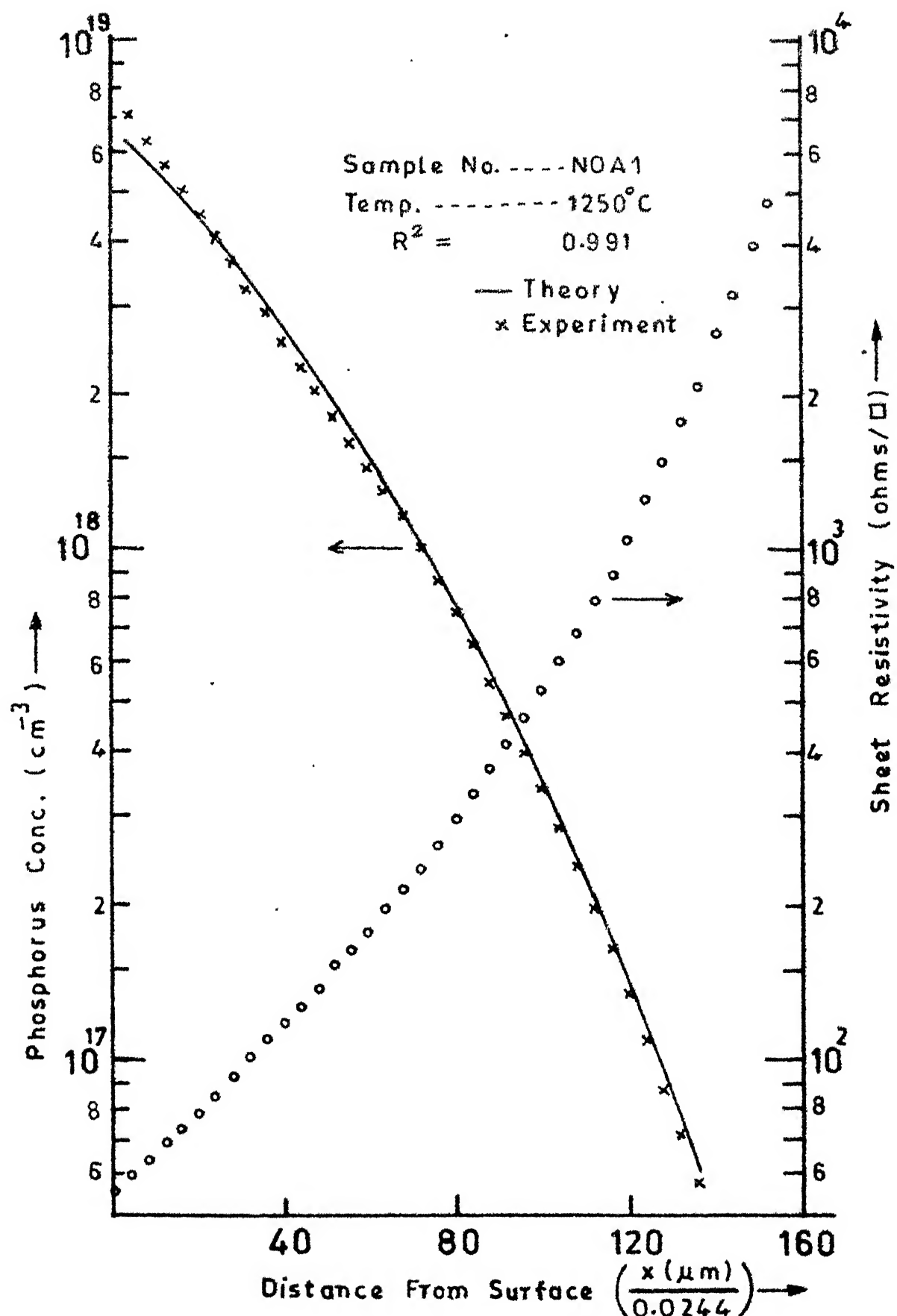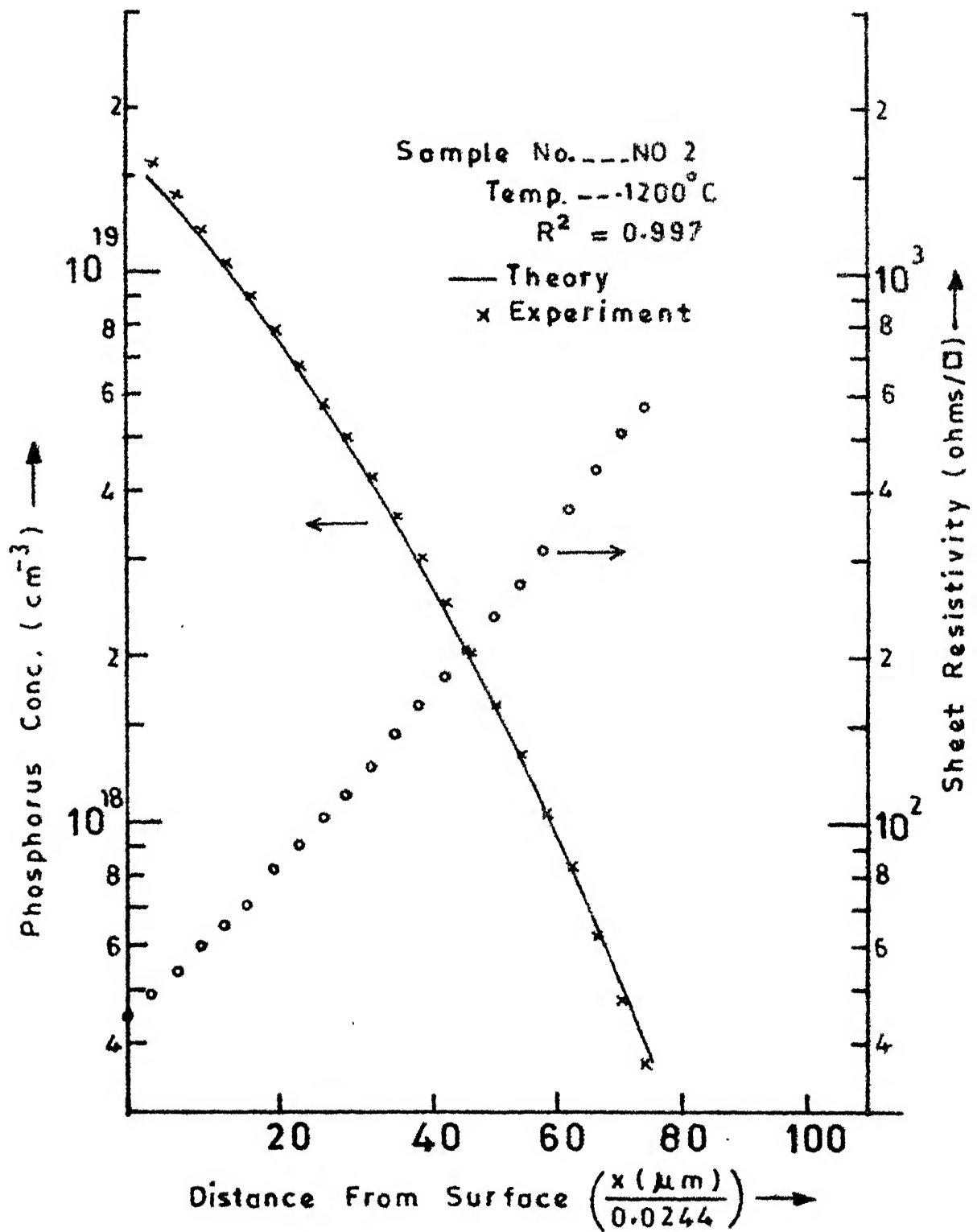FIG.3.17a Sheet Resistivity and Phosphorus Distribution in Silicon.

FIG. 3.18 Sheet Resistivity and Phosphorus Distribution in Silicon.
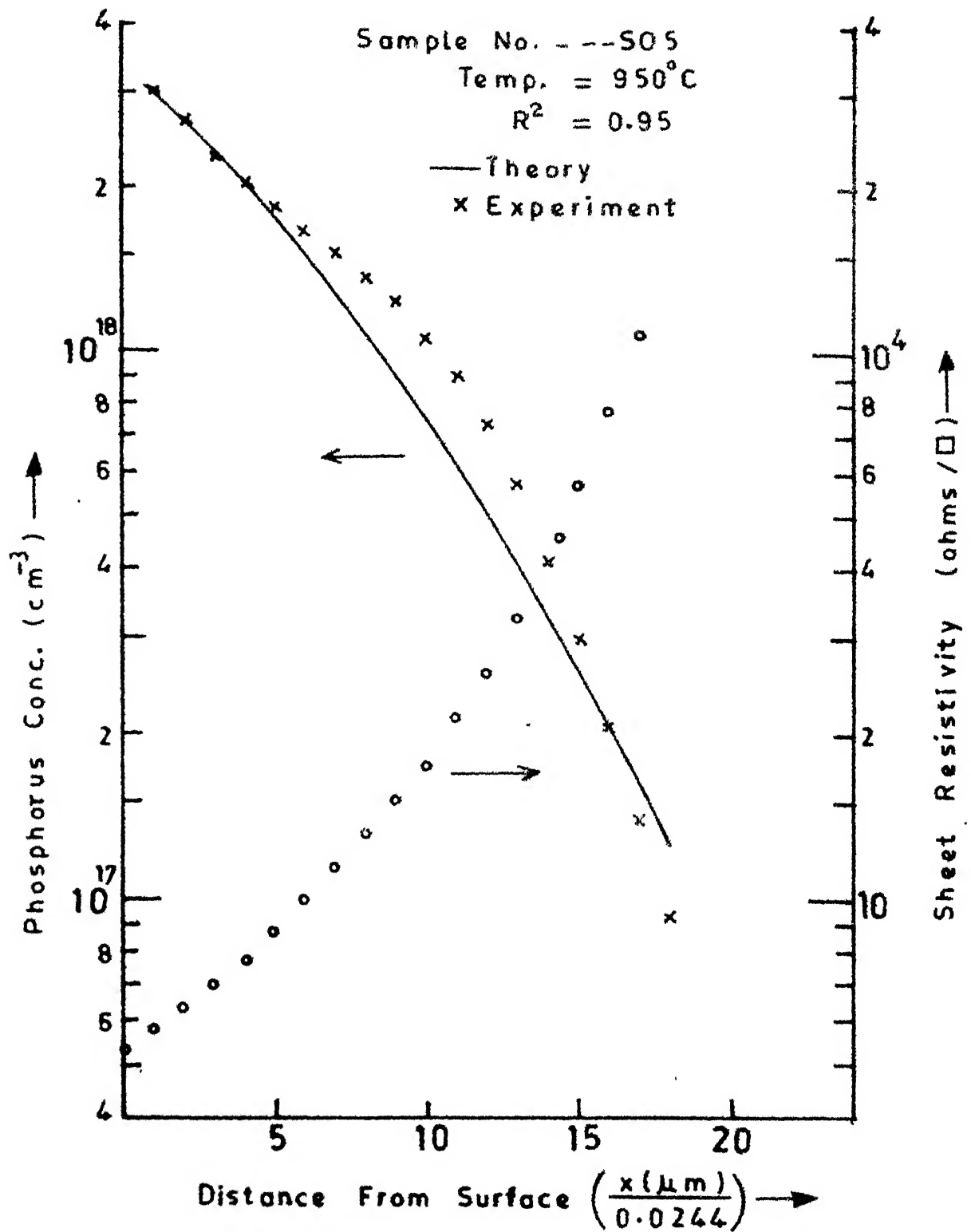
FIG.3.19 Sheet Resistivity and Phosphorus Distribution in Silicon.
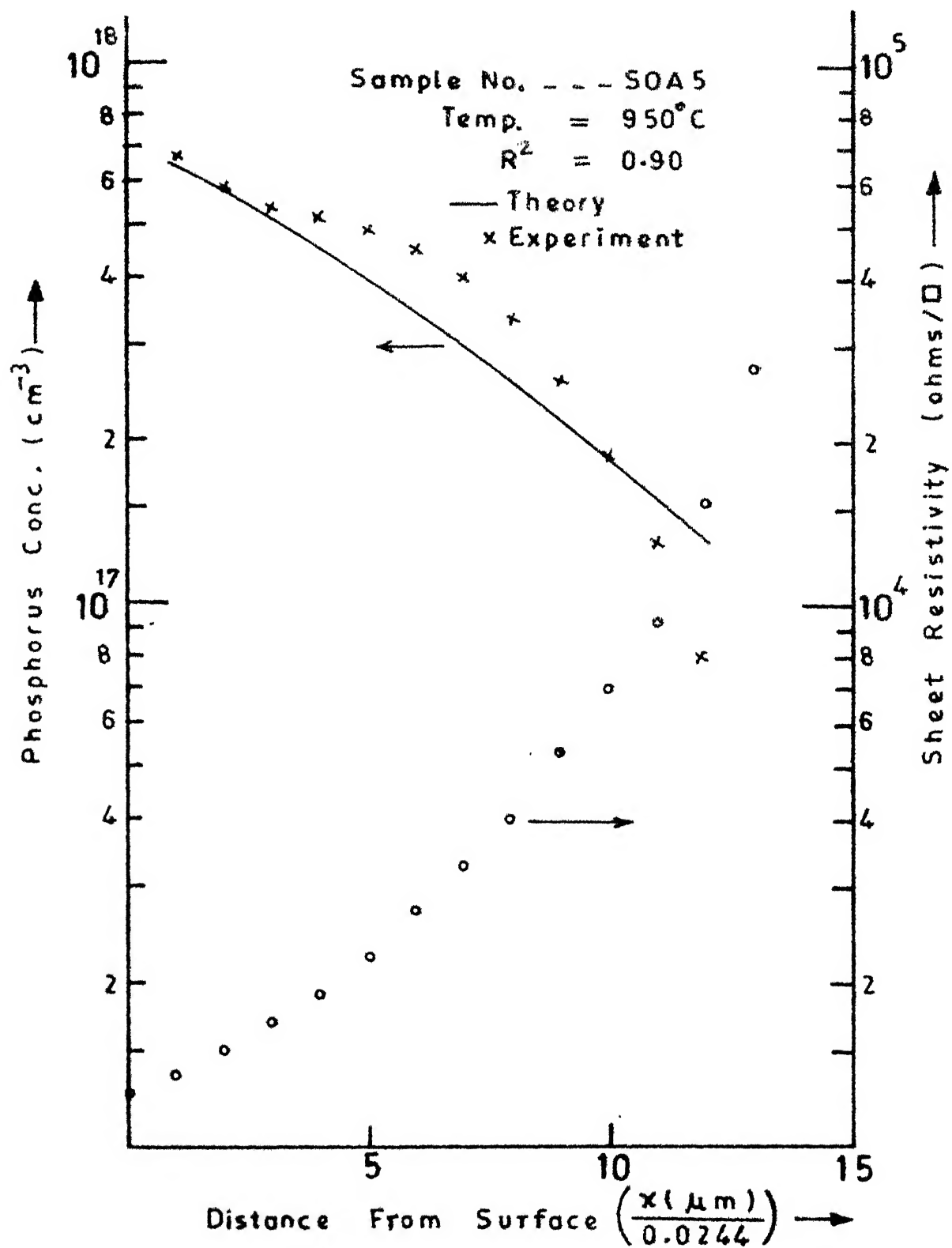
FIG.3.19a Sheet Resistivity and Phosphorus
Distribution in Silicon.
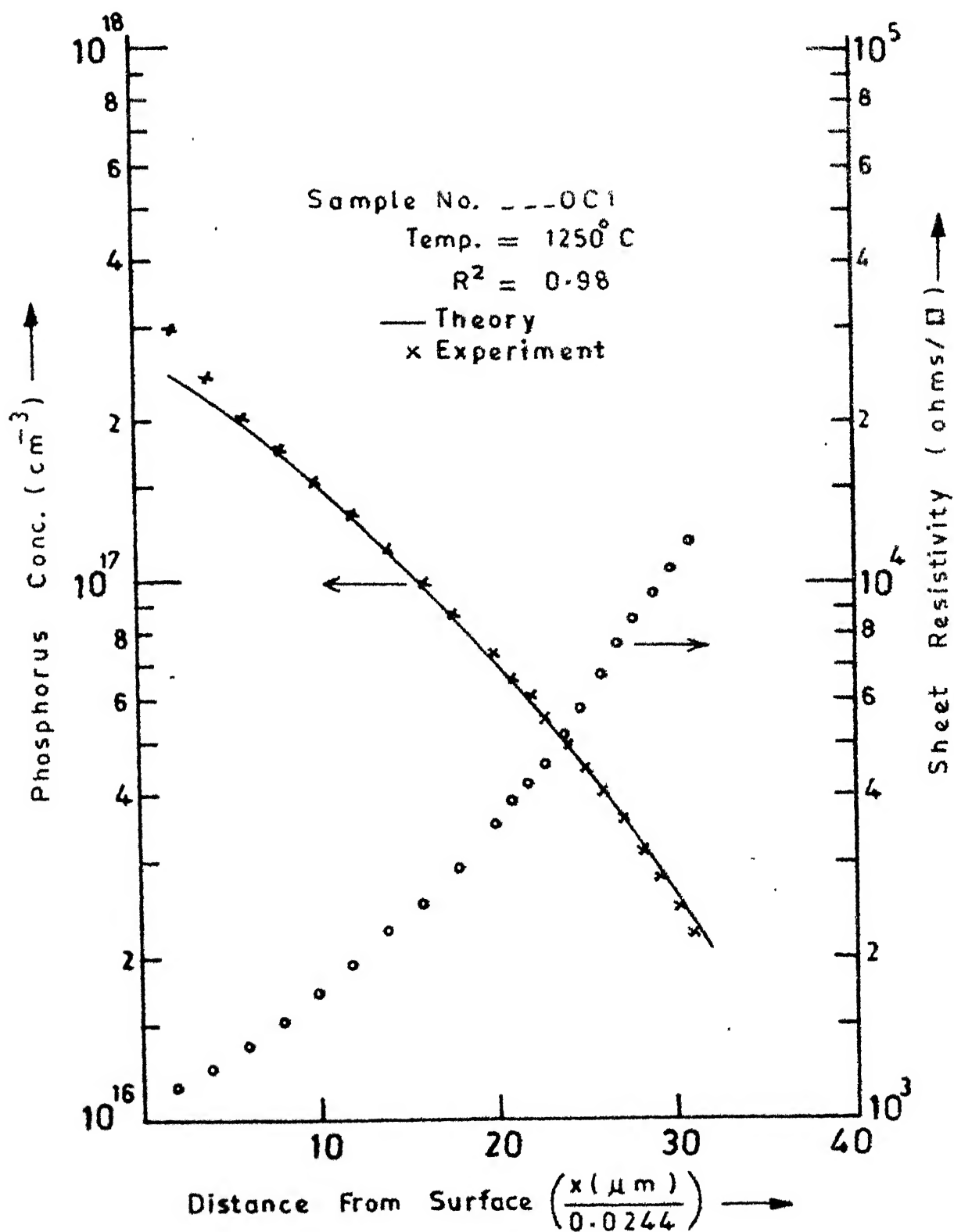
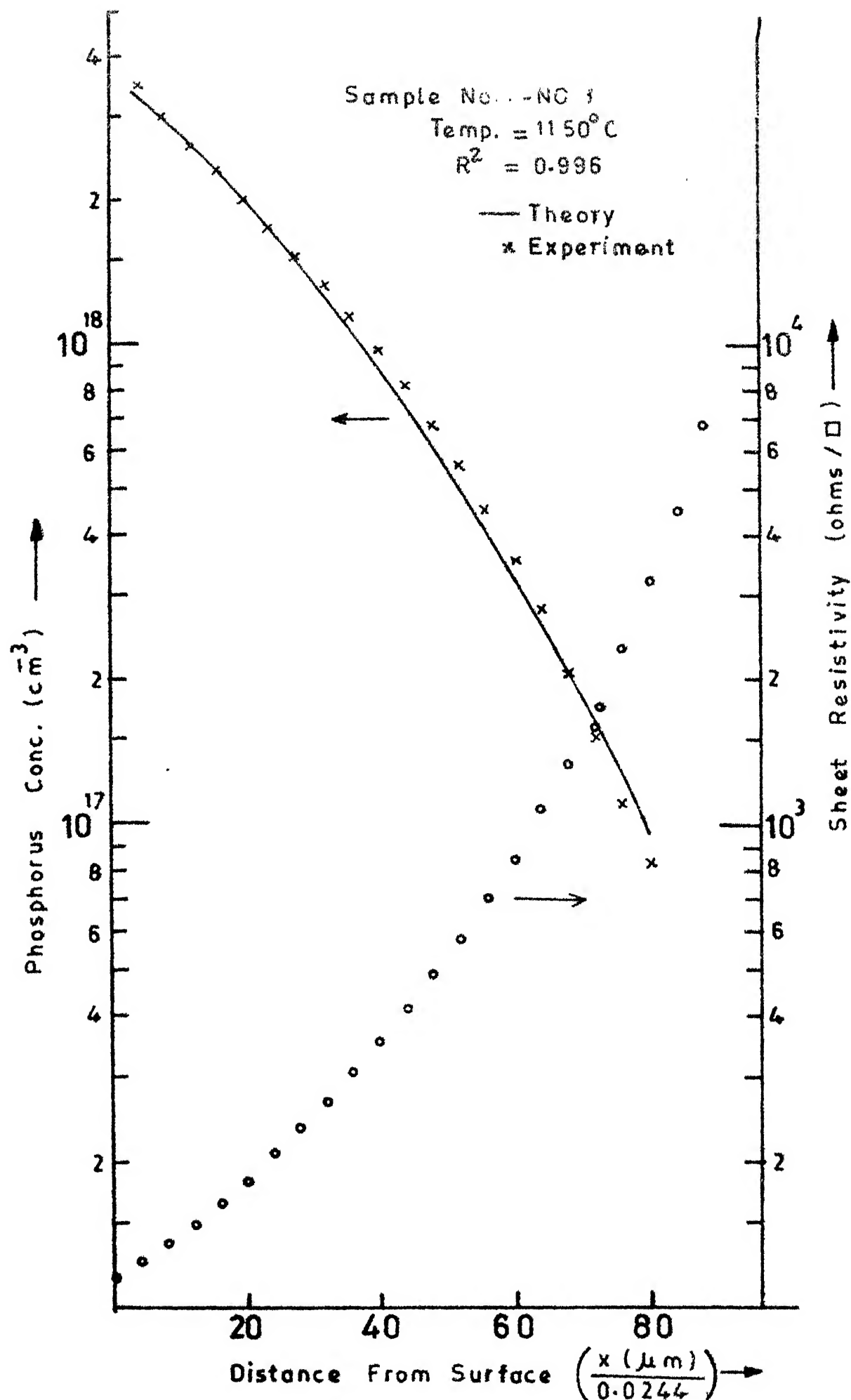FIG.3.20 Sheet Resistivity and Phosphorus Distribution in Silicon.
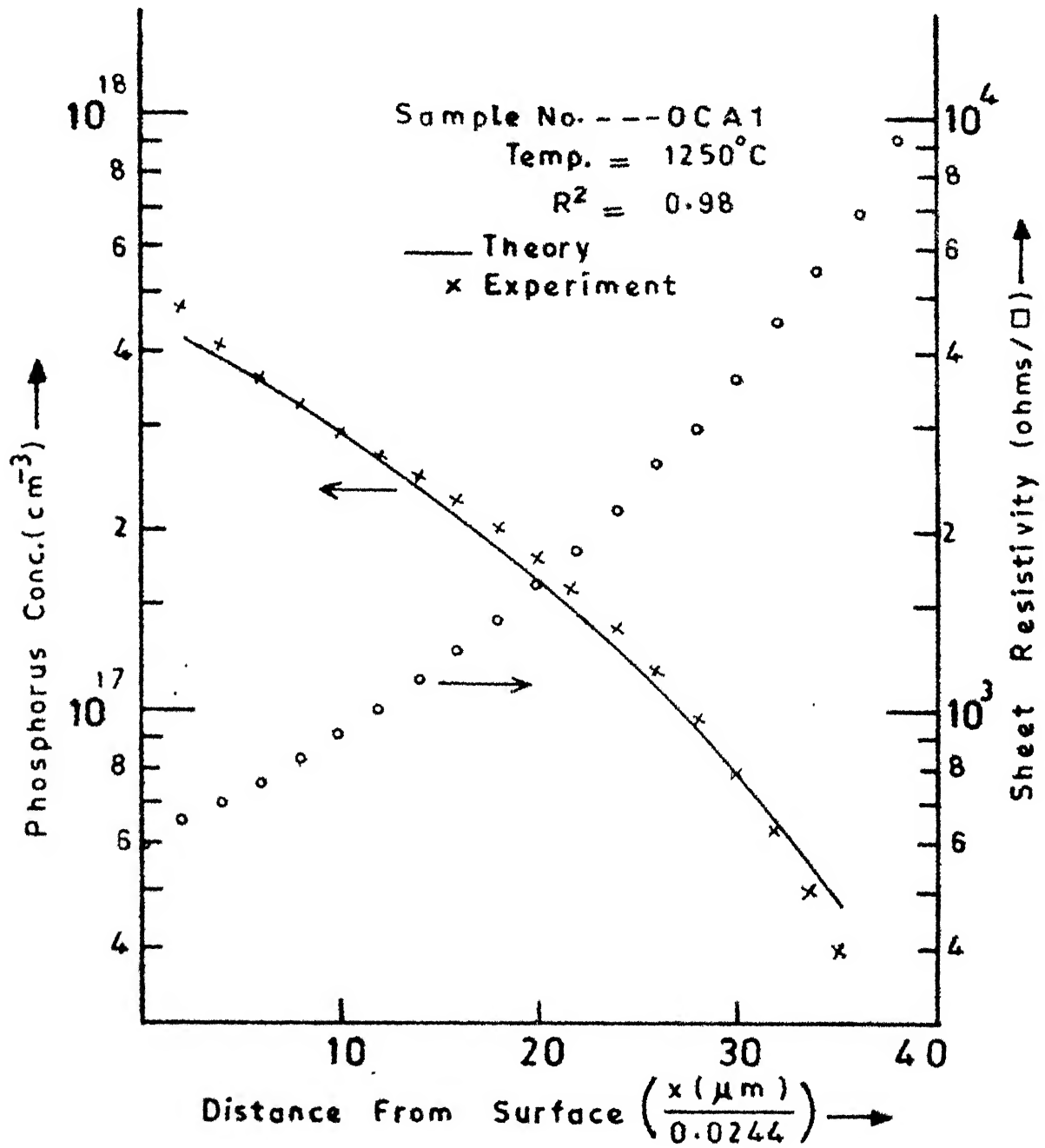
FIG.3.20a Sheet Resistivity and Phosphorus Distribution in Silicon.
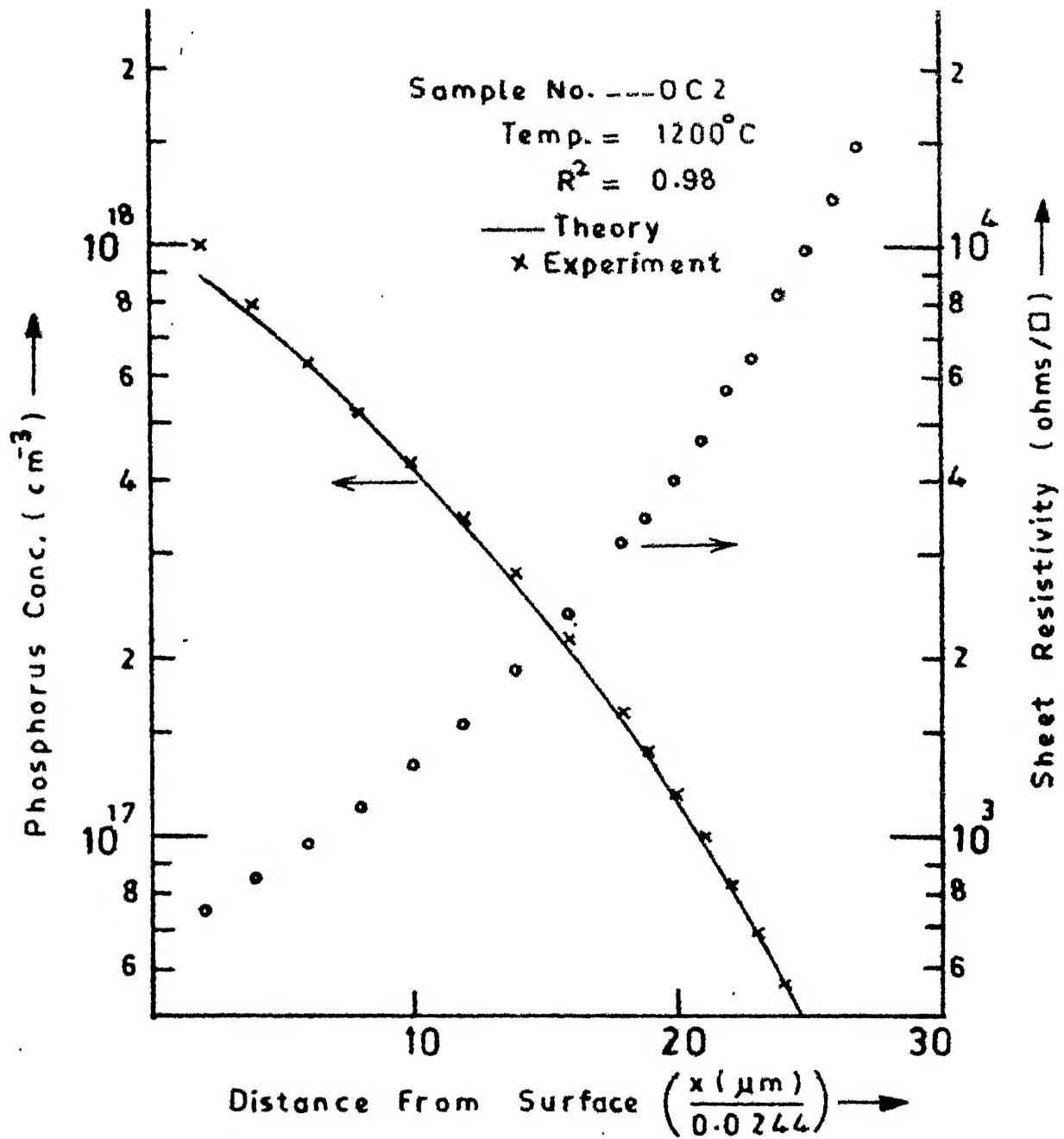
FIG. 3.21 Sheet Resistivity and Phosphorus Distribution in Silicon.
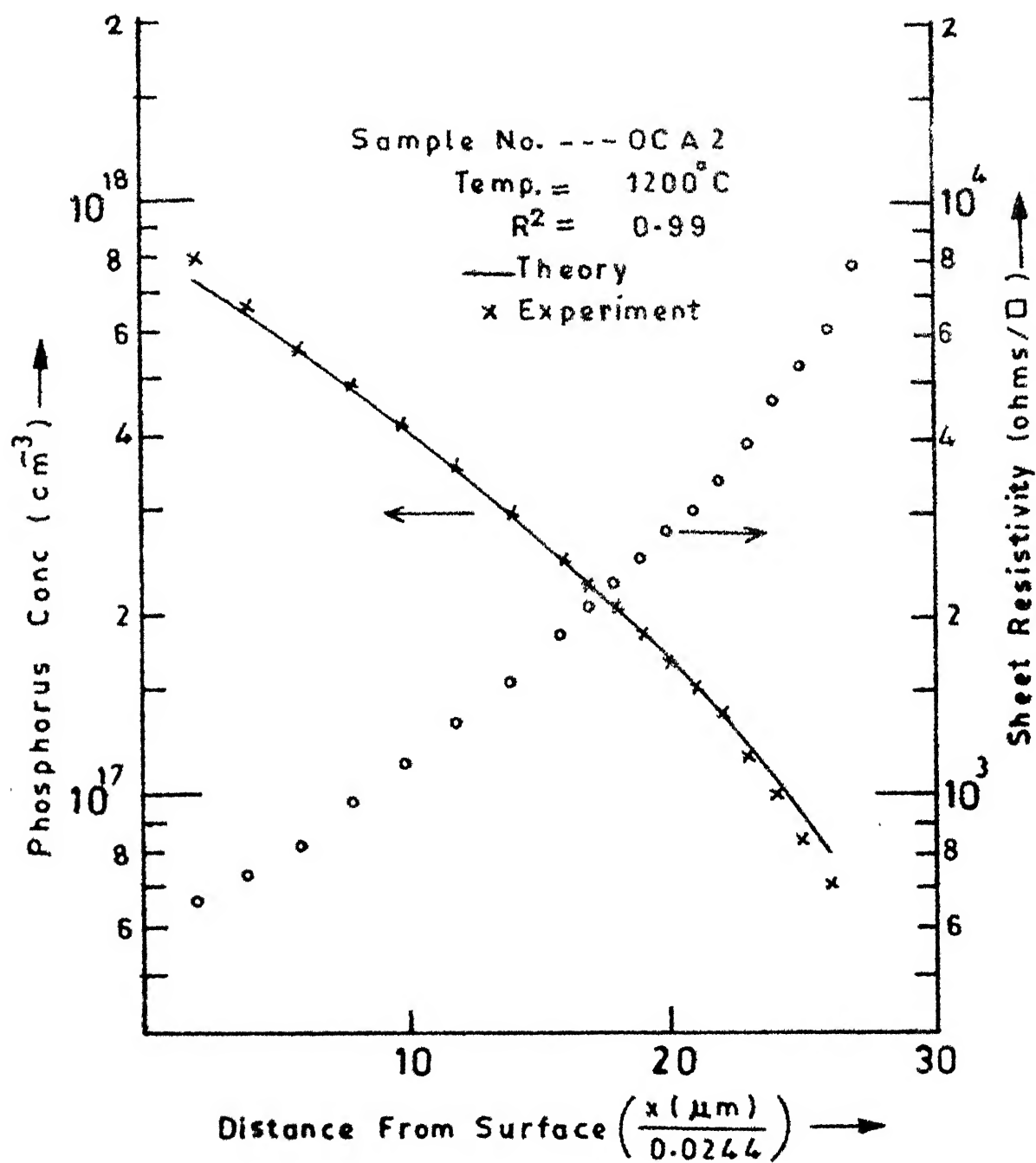
FIG.3.21a Sheet Resistivity and Phosphorus Distribution in Silicon.
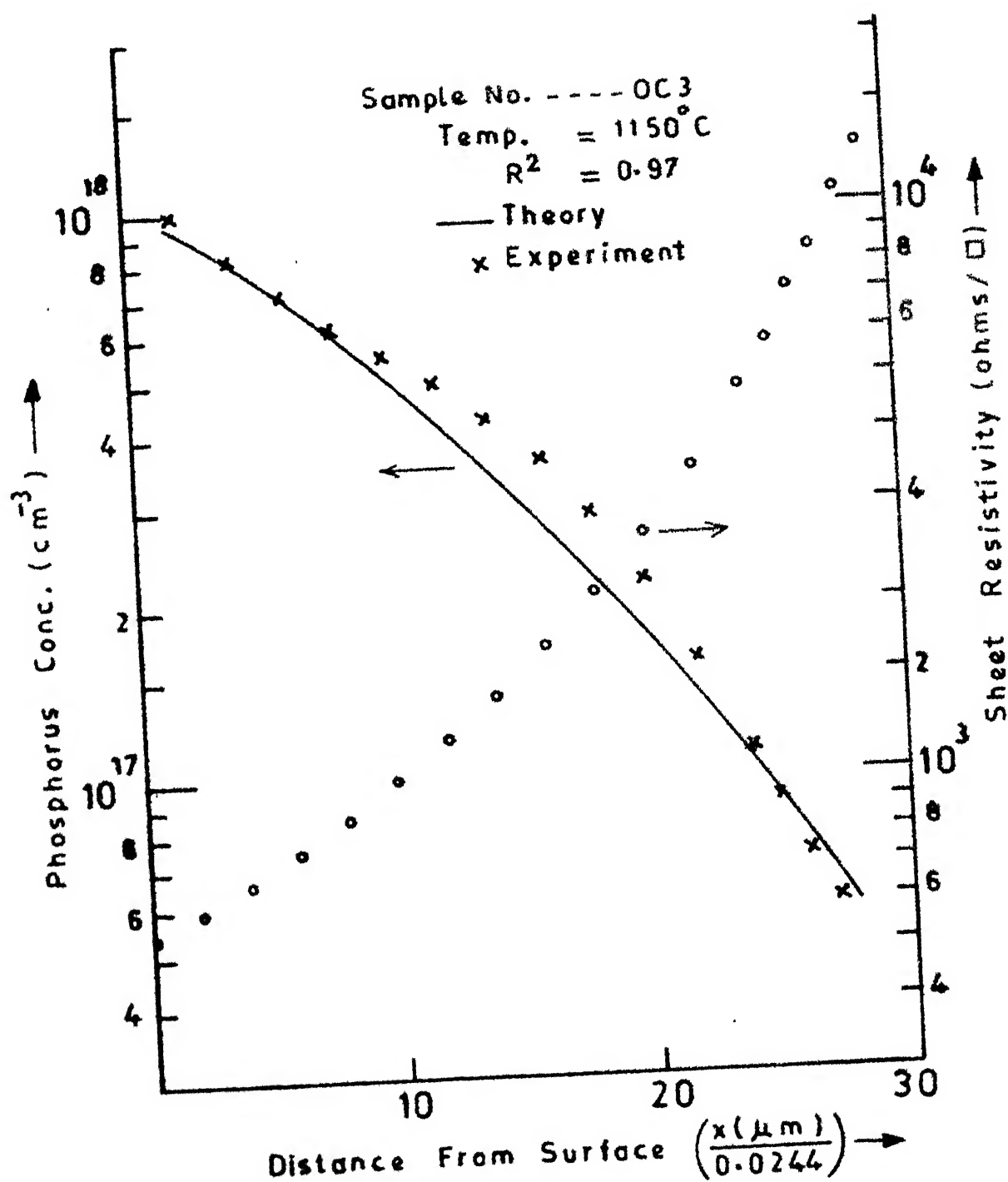
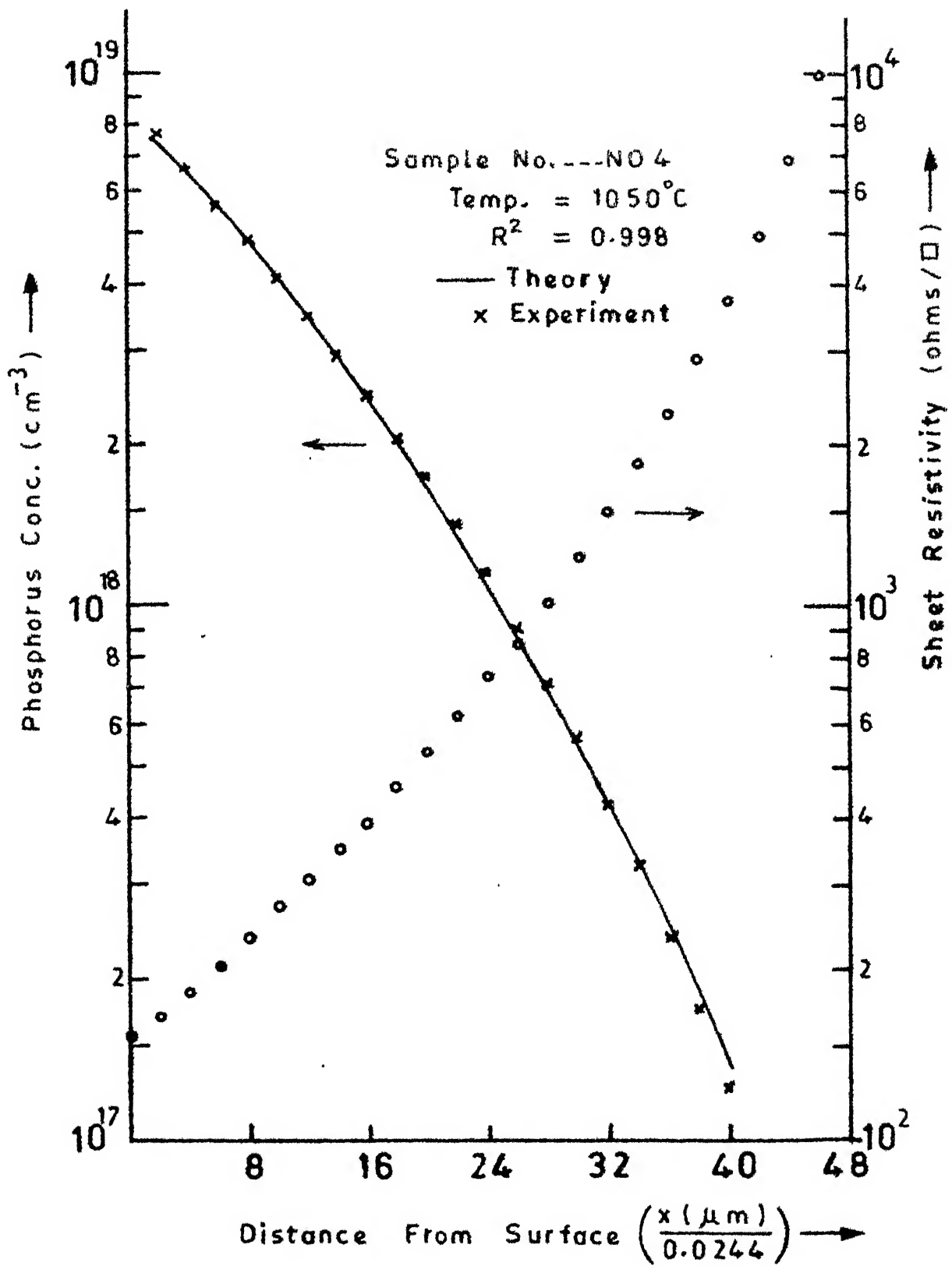FIG.3.22 Sheet Resistivity and Phosphorus Distribution in Silicon.
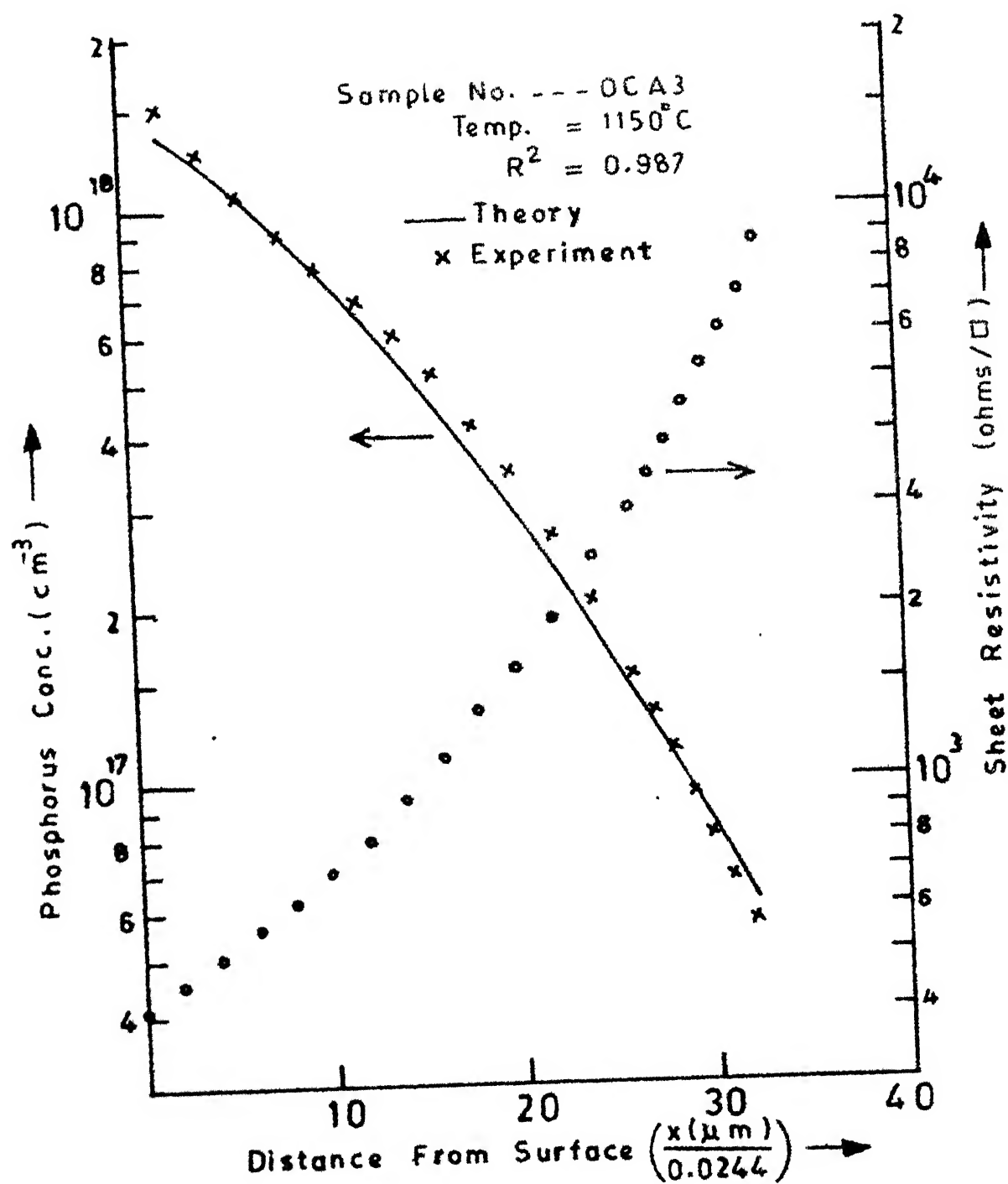
FIG.3.22 a Sheet Resistivity and Phosphorus
Distribution in Silicon.
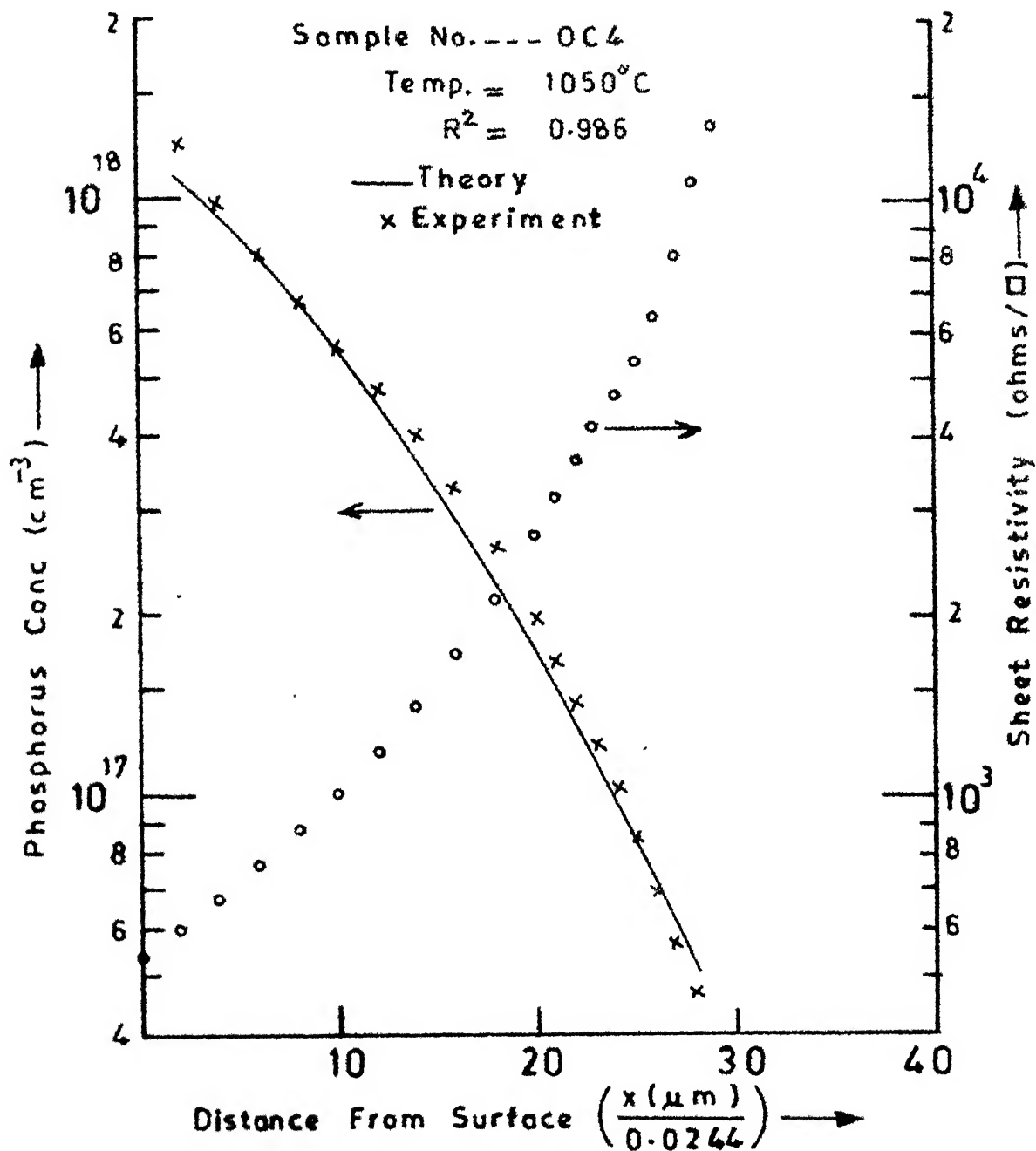
FIG.3.23 Sheet Resistivity and Phosphorus Distribution in Silicon
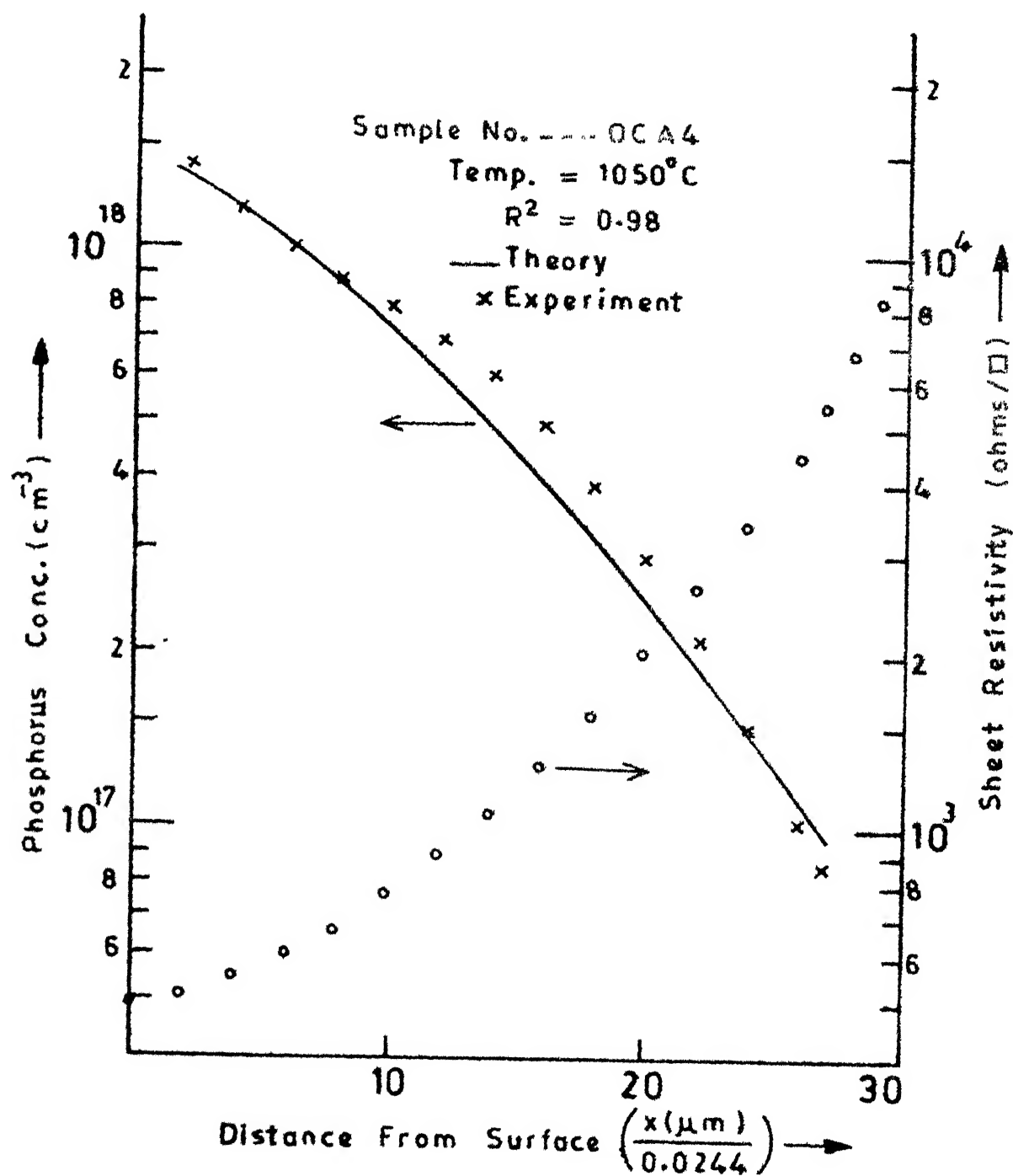
FIG.3.23a Sheet Resistivity and Phosphorus Distribution in Silicon.
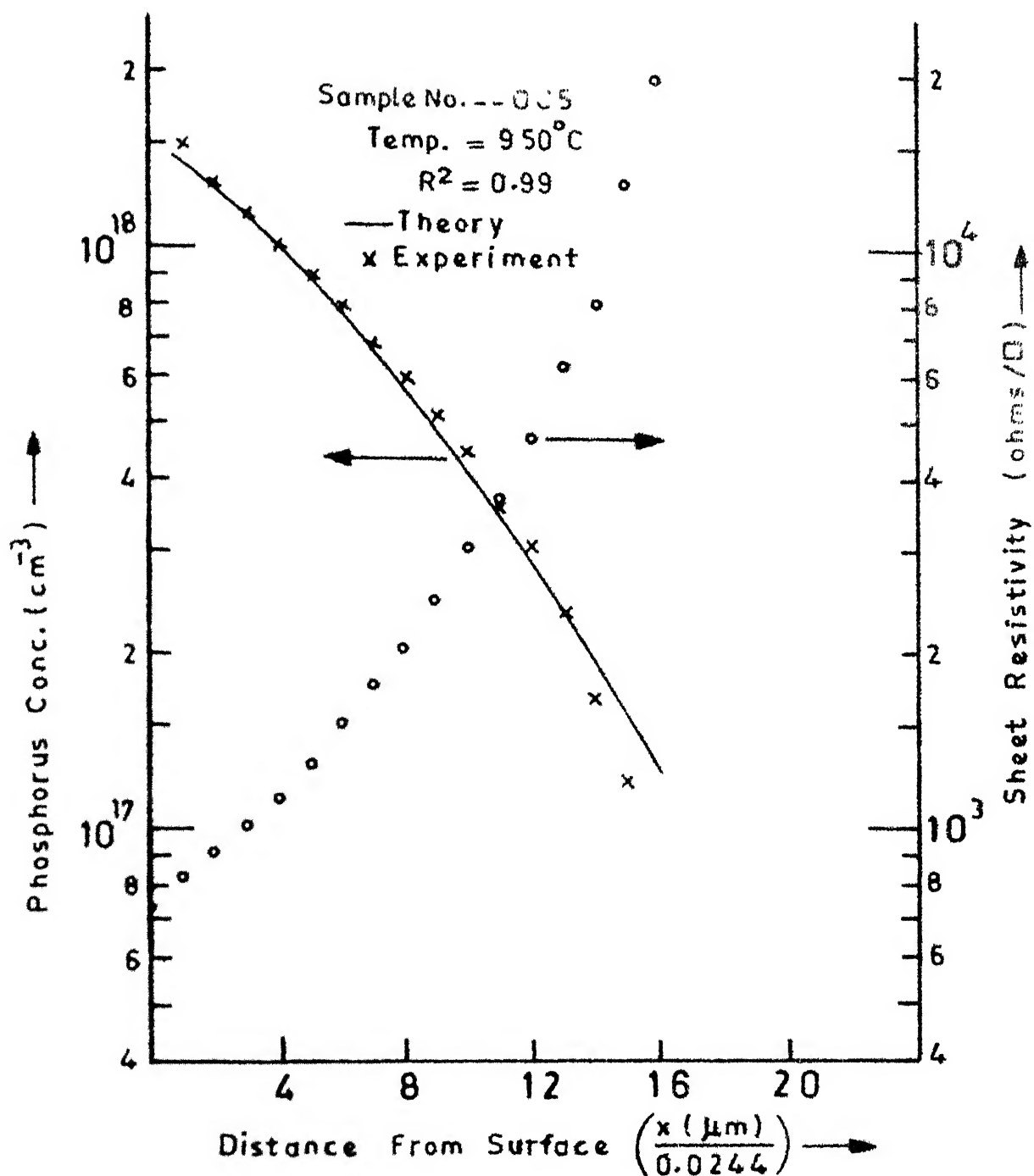
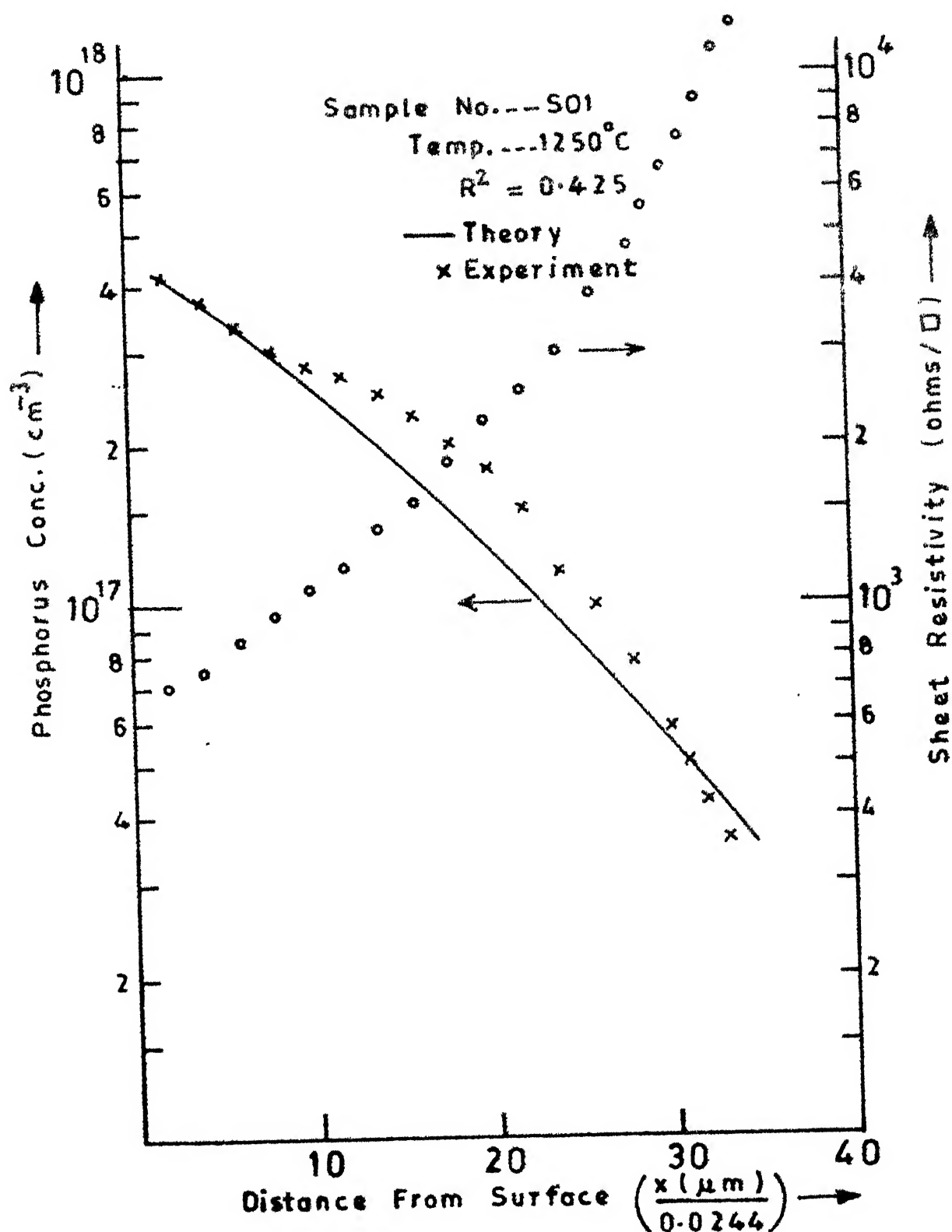FIG.3.24 Sheet Resistivity and Phosphorus Distribution in Silicon.

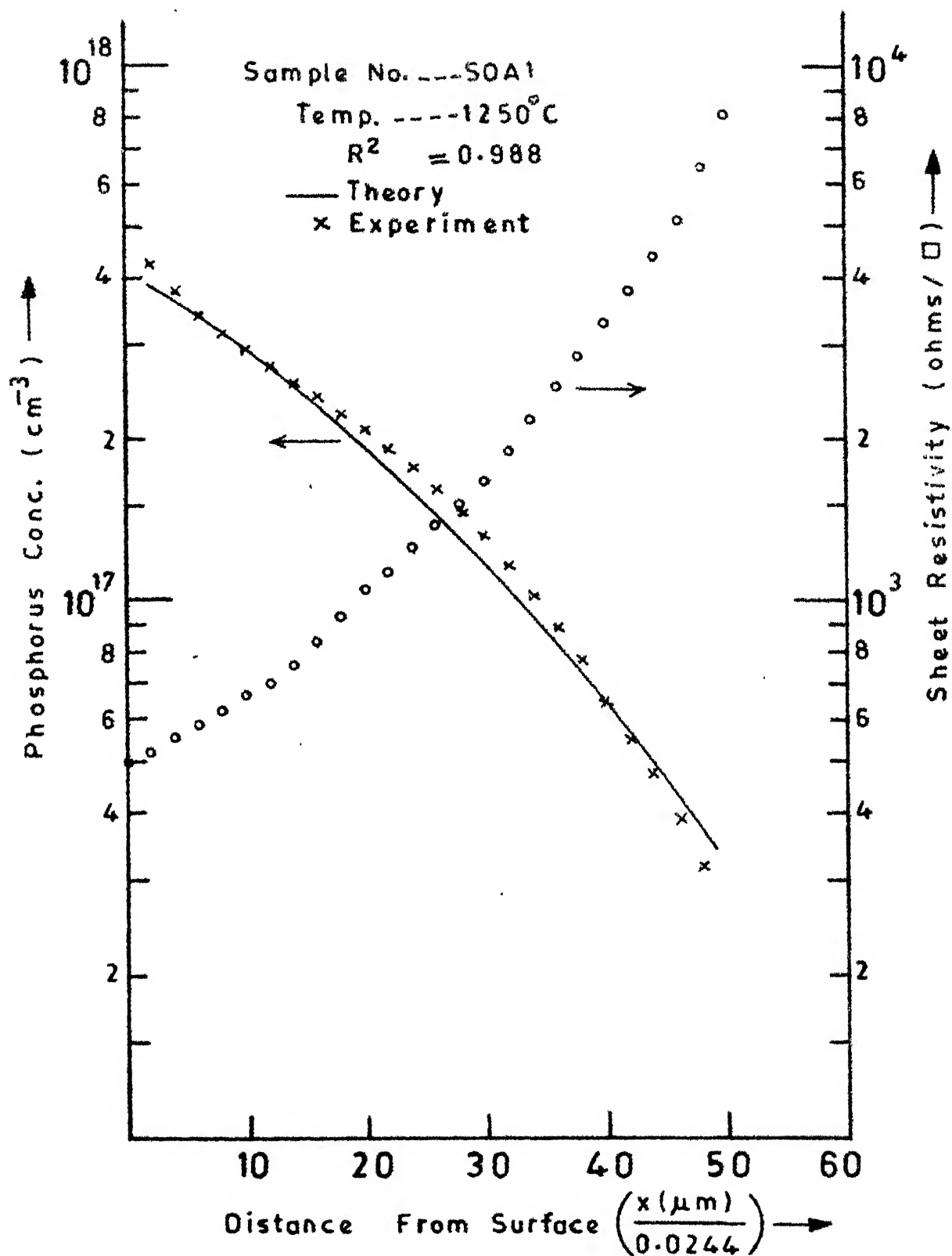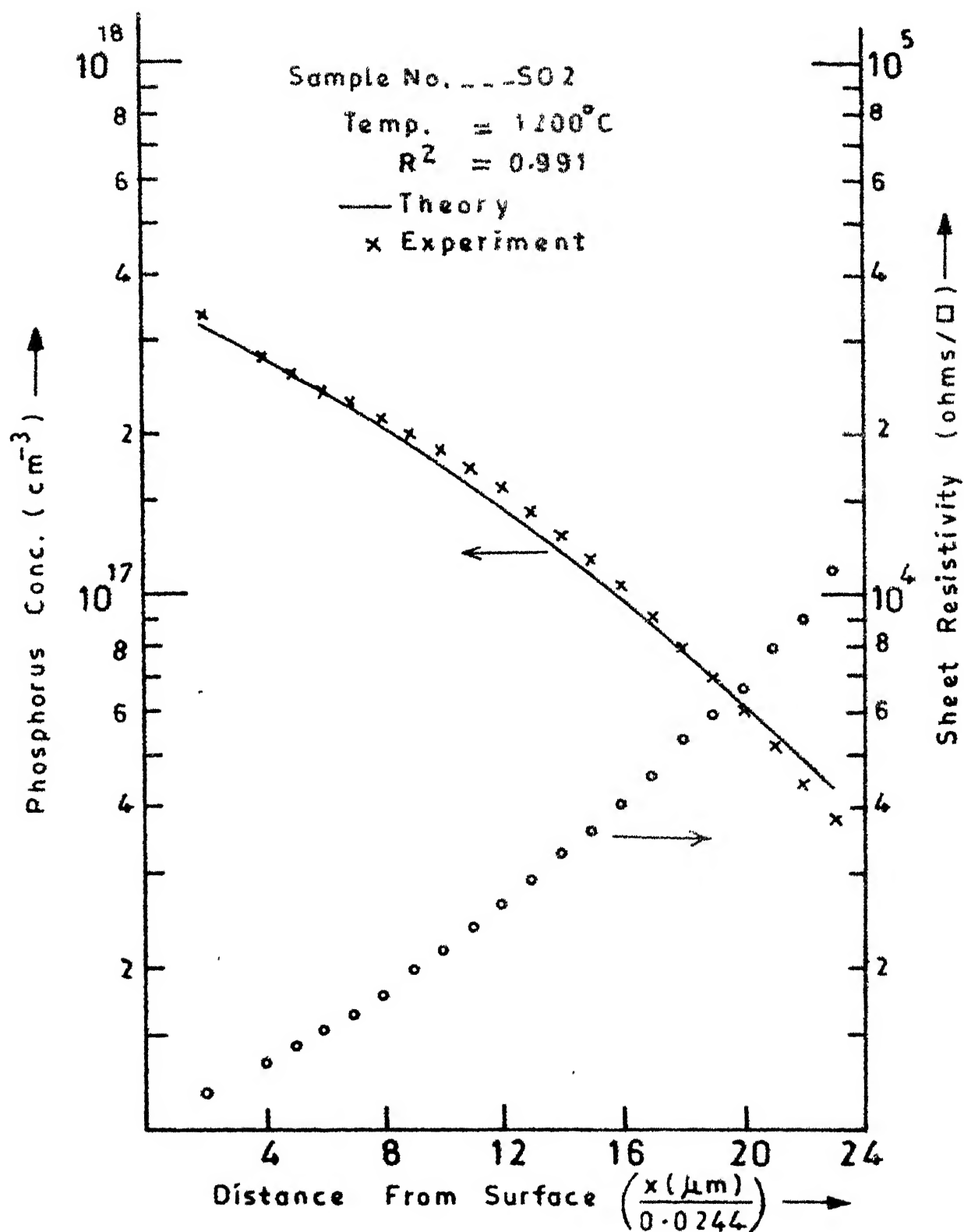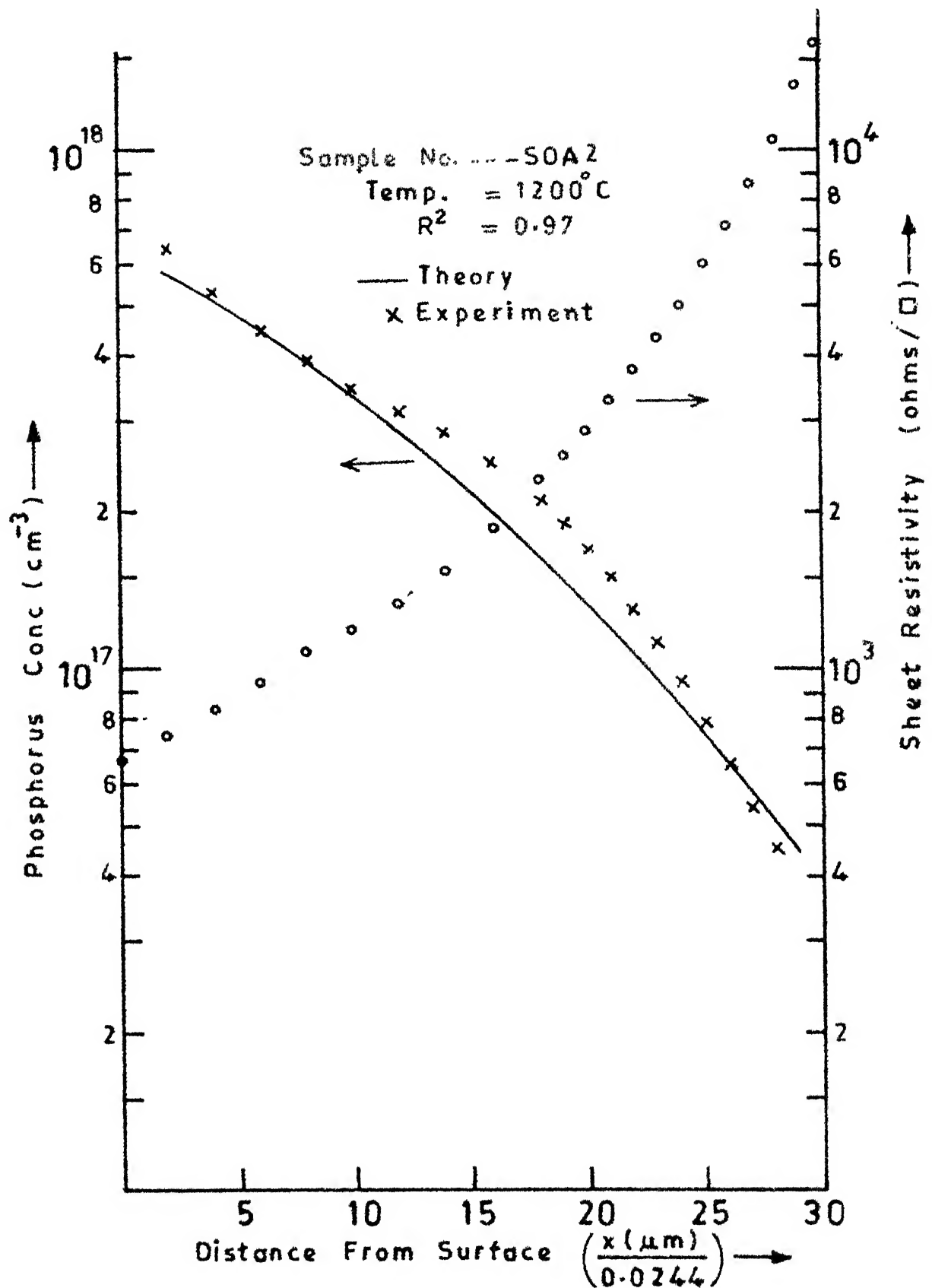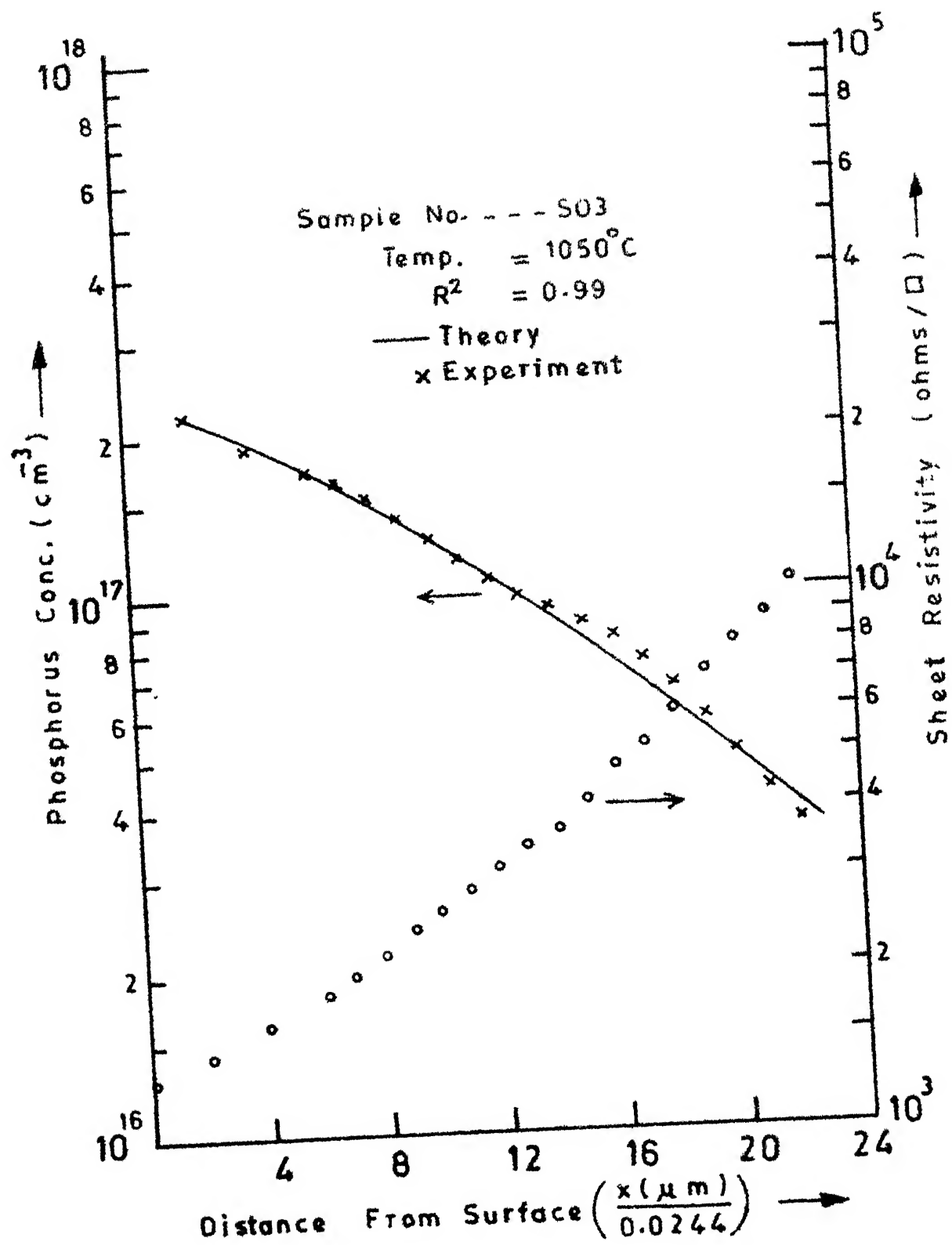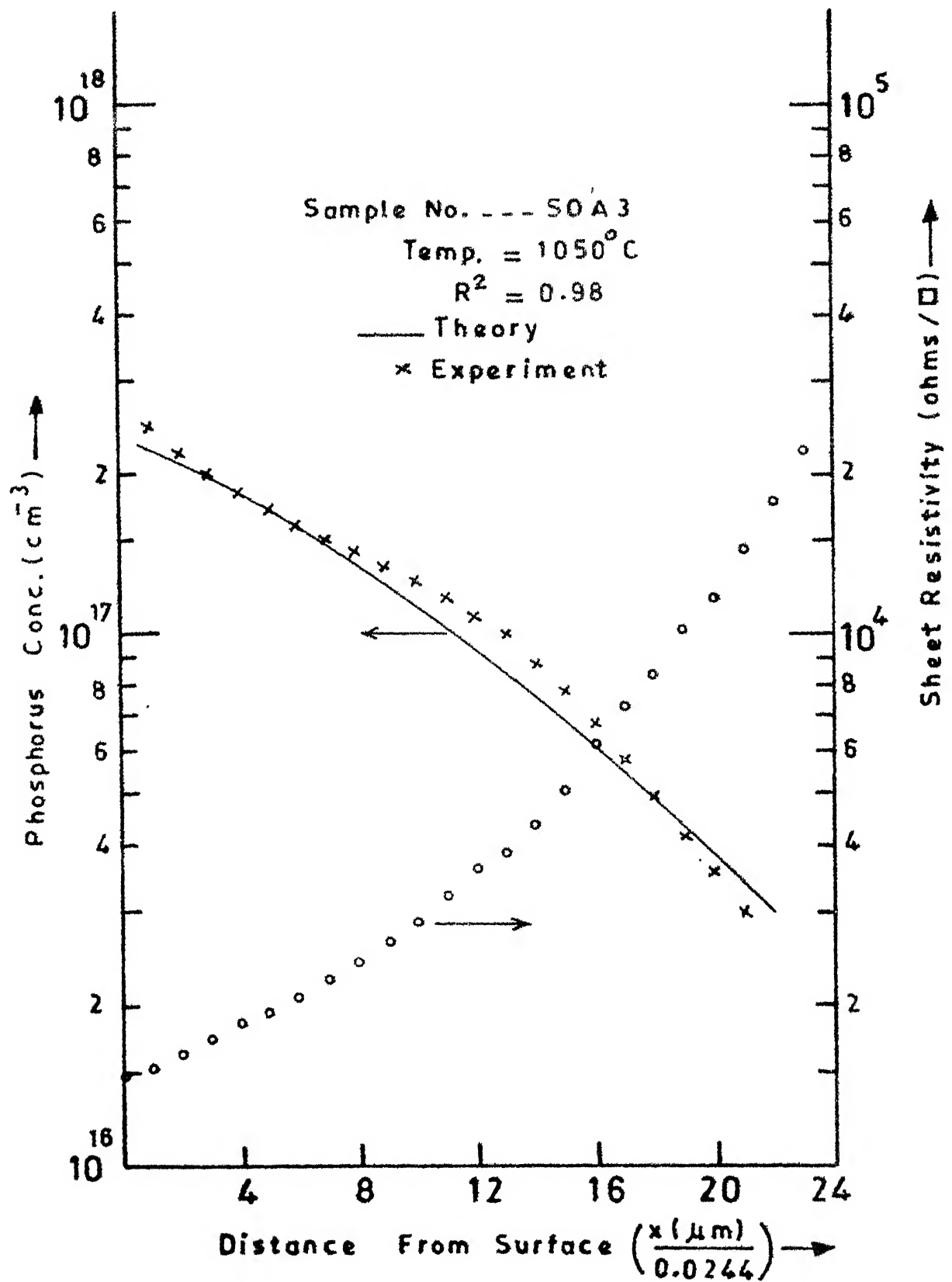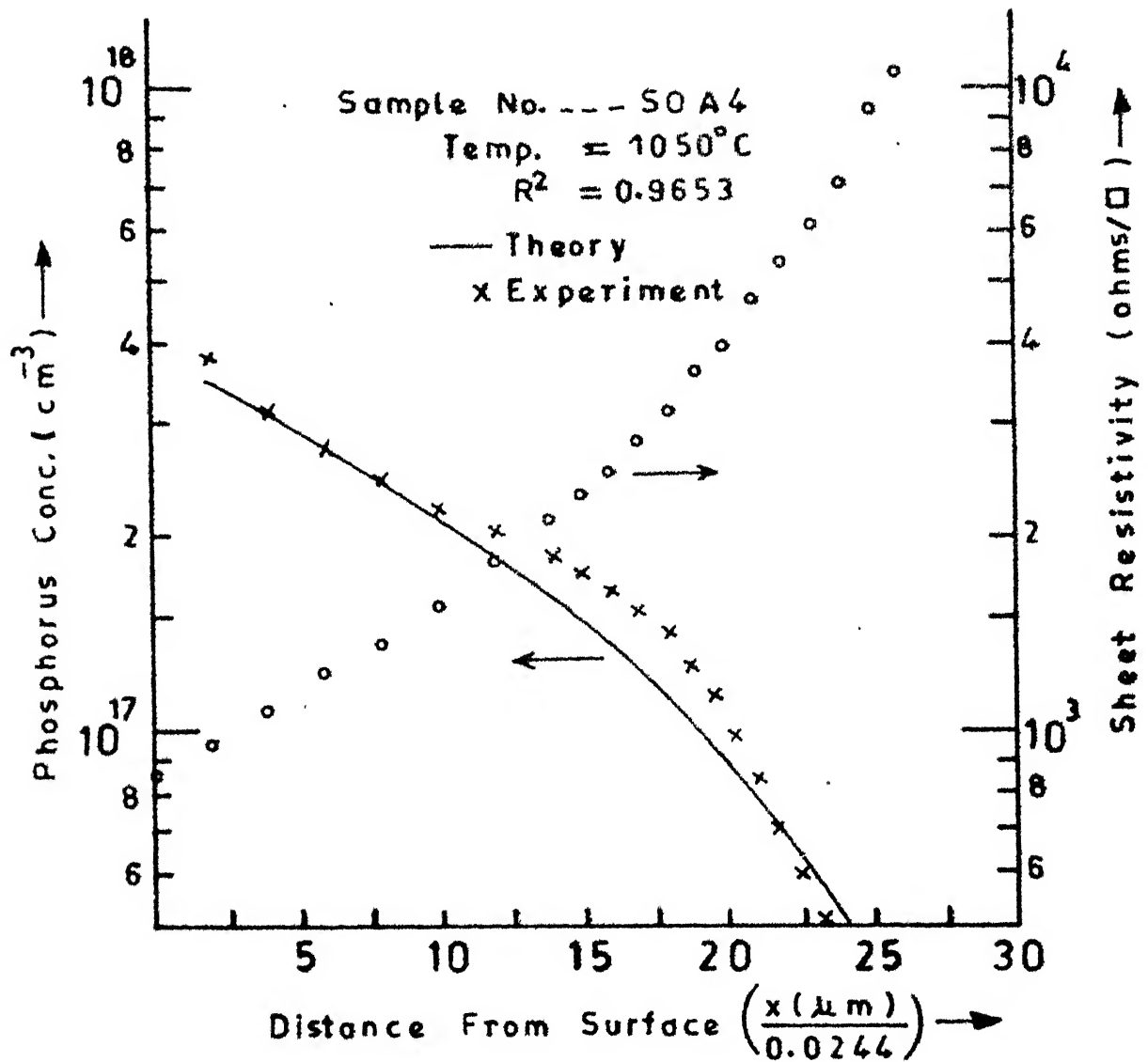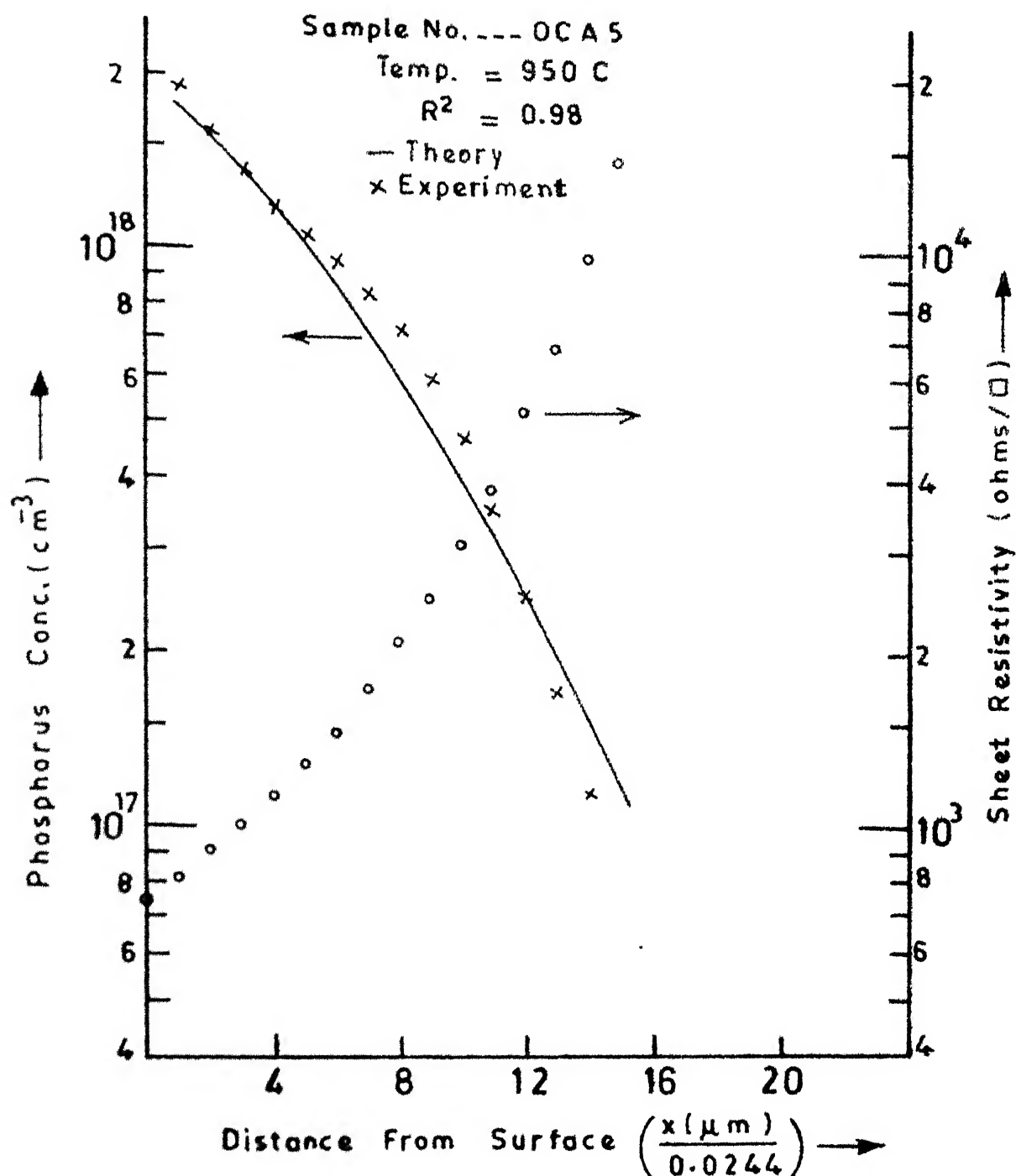FIG.3.24a Sheet Resistivity and Phosphorus Distribution in Silicon.

contains a small amount of oxygen and therefore a thin PSG layer is expected to be present. The impurity therefore enters the silicon from PSG rather than from ambient. The value of 'α' determined thus, should be expected to correspond to PSG-Si interface.

The parameters A and D_2 were determined by using eqns. (2.16) and (2.21) for diffusion in inert and oxidising/chlorooxidising ambients respectively. These equations have two unknowns, A and D_2. The values of these parameters were determined by simultaneously solving the eqn. (2.16)(or eqn. (2.21)) at two points on the experimentally determined impurity distribution (see Appendix V). From the values of A and D_2, thus determined, the theoretical impurity profile was generated using eqn. (2.16) (or eqn. (2.21)). The theoretical profiles along with their experimental counterparts are plotted in Figs. 3.7-3.24a. In most cases the two profiles are in good agreement. The details of the experimental results are discussed in the following chapter.

CHAPTER IV

EXPERIMENTAL RESULTS AND DISCUSSION

4.1 PHOSPHORUS DIFFUSION IN PSG

It was mentioned in Sec. 3.5 that in case of strong oxidising ambient, the dopant concentration at silicon surface is time invariant and therefore the impurity distribution in silicon is given by,

$$C_2(z,t) = A.\text{erfc}\left(\frac{z+r\sqrt{B}t}{2\sqrt{D_2}t}\right) \qquad (4.1)$$

where,

$$A \approx \frac{m\,C_0}{1+\sqrt{\pi}\,\delta e^{\delta^2}\,\text{erf}\phi(\delta)\,F\left(\frac{r\sqrt{B}}{2\sqrt{D_2}}\right)} \qquad (4.1a)$$

$$F\left(\frac{r\sqrt{B}}{2\sqrt{D_2}}\right) = 1+mr\left[\frac{1}{\sqrt{\pi}\left(\frac{r\sqrt{B}}{2\sqrt{D_2}}\right)e^{r^2B/4D_2}\,\text{erfc}\left(\frac{r\sqrt{B}}{2\sqrt{D_2}}\right)} - 1\right] \qquad (4.1b)$$

The values of A, D_2 were determined as described in Sec. 3.5. From eqn. (4.1a), it is seen that the value of δ, and hence that of D_1, can be calculated if m, C_0, B and D_2 are known. D_1 was calculated with $m=10$ [1], measured values of C_0, B and estimated values of D_2 at each temperature.
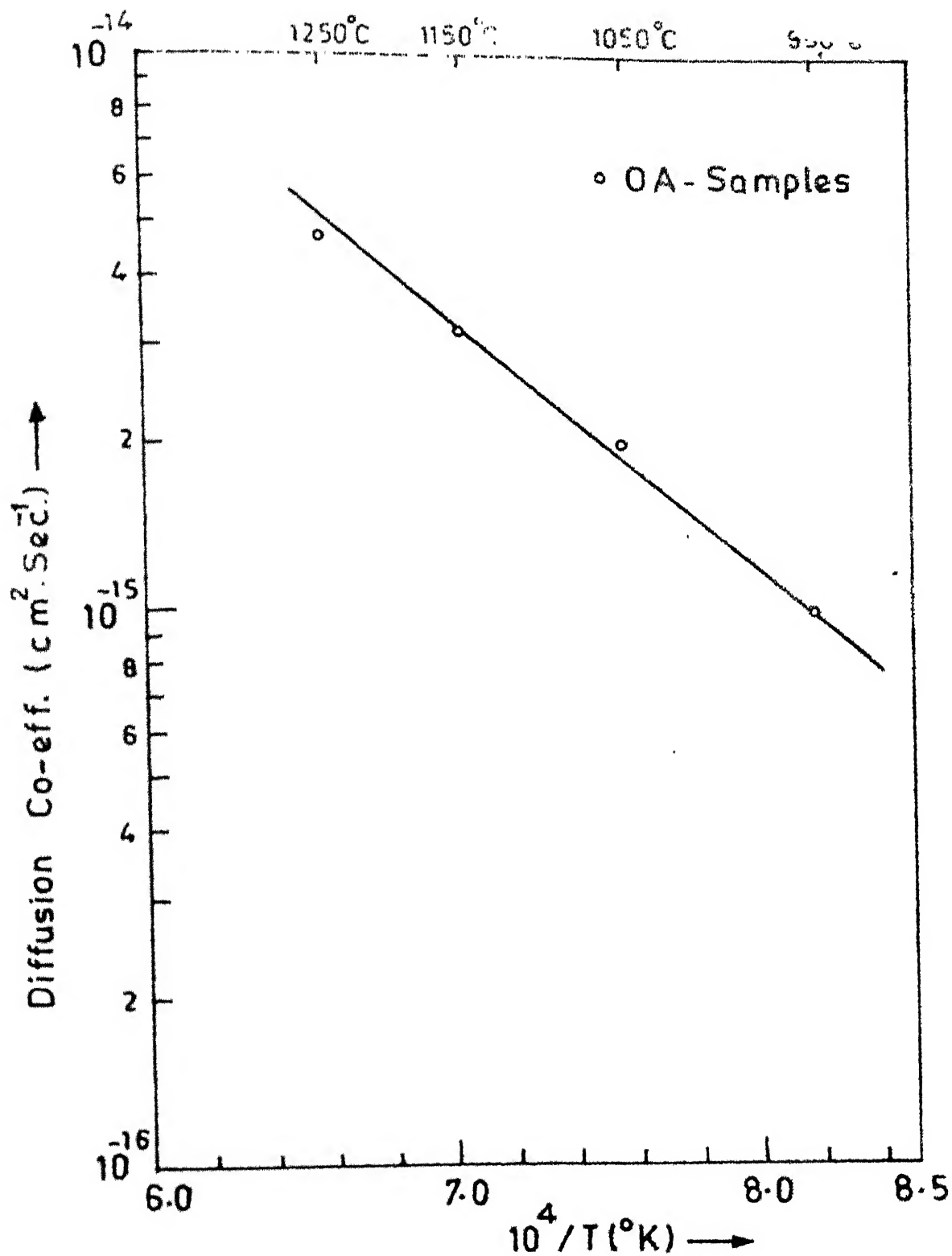
FIG.4.1 Diffusion Co-efficient of Phosphorus in PSG
(4 mole % $P_2 O_5$ in SiO_2)

The estimated values of D_1 for OA samples (see Table 3.1a, Chapter III) are plotted against $10^4/T(^{\circ}K)$ in Fig. 4.1. The least square fit to the experimental points is given by,

$$D_1 = 4.62 \times 10^{-12} . e^{-\frac{0.89}{kT} eV}$$

(4.2)

The value of activation energy of diffusion in the above equation, i.e., 0.89 eV, is considerably lower than the reported values of 1.4-1.6 eV in literature [2-5]. This is essentially due to the difference in the nature of the experiments. In the earlier reported studies, the experiment consisted of diffusing phosphorus from a doped oxide source [3] or from a $POCl_3$ source [2,4,5] into thermally grown SiO_2. The diffusing phosphorus, presumably in form of P_2O_5 [2-5], converted SiO_2 into PSG and D_1 was estimated either from the movement of PSG-SiO_2 interface [2,4,5] or from radiochemical profiling of diffusant in SiO_2 [3]. As pointed out by Eldridge and Balk [4], the activation energies reported by Sah et al [2] and Allen et al [5] (same applies to ref. [3]), actually refer to the overall process of PSG film formation rather than to diffusion process alone. In contrast, in the present work, the PSG of uniform composition is grown during the diffusion process and the estimated D_1 essentially refers to the diffusion of dopant species in PSG.

4.2 SURFACE CONCENTRATION CONTROL BY AMBIENT

The impurity concentration at the silicon surface for the case of diffusion in strongly oxidising ambient is given by,

$$C_{2s}(o,t) = A \cdot erfc(\frac{r\sqrt{B}}{2\sqrt{D_2}}) \qquad (4.4)$$

where A is given by eqn. (4.1a). A perusal of eqn. (4.1a) points to an interesting and useful method of controlling the surface concentration i.e. by altering the diffusion ambient composition. According to eqn. (4.1a), the value of A can be varied by orders of magnitude simply by varying B, i.e. the oxidation rate for the same value of C_o, D_1 i.e. constant dopant concentration in diffusion ambient. The oxidation rate can be controlled either by controlling the partial pressure of oxygen in the ambient or by changing the diffusion/oxidation temperature. For low surface concentration, large values of δ (high oxidation rate) and D_2 (high diffusion temperature) are desirable, according to eqn. (4.1a).

Figure 4.2 gives a plot of A vs $10^4/T^o K$, as estimated in Sec. 3.5, for OA samples detailed in Table 3.1. The ambient composition during all these diffusions was kept the same. As would be expected, the composition of PSG grown in all these cases was also observed to be approximately the same (4 mole% P_2O_5 in SiO_2) as already mentioned in Sec. 3.3. In Fig. 4.2, A varies almost by two orders of magnitude in the temperature range $950^o C$-$1250^o C$. The lowest surface concentration is obtained at highest temperature, in agreement with the theoretical prediction.
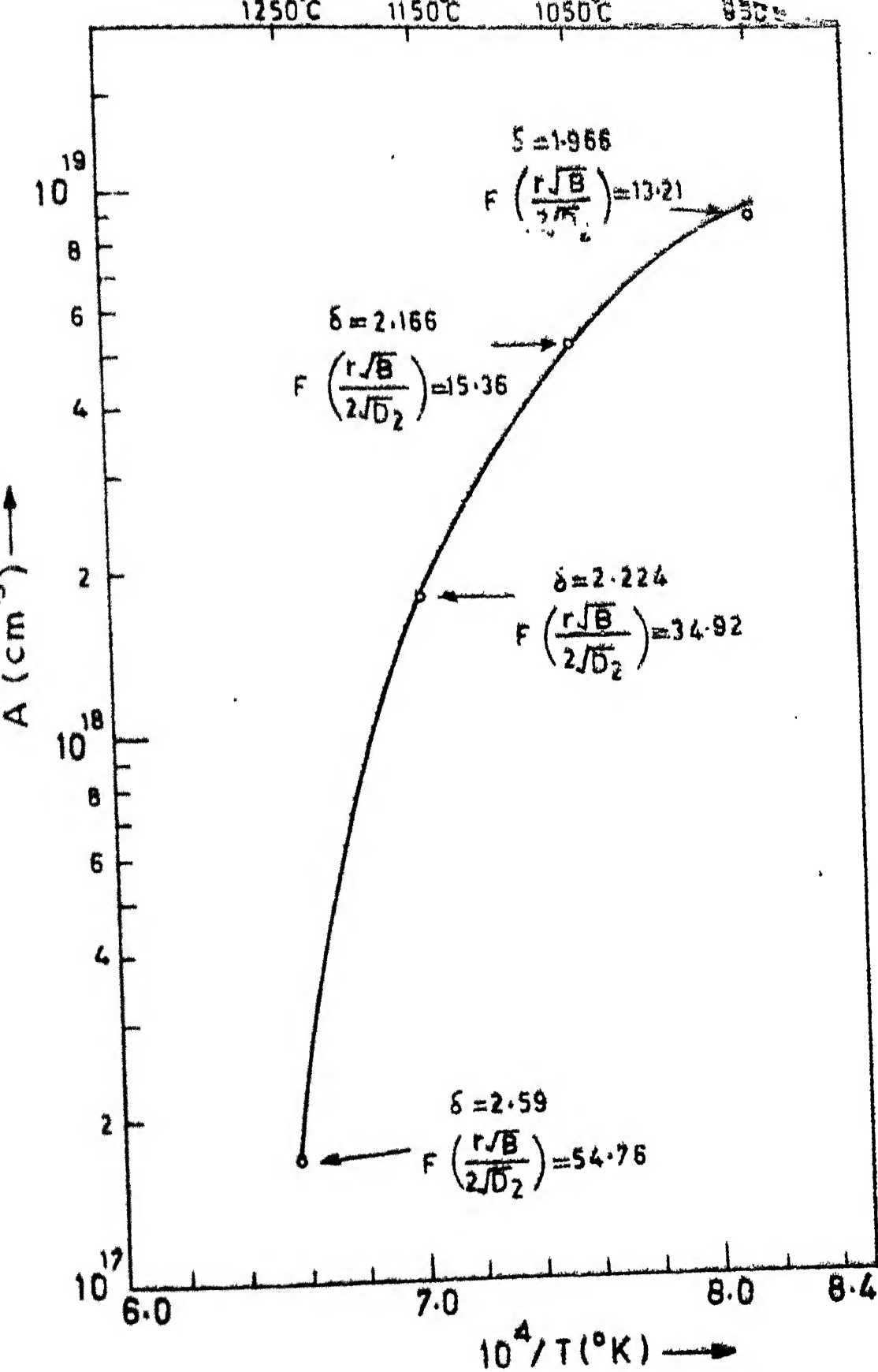
FIG.4.2 Variation of Surface concentration with Temperature and Oxidation Rate (OA-Samples)

In practical situations encountered in device fabrica-
tion such as low concentration diffusion for base of p-n-p
transistor, thyristor and hyperabrup varactor etc., this
method can easily be adopted in preference to usual low
temperature deposition/high temperature drive-in cycle. The
growth of PSG during diffusion has advantageous side effects
such as, (i) it getters the metallic impurities from bulk
silicon, and (ii) the presence of PSG improves the uniformity
of phosphorus diffusion over the surface.

4.3 PHOSPHORUS PROFILES DIFFUSED IN OXIDISING AMBIENT

The comparison of theoretical and experimental impurity
profiles in Figs. 3.7-3.24, brings out an interesting fact
that the profiles diffused in inert ambient (Figs. 3.11-3.14)
are in excellent agreement with theory, while the same diffused
in oxidising/chloro-oxidising ambient show a quantitatively
minor but qualitatively consistent deviation from the calcula-
ted profiles. In the latter cases, a pile-up near the surface,
a hump in the mid-region and a consequent kink in between the
two regions is observed in almost all the cases to varying
extent. A similar discrepancy between theory and experiment
(minus the near surface pile-up and hence, the kink) can also
be seen in the experimental profiles reported by Masetti et al.
[7,8], although they ignored it.

The presence of the above mentioned anamalous features in
the profiles diffused in oxidising ambient alone, indicates that

the phenomenon is oxidation related. The pile-up essentially implies that the phosphorus is incorporated into silicon at PSG-Si interface, at a rate larger than that at which it can diffuse away into silicon. This is also corroborated by an infinitely large value of α, hence that of reaction rate constant of phosphorus at the interface (see Sec. 3.5). The hump appears to be an indication of the presence of non-Fickian movement, in addition to the normal Fickian diffusion, of impurity atoms, as postulated by Dobson [9,10] to explain the observed hump in the high concentration ($> 10^{20}$ cm^{-3}) phosphorus profiles diffused in partially oxidising ambient. Dobson [10] assumed that oxidation of silicon induces a 'convective material flux', which includes both the self-interstitials generated during oxidation as well as impurities. This flux was assumed to be proportional to oxidation rate and impurity concentration. The inclusion of this 'convective flux' in the model brings about an excellent agreement between theory and experiment as demonstrated by Dobson by deriving the equation for impurity distribution, assuming a linear PSG growth. For parabolic PSG growth also, as assumed in the model in Chapter II, the expression for impurity distribution in silicon can be easily derived including the convective flux. The detailed analysis of the experimental results, on the basis of Dobson's model, however, has not been attempted because of the following reasons: (i) The physical basis of

the hypothesis is not clear. The mathematical representation of the 'convective flux' indicates that this flux is caused by a driving force [63]. This driving force is not clearly identified. (ii) The extent of deviation from theory, in this work, does not present a consistent picture i.e. the deviation does not show a systematic variation with temperature or crystal orientation. Therefore, the analysis of these results may not yield any meaningful information. This inconsistency is believed to be caused by two factors. (i) The smoothing of sheet resistance data tends to suppress the anamalous features. For different samples, the extent of data smoothing was different, causing the suppression of anamalous features to varying extent. (ii) There is possibly some unidentified and non-reproducible surface effect contributing to this deviation. More experiments, preferably using direct methods such as SIMS, radiochemical analysis for impurity distribution evaluation, which may be free from data smoothing, are therefore required to be carried out to study these effects.

It may be noted that in most cases, the quantitative agreement with theory is reasonably good. For the purpose of this work, the effective diffusion coefficient using the model of Chapter II has been calculated as described in Sec. 3.5.

4.4 OED OF PHOSPHORUS IN SILICON-EXPERIMENTAL

4.4.1 Diffusion in Inert Ambient

The logarithm of the estimated diffusion coefficients are

plotted against $10^4/T(^\circ K)$ in Fig. 4.3. As can be seen, a straight line can be fitted to the experimental data.

$$D_i = 1.74 \ e^{-\frac{3.56}{kT}} \ eV \qquad (4.5)$$

The activation energy of diffusion, 3.56 eV, is in close agreement with the other literature reported values 3.66 eV [11] and 3.5 eV [7-8] respectively. The former was obtained by Fair [11] by fitting a straight line to the (ln D) vs. 1/T experimental data reported by a number of authors [12-15] while the later was reported by Masetti et al. [7-8], on the basis of their experiments on phosphorus redistribution during drive-in in inert ambient. At $1250^\circ C$, the diffusion coefficient is seen to be exactly same for both <100> and <111> crystal orientation in agreement with the observation of other workers, that the phosphorus diffusion is independent of crystal orientation, in inert ambient [11].

4.4.2 Diffusion in Strongly Oxidising Ambient

The ln D vs $10^4/T^\circ(K)$ plots are given in Figs. 4.3-4.5. The main features of phosphorus diffusion in oxidising ambient are summarized below.

(i) The phosphorus diffusion in oxidising ambient is enhanced in comparison to that in inert ambient; enhancement increasing with decreasing temperature. The diffusion enhancement ratio, D_{ox}/D_i, increases from 1.3 at $1250^\circ C$ to about 4.7 at $950^\circ C$.
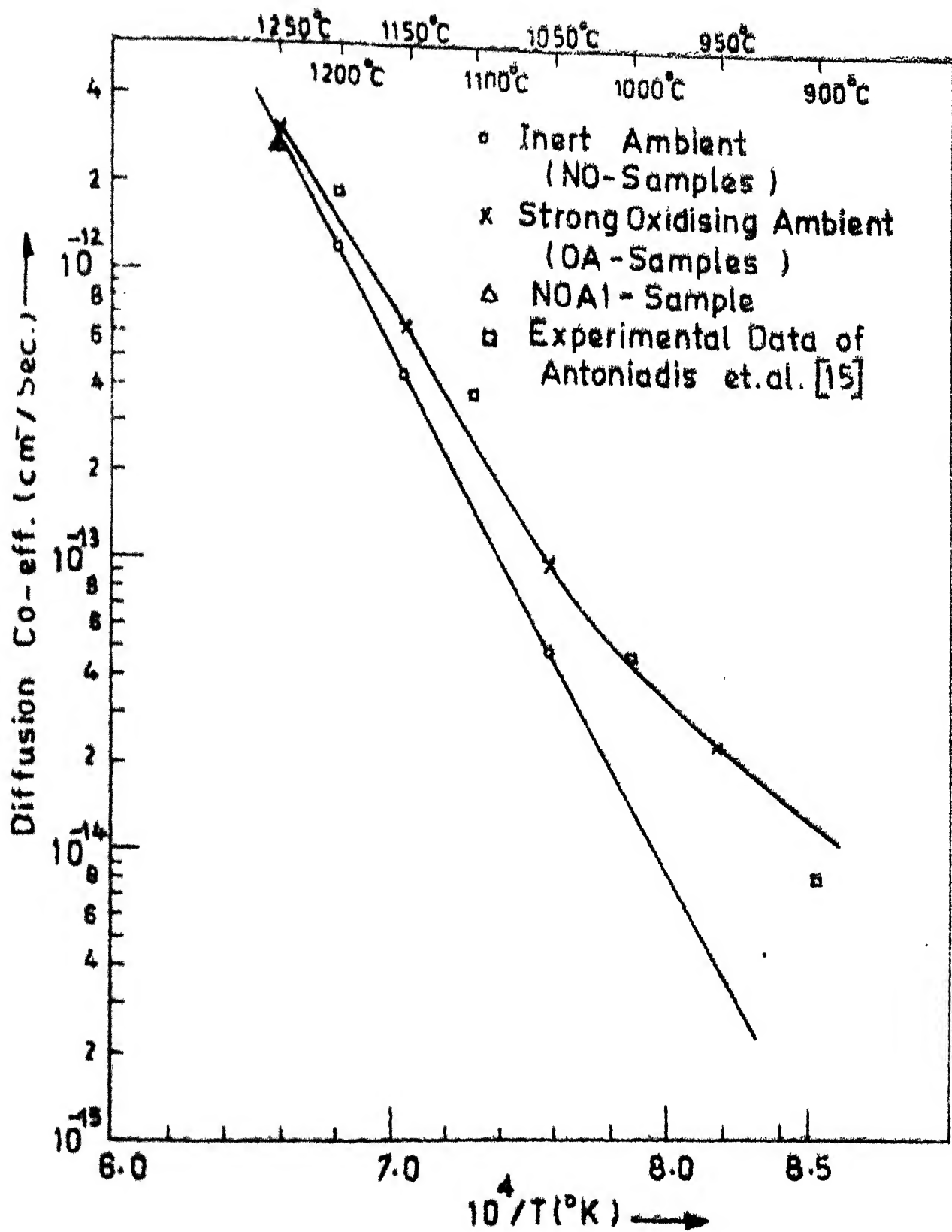
FIG.4.3 Oxidation Enhanced Diffusion in <100> Silic
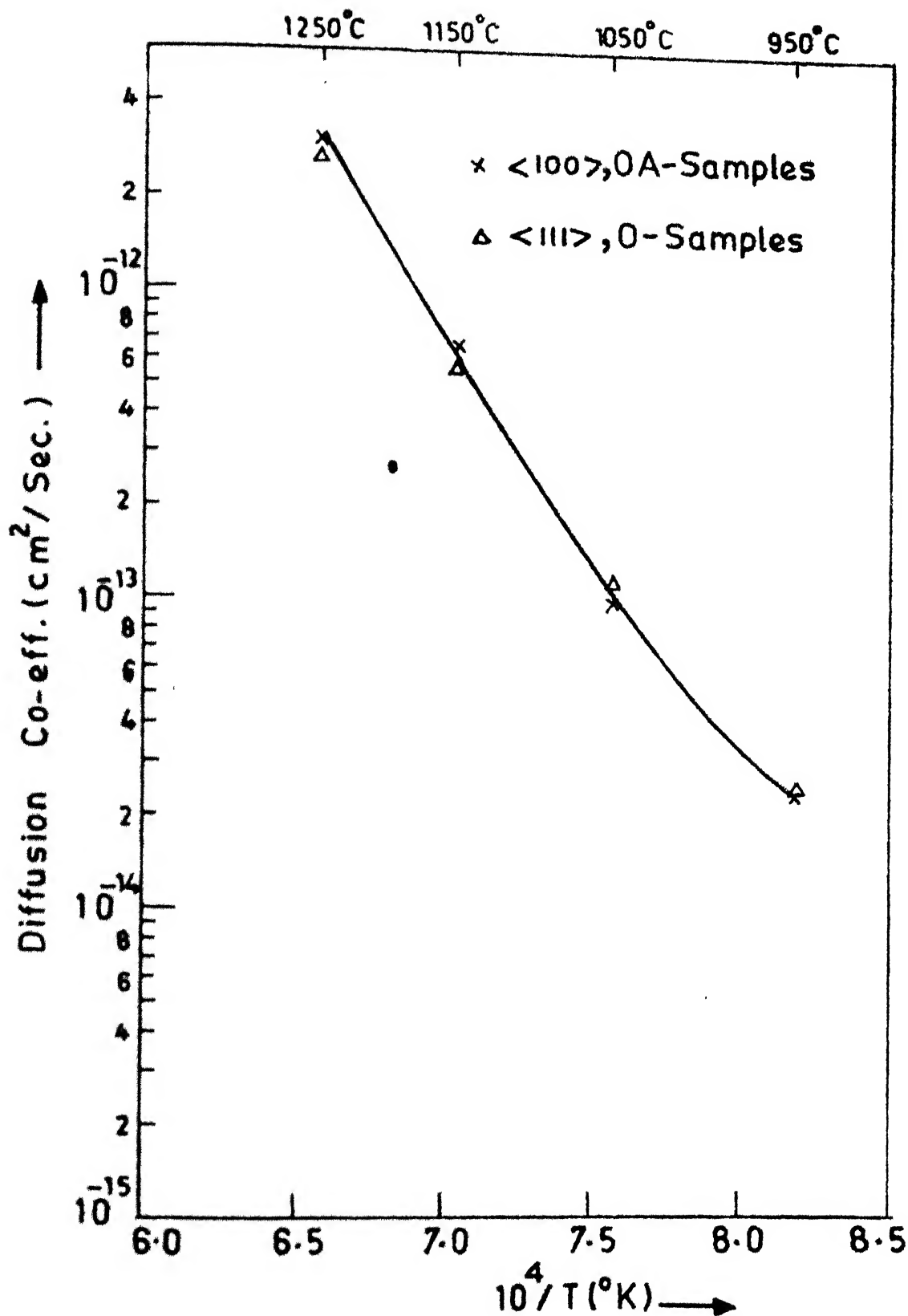
FIG.4.4 Orientation Dependence of Oxidation Enhanced Diffusion.
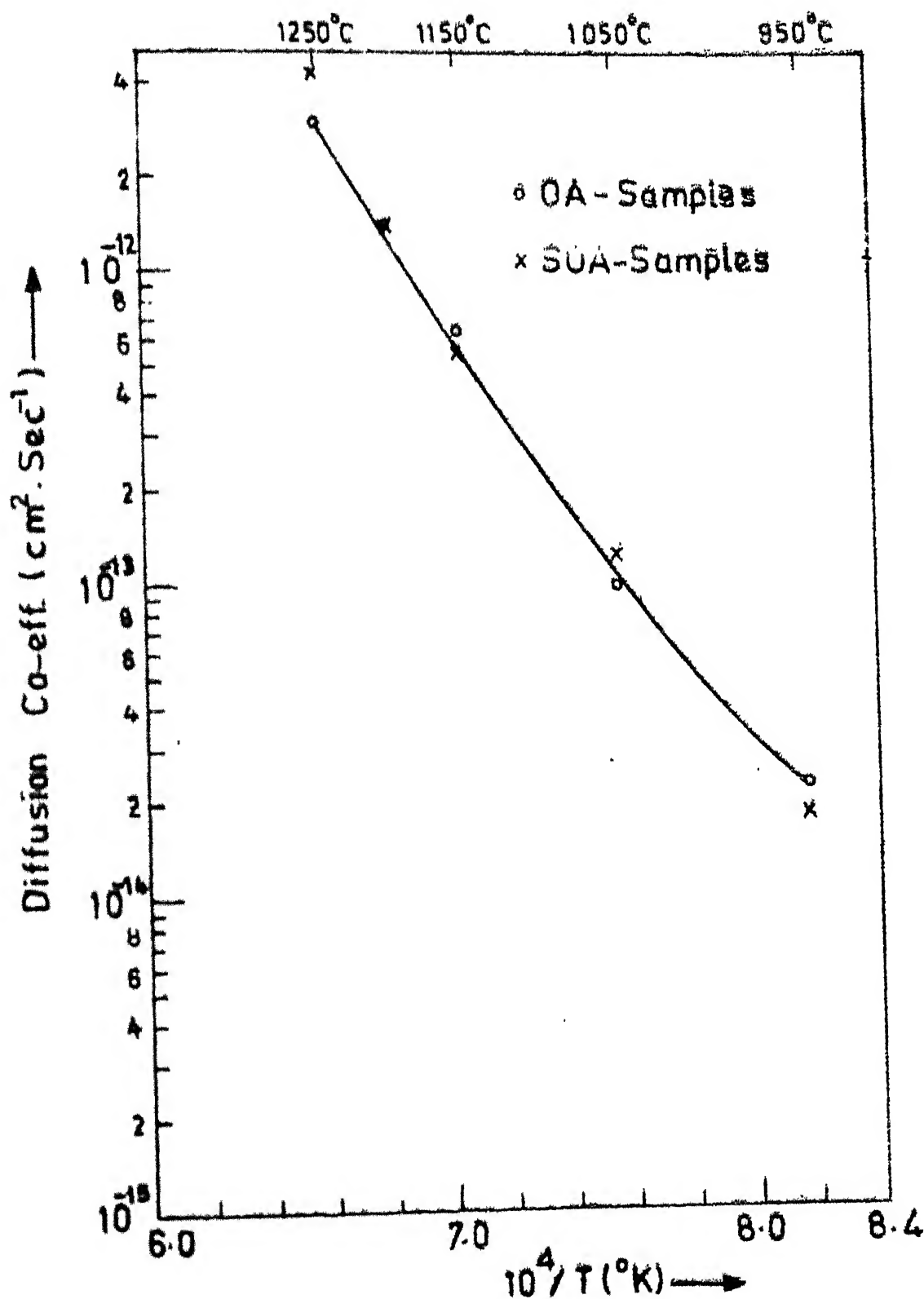
FIG.4.5 Variation of Phosphorus Diffusion Co-efficient in <100> Silicon with Oxidation/Diffusion Time (Also see Tables II & III)

Also plotted in Fig. 4.3, are the OED data of Antoniadis et al. [16], obtained from redistribution of phosphorus during oxidation in dry O_2. These are in good agreement with the results of this work.

(ii) The phosphorus diffusion coefficient in oxidising ambient and therefore OED, is independent of crystal orientation (see Fig. 4.4). This is in contrast to the behaviour of boron which exhibits an orientation dependent OED in silicon [17].

(iii) The OED is almost independent of oxidation/diffusion time (see Fig. 4.5).

In the following section the theoretical models proposed in literature to explain the OED as well as other oxidation related phenomena, are described and critically examined.

4.5 OED OF PHOSPHORUS IN SILICON-THEORETICAL

To understand and model the phenomenon of OED, it is essential to know the identity and kinetics of the point defects involved in OED as also the relationship between the point defect concentration and diffusion coefficient.

4.5.1 Point Defects Involved in OED

Since the diffusion in silicon proceeds via the motion of lattice point defects [18], the OED implies that oxidation introduces excess point defects in silicon. These point

defects, however, cannot be identified merely from the OED phenomenon, because the diffusion mechanism of phosphorus in silicon is still not known uniquely [18-22]. The possible diffusion mechanisms of phosphorus are considered to be interstitialcy [10,20], vacancy [11] and a combination of both [18,20,21]. On the basis of OED alone, therefore, the point defects generated during oxidation could be either interstitials or vacancies.

The oxidation is also found to cause the growth of stacking faults in silicon. The oxidation induced stacking faults (OSF's) have been determined, by TEM analysis, to be two dimensional extrinsic defects lying in <111> planes and bounded by Frank partial dislocations [23,24]. These extrinsic OSF's can grow either via absorption of self interstitials or omission of vacancies. The former implies the presence of supersaturation of self-interstitials and the latter that of an undersaturation of vacancies. Since both the OED and the OSF growth are observed to occur during oxidation under same conditions the point defects generated during oxidation are uniquely identified to be self-interstitials [21,25].

4.5.2 Self Interstitials and Phosphorus Diffusion

Since the oxidation causes injection of self-interstitials, the diffusion in oxidising ambient may be assumed to proceed either via interstitialcy or via a combination of both, the

interstitialcy and vacancy mechanisms. The diffusion coeffi-
cient of phosphorus then may be expressed by a general eqn.[26],

$$D_{ox} = D_{2I} \left(\frac{C_I}{C_I^{eq}}\right) + D_{2V} \left(\frac{C_V}{C_V^{eq}}\right) \tag{4.6}$$

where D_{2I} and D_{2V} are diffusion coefficients for interstitialcy
and vacancy mechanisms, C_I, C_V the concentrations of self inter-
stitials and vacancies during oxidation and C_I^{eq}, C_V^{eq} are the
thermal equilibrium concentrations of self interstitials and
vacancies respectively.

As postulated by Hu [27] and experimentally verified by
Antoniadis and Moskowitz [26], the recombination of vacancies
and interstitials is a very slow process, limited by an energy
barrier of about 1.4 eV. Under oxidising conditions, therefore,
$C_V \approx C_V^{eq}$ and eqn. (4.6) can be written as,

$$\begin{aligned}
D_{ox} &= D_{2I} \left[\frac{C_I}{C_I^{eq}}\right] + D_{2V} \\
&= D_i + D_{2I} \frac{C_I - C_I^{eq}}{C_I^{eq}} \\
&= D_i + D_e \tag{4.7}
\end{aligned}$$

where $D_i = D_{2I} + D_{2V}$ is the diffusion coefficient in inert
ambient and D_e denotes the oxidation enhanced diffusion. Since
C_I is oxidation rate and hence time dependent (this will be
further discussed in following subsection), D_e and D_{ox} are also

functions of time. It has been shown by Lin et al. [28], that when the diffusion coefficient is a function of time alone, the measured diffusion coefficient is simply the time-averaged value of actual time-dependent diffusion coefficient. In terms of time-averaged quantities, eqn. (4.7) can be written as [20,21],

$$\langle D_{ox} \rangle = D_i + \frac{D_{2I}}{C_I^{eq}} \cdot \frac{1}{t} \int_0^t (C_I - C_I^{eq}) dt \qquad (4.8)$$

where $\langle D_{ox} \rangle$ is the measured value of diffusion coefficient in the oxidising ambient. Eqn. (4.8) relates the diffusion coefficient with the concentration of excess self-interstitials and hence with the oxidation process. It may be noted that the depth dependence of C_I has been ignored in deriving eqn.(4.8). This is a reasonable approximation to describe OED because junction depths are usually much smaller than the diffusion length of self-interstitials in silicon.

4.5.3 Kinetics of Self-Interstitials Generated During Oxidation

The formulation of the kinetics of the excess self-interstitials would require the knowledge of the exact relationship between oxidation process and the generation rate of self-interstitials and also the mechanisms of their motion and annihilation in silicon. Furthermore, the model should be able to account for the other oxidation related phenomenon which is

observed under the same conditions i.e. OSF growth, both quantitatively as well as qualitatively. Besides the experimental results detailed in Sec. 4.4, the other relevant experimental observations to be accounted for, by the model ,are the following.

(i) The OSF's grow with time as t^n (n = 0.77-0.84) while OED (of boron) varies as $t^{-1/4}$. Since OSF growth rate $(d(l_{OSF})/dt)$ is proportional to excess self-interstitial concentration,both these observations are consistent with each other and point towards $t^{-1/4}$ dependence of excess self-interstitial concentration [25].

(ii) Both the OSF growth rate and OED (of boron) are crystal orientation dependent and are larger on <100> than on <111> surfaces [25].

(iii) Both OSF growth and OED increase with oxidation rate [25].

(iv) The concentration of self-interstitials at any point in silicon is diffusion limited. This is evident from the observations that OED has been reported to be a function of junction depth [29] and the delay in the onset of the growth of an OSF has been observed to be a function of the distance of the OSF from the oxidising surface [30].

Various models have been proposed to describe the kinetics of excess self-interstitials [33-37]. The models proposed by Murarka [33] and Leroy [34] have already been critically

examined by Hu [25] and will not be considered here. The
models proposed by Lin et al. [35], Tan and Gosele [36] and
Hu [37] are described below and examined in context with the
various experimental observations.

(A) The Model of Lin et al. [35]

An schematic representing the kinetics of excess self-
interstitials in the Lin's model [35] is shown in Fig. 4.6(a).
It was pointed out, following Tiller [31-32], that the thermal
oxidation requires the creation of free volume at the inter-
face at the rate of 1.25 V_i, where V_i is the interface velocity.
This free volume may be supplied either by a flux of self-
interstitials leaving the interface or a viscous flow of the
oxide. It was argued that if about 45% Si at the interface is
oxidised and the rest (55%) is placed at interstitial sites in
the oxide, the free volume will not be immediately needed.
However, since oxidation is experimentally determined to be
more than 99% complete, these excess interstitials placed in
oxide will have to be oxidised in other reactions. Based on
the above arguments Lin et al proposed a two step oxidation
process. In the first step, the lattice silicon atoms at the
surface undergo a reaction with oxygen to form SiO_2,

$$Si_L + (1-\gamma)O_2 \rightleftharpoons (1-\gamma)SiO_2 + \gamma Si_I \tag{4.9}$$
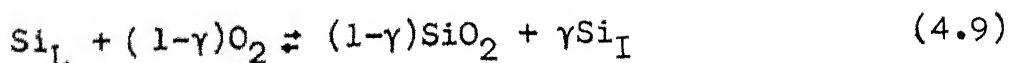
where Si_L and Si_I represent lattice and interstitial silicon at
interface respectively, γ is the fraction of excess silicon at

interface and has a value between 0-0.55. A small part of these excess silicon atoms flow into silicon (J_1 in Fig. 4.6(a)) and remaining excess silicon atoms form the flux J_2 into SiO_2. The generation rate of excess self-interstials, as per eqn. (4.9) is related to J_1, J_2 and interface velocity V_i, by,

$$G = \frac{rV_i}{\Omega} = \frac{r}{\Omega} \left(\frac{dX_o}{dt}\right) = J_1 + J_2 \qquad (4.10)$$

where r is SiO_2 to Si volume ratio and Ω is volume of a silicon atom.

The loss of self-interstitials via recombination with vacancies and absorption by stacking faults and other defect structures is approximated by an infinite sink of interstitials at a distance L_s from interface. This distance L_s is of the order of the range of OED (25µm as reported by Taneguchi [29]). Ignoring the convective flux due to the interface movement, the expression for J_1 is written as,

$$J_1 = D_I \left(\frac{C_I - C_I^{eq}}{L_s}\right) \qquad (4.11)$$

where D_I is diffusion coefficient of self-interstitials in bulk Si.

In the second step, it is hypothesized that interstitial Si, incorporated into SiO_2 in the first step, are oxidised by the following reaction,

$$Si + \frac{x}{2} O_2 \rightleftarrows SiO_x \qquad (4.12)$$

where x is an unknown parameter and possibly represents a mixture of several different SiO_x type reactions. This SiO_x is assumed to be further oxidised to SiO_2 later.

The flux J_2 is determined by reaction (4.12) and is given by,

$$J_2 \propto [p_{O_2}]^{x/2} (C_I' - C_I'^*)$$

$$\propto (\frac{dX_o}{dt})^{x/2} (C_I' - C_I'^*)$$

$$= K_I (\frac{dX_o}{dt})^{x/2} \cdot (C_I' - C_I'^*) \qquad (4.13)$$

Neglecting J_1 in eqn. (4.10) and combining with (4.13) leads to,

$$(C_I' - C_I'^*) = \frac{r}{\Omega \cdot K_I} (\frac{dX_o}{dt})^{1 - \frac{x}{2}} \qquad (4.14)$$

It is further assumed that self-interstitial concentrations in SiO_2 and Si at the interface, are related with each other by an equilibrium segregation constant m_I,

$$m_I = \frac{C_I - C_I^{eq}}{C_I' - C_I'^*} \qquad (4.15)$$

Using eqns. (4.14) and (4.15), the eqn. for excess self-interstitial in silicon, at the interface is given as,

$$(C_I - C_I^{eq}) = \frac{m_I r}{\Omega \cdot K_I} (\frac{dX_o}{dt})^{1 - \frac{x}{2}} \qquad (4.16)$$
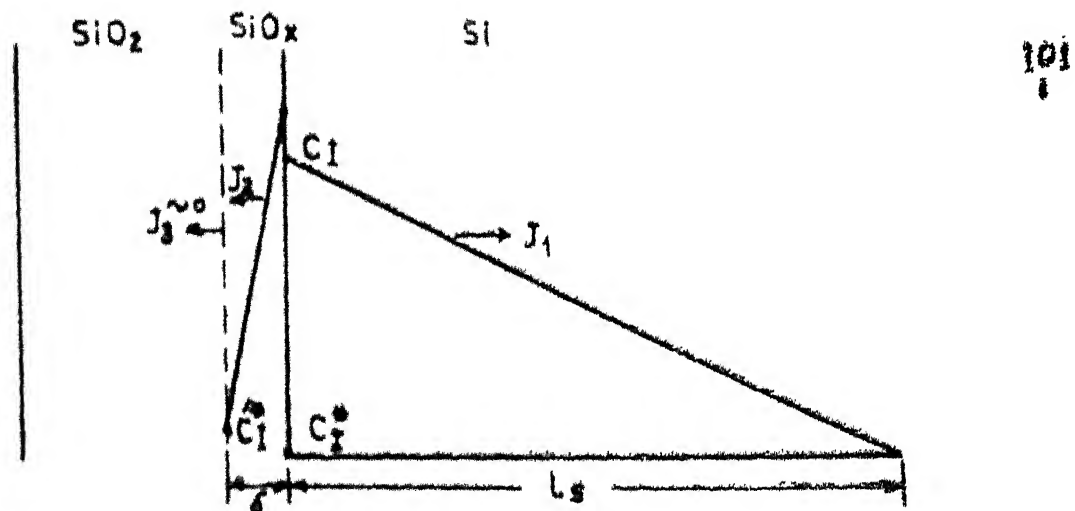
(a) Self-Interstitial fluxes during thermal oxidation
[ref.(35)]
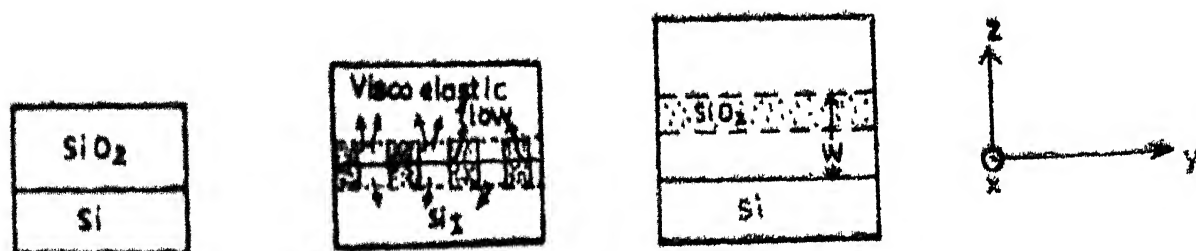
(b) Thermal Oxidation Process according to Tan &
Goesele [36]. Self interstitials are injected into Silicon
due to compressive stress in SiO_2 near interface.
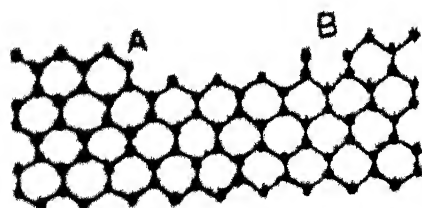
(c) Surface annihilation of excess self-interstitials
at kink sites. [37]

FIG.4.6 Models for kinetics of excess self
interstitials produced during thermal Oxidation.

On the basis of experimental results, Lin et al. proposed that the value of x is 1.2. For parabolic growth of oxide, $x = 1.2$ leads to the OSF growth as $t^{0.8}$ and OED variation with time as $t^{0.2}$, which compare well with their respective experimental values of (0.77-0.84) and 0.25 respectively. It is further speculated that m_I in eqn. (4.15) is orientation dependent and $m_{I<100>} > m_{I<111>}$, in analogy with the experimentally observed orientation dependence of boron segregation in SiO_2-Si system [17,38]. The orientation dependence of OED and OSF growth rate was attributed to the orientation dependence of m_I.

Although this model explains some of the experimental results mentioned earlier, it is unsatisfactory in some respects as described below.

(i) An orientation dependent m_I would predict orientation dependent OED irrespective of the impurity type. While boron exhibits orientation dependent OED [17,39-41], the phosphorus OED in this work, has been observed to be orientation independent even under intrinsic diffusion conditions.

(ii) It is implicitly assumed that the diffusion coefficient D_I of self-interstitials is very large as compared to the range L_s of the self-interstitials, while correlating the concentration of self-interstitials at the interface (as given by eqn. (4.16)) with the time dependence of OSF growth rate and OED. The finite range L_s of interstitials is attributed to the

loss mechanisms such as recombination with vacancies and absorption at defect structures and is essentially time invariant. The later experiments of Taniguchi [30] clearly demonstrated that the concentration of self-interstitials in bulk silicon is diffusion controlled.

(iii) In the first step of the oxidation it was postulated that a fraction of interface silicon atoms become interstitial in SiO_2 via reaction given by eqn. (4.9), thus obviating the need of the free volume for the formation of SiO_2. However, when these are oxidised subsequently, the free volume is still required. It was pointed out by Tan and Gosele [36] that the model does not explain clearly, how this free volume requirement is met.

(B) The Model of Tan and Gosele [36]

Tan and Gosele [36] proposed a macroscopic rather than atomistic model for relationship between generation of excess self-interstitials during thermal oxidation. In this model the free volume requirement of the growing SiO_2 is met by the viscoelastic flow of SiO_2 near the interface. The complete process is depicted in Fig. 4.6(b). It was argued that the growth of new SiO_2 layer at interface amounts to insertion of oxygen atoms in bond centered position of Si atoms which would lead to a linear expansion of 30% in x,y,z directions. In z-direction the expansion is accomplished easily as SiO_2 surface

is free. In x-y plane, however, the SiO_2 layer is subjected to an elastic strain and associated compressive stress 'τ'. This stress causes the viscoelastic flow of excess material into SiO_2 (Fig. 4.6b(iii) and injection of self-interstitials into silicon simultaneously. The viscoelastic flow of SiO_2, is stopped as soon as the planar strain in x-y plane is fully released (Fig. 4.6b(iii)). The viscous flow rate is equal to the required volume expansion rate (and therefore oxidation rate). The general relationship between viscous flow rate and stress τ is given by,

$$\text{Flow rate} \propto \tau^j \propto (\frac{dX_o}{dt}) \qquad (4.17)$$

where 'j' is a function of viscosity of the newly grown SiO_2 near interface. Super saturation ratio of self-interstitials, S_r, is taken to be directly proportional to compressive stress 'τ', so that

$$S_r = \frac{C_I - C_I^{eq}}{C_I^{eq}} \propto \tau^{1/j}$$

or

$$(C_I - C_I^{eq}) \propto (\frac{dX_o}{dt})^{1/j} \qquad (4.18)$$

Tan and Gosele argued that 'j' may take any value greater than or equal to unity. For well annealed amorphous SiO_2 $j = 1$. In contrast, the newly grown SiO_2 layer has a lower viscosity so that $j > 1$. It can be seen that for $j = 2$, $(C_I - C_I^{eq}) \propto t^{-1/4}$, which is the desired relationship to explain the time variation

of OSF growth and OED. It was argued that the scatter in the reported values of n (where OSF length $\propto t^n$) between 0.77-0.84 is due to the variation in 'j' which is a strong function of impurity incorporated in the SiO_2 near the interface.

It is noted that the model ignores the diffusional effects of self-interstitials in bulk silicon and therefore cannot account for the observations of Taniguch [30] mentioned earlier. Furthermore, the question of orientation dependence of OSF growth rate and OED has not been addressed at all.

The Model of Hu [37]

This model is based on the following postulates,

(i) The oxidation of silicon at $Si-SiO_2$ interface is usually incomplete, thus creating self-interstitials. The generation rate of self-interstitials at the interface is directly proportional to the oxidation rate.

(ii) At the silicon surface, there exists a certain density of active sites, possibly kinks of surface steps, which are capable of capturing the excess self-interstitials. The capture of self-interstitials by these kink sites, thus causes surface regrowth. On the basis of the calculations made by Burton et al. [42] which showed that the surface configuration entropy (and hence the density of the kinks) is a continuous function of temperature, Hu [21] proposed that the thermodynamic fluctuations can create the surface kink sites

at any temperature. He further explained that the density of kink sites is a function of crystal orientation and increases in the order $\langle 100 \rangle$, $\langle 110 \rangle$ and $\langle 111 \rangle$. Fig. 4.6(c) illustrates the process of capture of self-interstitials at kink sites. At site A the surface structure is restored by capture of two self-interstitials.

(iii) The diffusivity of self-interstitials is finite and the loss of self-interstitials in bulk silicon due to recombination with vacancies and absorption by OSF's is very small.

The distribution of self-interstitials in silicon, is given by the continuity equation,

$$\frac{\partial C_I}{\partial t} = D_I \frac{\partial^2 C_I}{\partial x^2} \qquad (4.19)$$

The boundary and initial conditions are,

$$C_I(\infty, t) = C_I(x, o) = C_I^{eq} \qquad (4.20)$$

and

$$\left[-D_I \frac{\partial C_I}{\partial x} + k_I(C_I - C_I^{eq}) \right]_{x=o} = \text{Generation rate} = G(t)$$

$$= A_I \, t^{-1/2} \qquad (4.21)$$

The solution to eqns. (4.19) - (4.21) is given by,

$$\Delta C_I = (C_I - C_I^{eq}) = A_I(\frac{\pi}{D_I})^{1/2} \, e^{-x_n^2} \, e^{(x_n + \sqrt{t_n})^2} \, erfc(x_n + \sqrt{t_n})$$

$$(4.22)$$

where

$$x_n = \frac{x}{2\sqrt{D_I t}}$$

$$t_n = t \, \frac{k_I^2}{D_I}$$

k_I = Annihilation velocity (cm S^{-1}) of self-
interstitials at silicon surface

C_I = Concentration of excess self-interstitials

The growth rate of OSF was taken to be proportional to the $<\Delta C_I>_{L_I}$, the average excess interstitial concentration over the diffusion length, L_I. The expression for $<C_I>_{L_I}$ is derived from (4.22) and is given by,

$$<\Delta C_I>_{L_I} = \int_0^1 C_I(x_n, t_n) dx_n$$

$$= A_I(\frac{\pi}{D_I})^{1/2} \frac{1}{2\sqrt{t_n}} [e^{-1} e^{(1+\sqrt{t_n})^2} erfc(1+\sqrt{t_n}) -$$

$$e^{t_n} erfc(\sqrt{t_n}) + erfc(1)] \qquad (4.23)$$

Hu demonstrated that the plots of $\ln(\Delta C_I)$ vs. $\ln(t_n)$ and that of $\ln(<\Delta C_I>_{L_I})$ vs. $\ln(t_n)$ have the slopes, of about (-0.25) and (-0.21) respectively in the range $t_n = 0.1-1.0$ and of about (-0.4) and (-0.35) respectively in the range of

$t_n = 1$ to 10. It follows that OED and OSF growth rate vary as $t^{-0.25}$ and $t^{-0.21}$ respectively (in the range $t_n = 0.1$ to 1), in agreement with the experimental results. Hu argued that most of the experimental results reported cover only about a decade of time span and are likely to correspond to range of $t_n = 0.1-1.0$. The small variation ($n = 0.77-0.84$) observed in the time dependence of OSF growth rate is merely due to the different value of t_n in the various experiments. The only variable in eqn. (4.22) that depends upon crystal orientation is k_I and is responsible for orientation dependence of OED and OSF growth rate. Since the <111> surface has a larger density of kink sites than <100> surface, k_I would be larger for <111> surfaces, resulting in smaller OSF growth rate and OED for <111> surfaces, as experimentally observed. The assumption of the diffusion controlled motion of self-interstitials is also consistent with the observations of Taniguchi [29,30] mentioned earlier. This model, thus, is qualitatively and to some extent quantitatively consistent with, the experimental observations reported earlier. It will be shown below that this model can also explain the orientation and time invariance of OED observed in this work.

In the model described above, k_I is considered to be dependent on the density of kink sites. It is proposed that k_I would also depend upon the impurity present at interface through its segregation coefficient in $Si-SiO_2$ system. Since the segregation coefficient of phosphorus in $Si-SiO_2$ system is

large (m = 10), it may be assumed that phosphorus will tend to pile-up on silicon side of interface, and effectively compete with self-interstitials in surface regrowth process. It is proposed that phosphorus is captured at kink sites in preference to self-interstitials. Since density of kink sites is estimated to be $\approx 10^{12}$ cm^{-2} [21], a phosphorus concentration of about 10^{18} cm^{-3} at the interface would be sufficient to eliminate the capture of self interstitials at the interface. This means that $k_I \approx o$ in eqn. (4.22). This situation will lead to the following effects.

(i) $C_I(x,t)$ and hence OED, would be orientation as well as diffusion time independent, for case of small junction depths such as $x_j \ll 2\sqrt{D_I}t$.

(ii) Larger OED than expected for the case of $k_I > o$ would be observed since $C_I(x,t)$ in eqn. (4.22) reaches its maximum value as $x_n, t_n \to o$. In the present work, since the surface concentration in almost all cases is of the order of 10^{18} cm^{-3}, all these effects may be expected to be present.

It follows from the above argument that for group V impurities (P,As,Sb), which have m $\gg$ 1, the concentrations of the order of 10^{18} cm^{-3} and above will lead to orientation and time invariant OED. For lower concentrations, say $< 10^{16}$ cm^{-3}, the OED (as well as OSF growth rate) should be both orientation and time dependent. Unfortunately no systematic steady has been

reported on orientation dependence of OED of P,As and Sb. However, it has been reported by Antoniadis and Moskowitz [26] that for concentrations of the order of 10^{16} cm^{-3}, P and As indeed exhibit a time dependent OED. Furthermore, for boron, it would be expected that OED is orientation dependent even for comparatively higher boron concentrations at the interface, because boron tends to segregate into SiO_2, thus causing the surface regrowth to occur dominantly by capture of self-interstitials. In literature, the orientation dependence of boron has been reported for impurity concentrations ranging from 10^{17}-10^{19} cm^{-3} [17,39-41].

Conclusion

The review of the models, proposed to describe the kinetics of excess self-interstitials leads to the following conclusions. (i) Only the model proposed by Hu [37] is consistent with all the experimental observations on OSF growth and impurity OED in silicon (ii) The surface regrowth process in Hu's model is a function of the segregation coefficient and concentration of the impurity present at the SiO_2-Si interface. It may, however, be pointed out that in all these models the SiO_2-Si interface has been assumed to be a source of self-interstitials which is consistent with the phenomena of OSF growth and OED. At high temperatures ($>1150^{o}$C) and long oxidation times, however, OSF shrinkage and ORD of phosphorus are observed [43,44] which point to the fact that under these conditions the interface acts as a

sink for self-interstitials [43]. This situation has not been considered in these models. The reason probably is that the precise mechanism of the oxidation process and generation of excess self-interstitials is still not well understood. A comprehensive model to describe the generation kinetics of excess self-interstitials at the interface is, therefore, yet to be developed. While the two basic features of Hu's model i.e. surface regrowth process and finite diffusivity of self-interstitials in bulk silicon have to be retained in any model, the generation process of self-interstitials at interface needs to be reformulated. However, as shown in the foregoing discussion, Hu's model in its present form satisfactorily accounts for all experimental observations on OSF growth and OED and hence can be considered to be valid under corresponding oxidising conditions.

4.5.4 Modelling of OED

Following Hu's model for kinetics of excess self-interstitials, generated during oxidation, the equation for oxidation enhanced diffusivity factor 'G', for the present work (i.e. $k_I = o$) can be written as (using eqns. (4.8) and (4.22)),

$$G = \frac{\langle D_{ox} \rangle}{D_i} - 1 = \frac{D_{2I}}{D_i} \frac{A_I}{c_I^{eq}} \left(\frac{\pi}{D_I} \right)^{1/2} \qquad (4.24)$$

It is evident that a plot of $\ln G$ vs $10^4/T(^{\circ}K)$ would be straight line. In the plot of Fig. 4.7, the experimental points
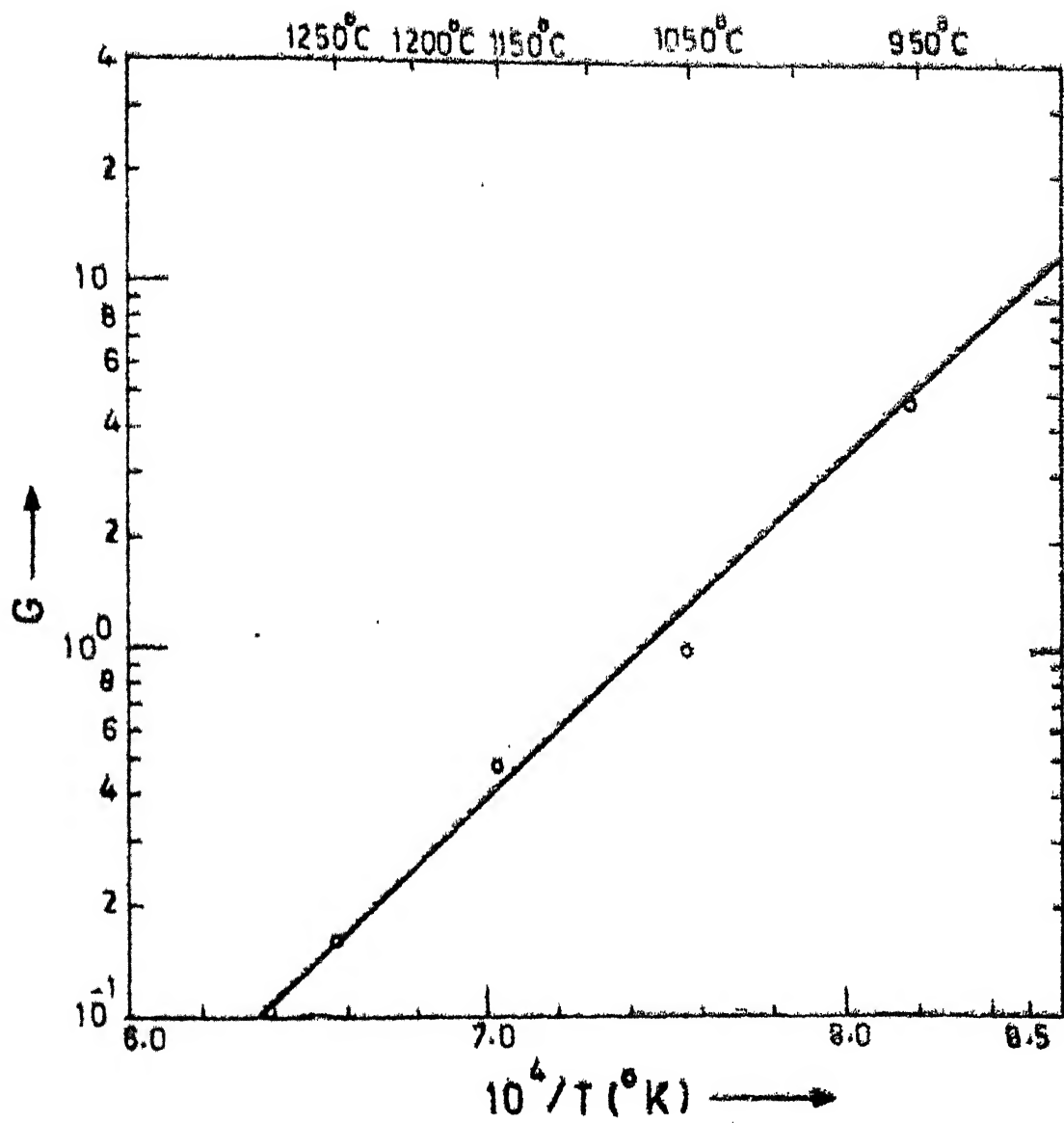
FIG.4.7 Oxidation Enhanced Diffusivity Factor in
<100> Silicon.

are best described by a straight line, given by the equation,

$$G = 1.246 \times 10^{-7} \ e^{\frac{1.84}{kT}} \ eV \qquad (4.25)$$

Equation (4.25) relates the oxidation enhanced diffusivity factor with temperature. This equation is valid only for diffusion in 90% O_2 ambient.

In eqn. (4.24), G is a function of oxidation conditions only through A_I. By evaluating G for different oxidation rates, it is possible to check whether or not the interstitial generation at interface is proportional to oxidation rate as assumed in the model of Hu [37].

The value of parameter $k_I/\sqrt{D_I}$ at low phosphorus concentrations ($\leq 10^{16}$ cm^{-3}) can be calculated, if the oxidation/diffusion time dependence of G is known. The only data available on oxidation time dependence of phosphorus diffusion coefficient are those reported by Antoniadis and Markowitz[26]. Their data, however, are reported only at one temperature i.e. 1000°C. More experimental data are required before a detailed evaluation of this parameter is attempted.

4.6 THE EFFECT OF CHLORINE ON PHOSPHORUS DIFFUSION

4.6.1 Experimental Results

The phosphorus diffusion coefficient in <111> and <100> silicon is plotted against $10^4/T(°K)$ in Fig. 4.8 and Fig. 4.9 respectively. It is seen that

(i) The presence of chlorine, (produced by decomposition of TCE [45]) in the ambient causes a reduction in the diffusion coefficient at all the temperatures.

(ii) In <100> silicon the reduction is less than the same in <111> silicon.

(iii) The effect of chlorine on the diffusion coefficient decreases with decreasing temperature.

(iv) At high temperatures (> $1150^{\circ}C$) the diffusion coefficient in chlorooxidising ambient is lower than its value in inert ambient. In <100> silicon, the diffusion coefficient at $1250^{\circ}C$ is reduced by 10% and in <111> silicon by 35%, with reference to its corresponding value in inert ambient.

In order to explain the above results it is essential to know the distribution of chlorine in SiO_2-Si system during chlorine oxidation and also the nature of interaction of chlorine atoms with the point defects involved in impurity diffusion.

4.6.2 Chlorine Distribution in the SiO_2-Si System

Recently, there has been considerable effort invested in understanding the effect of chlorine on thermal oxidation because chlorine in thermally grown oxides (i) neutralizes the positive alkali ions in the oxide [46], (ii) provides better reproducibility in breakdown voltages [47], (iii) and reduces stacking faults [48]. A brief review of the status of chlorine
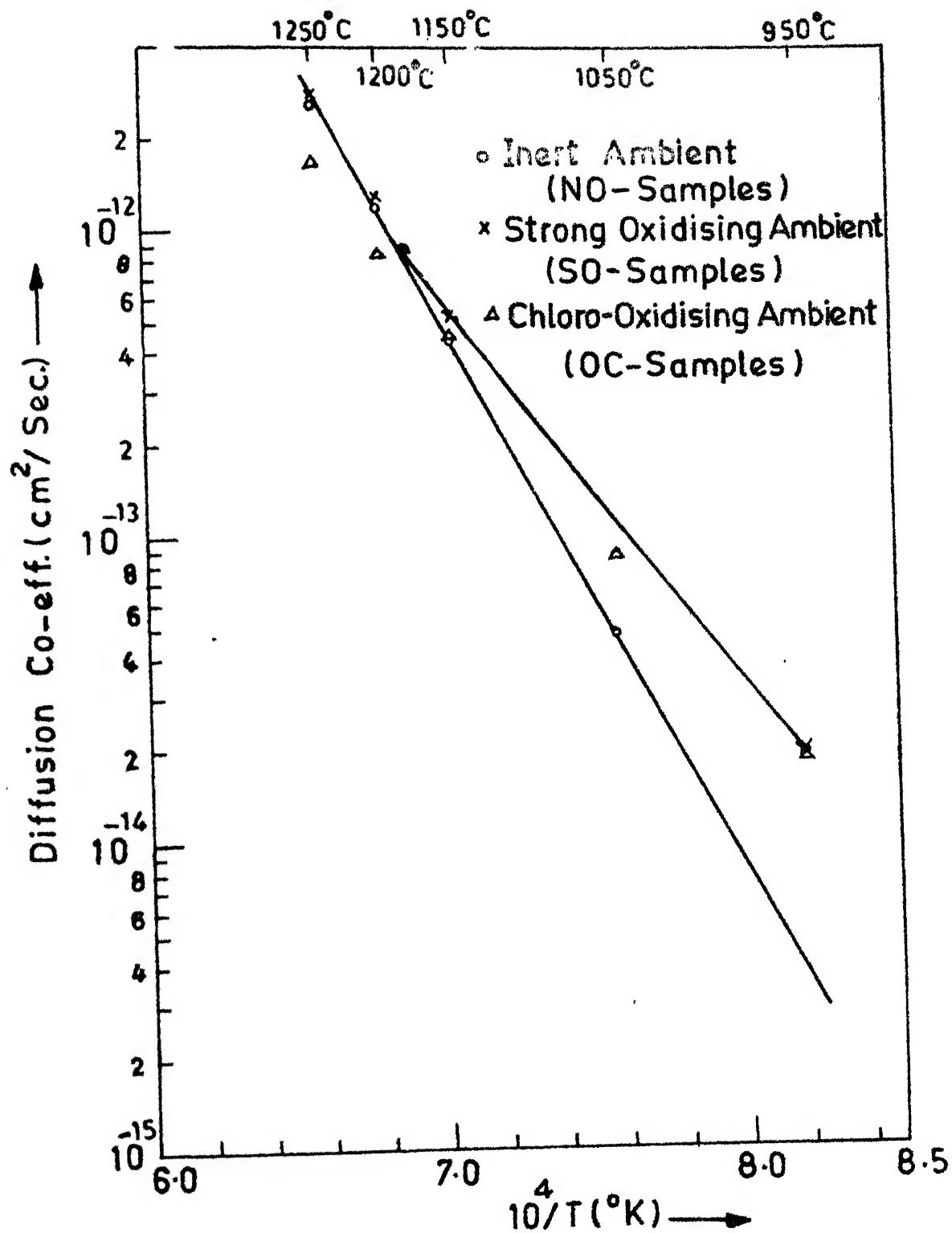
FIG.4.8   The Effect of Chlorine on Phosphorus
Diffusion in <111> Silicon.
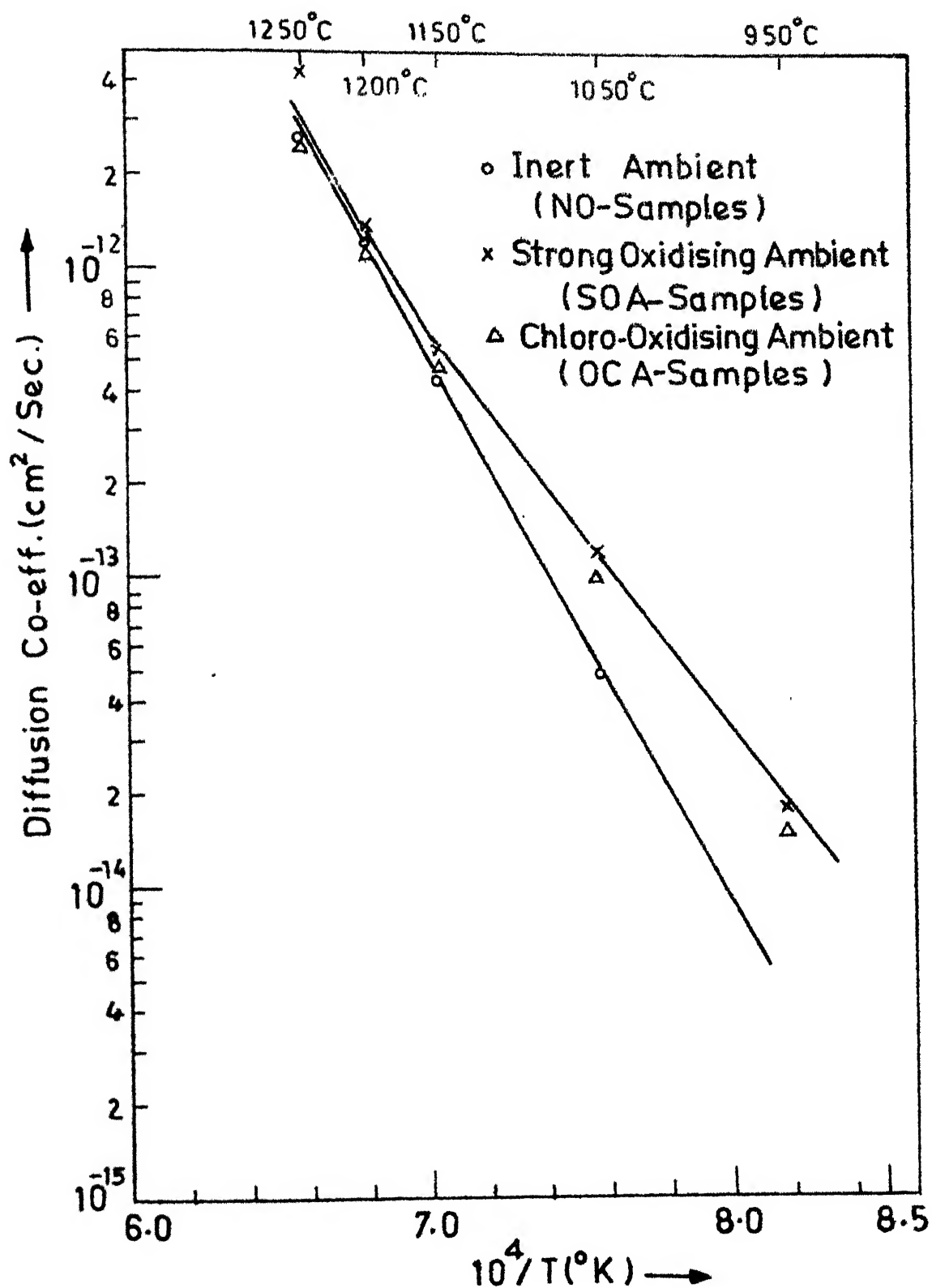
FIG. 4.9 The Effect of Chlorine on Phosphorus Diffusion in <100> Silicon.

oxidation in the fabrication process of LSI's is given by Hattori [49].

Rather a few investigations have been reported on the kinetics of chlorine during the thermal oxidation of silicon in chloro-oxidising ambient [50-53]. The chlorine distribution in SiO_2 in these studies was experimentally determined using nuclear backscattering [50], SIMS [51] and Auger sputter profiling/SIMS [52-53]. The main observations are as follows :

(i) The chlorine atoms segregate near the interface in SiO_2, where these are probably incorporated in various Si-Cl-O-H complexes. The peak in the chlorine concentration profile occurs very near the interface on SiO_2 side. There is a region of 100-200°A thickness near the interface where chlorine is accumulated in high concentrations [50-53]. The concentration of chlorine in the bulk SiO_2 is about two orders of magnitude lower than the peak concentration near the interface.

(ii) The chlorine concentration at interface is a strong function of temperature. The chlorine level varies from $6x10^{13}$ cm for 900°C oxides to about $1.7x10^{15}$ cm^{-2} for 1100°C oxides [50-53]. The clorine concentration also is a weak function of oxidation time [51,52] and increases linearly with chlorine partial pressure in ambient [51].

(iv) For identical oxidation conditions, the level of chlorine incorporated in SiO_2 on <111> silicon is larger than in SiO_2 on <100> silicon. This experiment, however, was carried out only for oxides grown at 1100°C [51] and 1000°C and 1100°C [52].

(v) The linear rate constant of oxidation is increased in presence of chlorine [54-56].

4.6.3 Interaction of Chlorine with Self-Interstitials at the Interface

It is now well established that oxidation in chloro-oxidising ambient causes the retarded growth or elimination of OSF [57-59]. The reduction in OED of phosphorus and boron, in chloro-oxidising ambient, has also been reported by Nabeta et al. [60]. As pointed out in previous section, both these phenomena i.e. OSF growth and OED are caused by the excess-self-interstitials generated at the interface during thermal oxidation process. It thus follows that the chlorine incorporated at the interface during thermal oxidation causes the interface to act as a sink for self-interstitials.

A two step mechanism has been proposed by Murarka [61-62] that possibly reduces the concentration of self-interstitials near the interface. In the first step, it is postulated that the interface chlorine atom reacts with the lattice silicon atom to form SiClu, by the reaction,

$$Si_L + \frac{u}{2} Cl_2 \rightleftharpoons SiClu + Si_V \qquad (4.26)$$
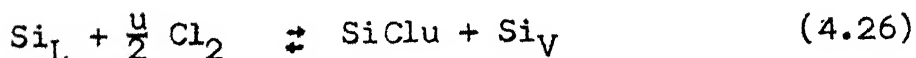
The silicon vacancy generated in this reaction recombine with the self-interstitial present at the interface,

$$Si_I + Si_V \rightleftharpoons Si_L \qquad (4.27)$$

In eqn. (4.26), the interface chlorine atom has been assumed to react with lattice silicon atom alone. While it is consistent with the observed increase in linear rate constant during chlorine oxidation [53-55,62], it is unlikely that the free self-interstitials generated at the interface would not directly react with chlorine atoms. The exact chemistry of the interaction of chlorine atoms with various species such as self-interstitials, O and H-atoms present at the interface is not yet known. It appears, however, reasonable to assume that in general the interface chlorine atoms react with self-interstitials forming various immobile $SiCl_u$ or Si-Cl-O-H complexes [52]. The SiO_2-Si interface containing chlorine, thus, acts as a sink for self-interstitials generated at the interface.

4.6.4 Discussion

In general, the loss rate, R, of self-interstitials at the interface due to reaction with chlorine atoms may be expressed as,

$$R(t) = k_{Cl} \cdot C_{Cl} \cdot C_I(o,t) \tag{4.28}$$

where k_{Cl} is a constant, C_{Cl} and C_I are the concentrations of chlorine and excess self-interstitials at the interface respectively. Considering that C_{Cl} is a weak function of time and can be treated essentially as a constant [52], it is easy to formulate the effect of chlorine on C_I, in Hu's model

described in previous section. The effect of the presence of chlorine, as expressed by eqn. (4.28) can be included in the boundary condition given by eqn. (4.21). The modified eqn. (4.21) is,

$$[-D_I \frac{\partial C_I}{\partial x} + (k_I + k_{Cl} C_{Cl}) \cdot (C_I - C_I^{eq})]_{x=o} = A_I \cdot t^{-1/2} - k_{Cl} C_{Cl} C_I^{eq}$$

$$(4.21a)$$

The expression for excess self-interstitial distribution at silicon surface is determined to be (see Appendix VI),

$$(C_I - C_I^{eq})|_{x=o} = \Delta C_I(o,t) = A_I (\frac{\pi}{D_I})^{1/2} e^{t'_n} \text{erfc}(\sqrt{t'_n}) -$$

$$C_I^{eq} [1 - e^{t'_n} \text{erfc}(\sqrt{t'_n})] \qquad (4.29)$$

where,

$$t'_n = \frac{(k_I + k_{Cl} C_{Cl})^2}{D_I} \cdot t \qquad (4.29a)$$

Combining equations (4.8) and (4.29), the eqn. for diffusion coefficient in chloro-oxidising ambient is written as :

$$\langle D_{ox,Cl} \rangle = D_i + \frac{D_{2I}}{C_I^{eq}} [\frac{\{A_I (\frac{\pi}{D_I})^{1/2} - C_I^{eq}\}}{(k_I + k_{Cl} \cdot C_{Cl})^2 \, t/D_I} \{\frac{2\sqrt{t'_n}}{\sqrt{\pi}} +$$

$$e^{t'_n} \text{erfc}(\sqrt{t'_n}) - 1\} - C_I^{eq}] \qquad (4.30)$$

The experimental results are now easily explained on the basis of the qualitative discussion presented in subsection 4.6.2-3 and its quantitative representation in eqn. (4.30). It is seen that the second term on RHS of eqn. (4.30) decreases as C_{Cl} increases and A_I decreases. The orientation dependence of the effect of chlorine on diffusion coefficient is essentially due to orientation dependence of C_{Cl}. As mentioned in subsection 4.6.2, the C_{Cl} is larger for $\langle 111 \rangle$ surface. This is consistent with larger reduction in diffusion coefficient for the case of $\langle 111 \rangle$ silicon, than for $\langle 100 \rangle$ silicon, in identical ambients. The decrease in the effect of chlorine on $\langle D_{ox,cl} \rangle$ with decreasing temperature is due to the fact that C_{Cl} sharply decreases with decreasing temperature, as mentioned in Sec. 4.6.2.

Lastly we come to the observation that at high temperatures ($> 1150^{\circ}C$), the diffusion coefficient in chloro-oxidising, ambient is lower than its value in inert ambient. This essentially implies that the second term in eqn. (4.30) is negative, signifying a situation when $C_I < C_I^{eq}$ at the interface. It is pointed out that if D_i is entirely due to the vacancy mechanism as believed by some investigators [11], the situation $C_I < C_I^{eq}$ at the interface (hence in the impurity diffusion region) will either leave D_i unchanged or will cause an enhancement in D_i. The former situation would arise, if the process of recombination of self-interstitials and vacancy is slow [26], so that

vacancy concentration in the diffusion region, (hence D_i) remains nearly equal to its thermal equilibrium value. On the other hand if the recombination process is fast, the concentration of vacancies in the diffusion zone will rise, causing an enhancement in D_i. The observed reduction in diffusion coefficient below D_i, in chloro-oxidising ambient, therefore, uniquely proves that in inert ambient phosphorus diffuses via a pure/partial interstitialcy mechanism.

The fractional contribution of the interstitialcy mechanism (if a partial interstitialcy mechanism of phosphorus diffusion is assumed) to the phosphorus diffusion in inert ambient may also probably be experimentally determined by evaluating the effect of chlorine at higher chlorine concentrations.

It can be seen from eqn. (4.29) that for large C_{Cl} such that $\dfrac{(k_I + k_{Cl} C_{Cl})}{D_I} \gg 1$, $\Delta C_I \rightarrow -C_I^{eq}$, which signifies that the interface is a perfect sink for self-interstitials. For such a situation the expression for $D_{ox,cl}$ simply reduces to,

$$\langle D_{ox,Cl} \rangle = D_i - D_{2I} \qquad (4.31)$$

If diffusion mechanism is partially interstitialcy, D_i may be written as, $D_i = D_{2V} + D_{2I}$. Thus at sufficiently high C_{Cl}, $\langle D_{ox,Cl} \rangle$ will saturate to a minimum value, equal to D_{2V}. The fractional contribution of interstitialcy mechanism, then can be calculated by the equation,

$$f_I = [1 - \frac{D_{i\ min}}{D_i}]$$
(4.32)

It may be pointed out that in the present work, the volume percent of N_2, bubbled through ICE (the source of chlorine in the present experiments) was merely 5% of the total ambient gases. This can probably be increased by a factor of two without causing any damage to the surface [52]. This method may allow determination of f_I, if f_I is less than, say 0.6.

CHAPTER V

SUMMARY

It is well established that the phosphorus diffusion in silicon is influenced by the diffusion ambient i.e. the presence of O_2 and Cl_2 in the ambient. The objective of the present work is to understand and quantitatively model the ambient effects on the phosphorus diffusion.

Several workers have systematically investigated the effect of oxygen on phosphorus diffusion. Their experiments consisted of evaluating the redistribution of deposited phosphorus (either by CVD or ion implantation) in oxidising ambient. The analysis of these profiles for extraction of diffusion parameters is rather complicated, approximations are to be made for the initial deposited profile and the finer details of the nature of experimental profiles are likely to be overlooked. In the present work, the constant source diffusion using PH_3, has been utilized to investigate the effect of O_2 and Cl_2 on phosphorus diffusion in silicon.

A model for constant source diffusion in oxidising ambient is presented. Since in general, the surface concentration in silicon is time-variant, a reaction rate limited flux boundary condition has been assumed at the interface. It is shown that

in extreme cases such as negligible PSG growth and infinitely large reaction rate constant, the model yields Smit's equation and Grove's equation respectively, for impurity distribution in silicon. For the case of small diffusion lengths, the model leads to a series solution.

To investigate the ambient effects, the phosphorus diffusion was carried out in inert ambient, 90 V% O_2 and 95 V% O_2 + 4.5 V% (N_2+TCE) respectively, at various temperatures in the range $950^{\circ}C$-$1250^{\circ}C$. The sheet resistance profiles were measured by Vander Pauw/four-point probe and anodic stripping of silicon layers. The impurity distribution in silicon was determined by incremental sheet resistivity method. The diffusion coefficient of phosphorus was calculated by solving the appropriate theoretical equation for impurity distribution at suitable points on experimentally determined profile. The main results are the following.

(i) For the case of strong oxidising ambient, the model predicts a strong dependence of surface impurity concentration in silicon, on the ratios of PSG thickness (X_0) to the diffusion lengths in PSG ($L_1 = 2\sqrt{D_1 t}$) and silicon ($L_2 = 2\sqrt{D_2 t}$) respectively. The low surface concentration requirements are a large value of X_0/L_1 (i.e., strong oxidising ambient with low dopant partial pressure) and small value of X_0/L_2 (high temperature). It is verified experimentally also. It was observed that for the identical oxidising diffusion ambients, the

surface concentration varies by two orders of magnitude from its lowest value at 1250°C to its highest one at 950°C.

(ii)   It has been observed that the detailed nature of experimental profiles, diffused in strong oxidising ambient deviates from theory, qualitatively. The experimental profiles show a pile-up near the surface and a hump in the bulk. The pile-up is attributed to the infinitely large value of reaction rate constant of phosphorus at silicon surface, which causes the incorporation of phosphorus into silicon (at the interface) at a   larger rate than that at which the phosphorus can diffuse into bulk silicon. The hump essentially indicates the presence of non-Fickian impurity motion, the origin of which is not known at present. The deviation in most cases, however, is very small and has been ignored in calculating the diffusion coefficients.

(iii) The amount of OED observed in 90% O_2 diffusions is approximately the same as reported by other investigators in dry O_2 ambient. The OED has been found to be independent of the crystal orientation and oxidation/diffusion time. The models reported in literature, to explain the oxidation induced phenomena, have been discussed in context with the experimental observations of this work coupled with the other related observations reported in literature such as $t^{-1/4}$ dependence of OSF growth rate and OED, their orientation dependence etc. It is

shown that only the model proposed by Hu can account for all the experimental observations reported so far. It is suggested on the basis of the observations of this work that the surface regrowth process in Hu's model depends upon the type of impurity as well as on its concentration at the interface. Finally, it is observed that more experimental data are required for quantitative evaluation of parameters in Hu's model.

(iv) The presence of chlorine in the diffusion ambient has been observed to cause a reduction in OED. The effect of chlorine is found to be dependent on crystal orientation and temperature. The reduction in OED is consistent with the reported observation of retarded growth/elimination of OSF in chloro-oxidising ambient and is attributed to the fact that the chlorine segregates in SiO_2 at the interface and the interface containing chlorine acts as a sink for self-interstitials generated during oxidation. Hu's model is extended to take into account the effect of chlorine on OED. It is shown that the effect of chlorine on OED varies inversely as chlorine concentration at interface, C_{Cl}. The observed orientation dependence of the effect of chlorine is explained to be due to the reported orientation dependence of C_{Cl}. Comparatively small effect of chlorine on OED at lower temperature ($\leq 1050^{\circ}C$) is attributed to the reported sharp decrease in C_{Cl} with decreasing temperature. The larger generation of self-interstitials at these temperatures further obscures the effect of chlorine on OED.

The most important observation is the reduction of the phosphorus diffusion coefficient in chloro-oxidising ambient below its value in inert ambient. It leads to the conclusion that in inert ambient, the phosphorus diffusion in silicon proceeds via either partial or pure interstitialcy mechanism.

Lastly it is suggested that these experiments may be repeated for higher chlorine concentration in the ambient to experimentally determine the fractional contribution of interstitialcy mechanism to phosphorus diffusion in silicon.

APPENDIX I

Applying boundary condition given by eqn. (2.3), to the expression for $C_1(x,t)$, gives

$$C_1(o,t) = C_o = \sum_{n=o}^{\infty} (D_1 t)^{n/2} [a_n \cdot h_n(o) + A_n \cdot i^n \text{ erfc}(o)] \quad (1)$$

The coefficients A_n may be eliminated by comparing the coefficients of like powers of $t^{n/2}$ on both the sides

$$C_o = a_o \cdot h_o(o) + A_o \cdot i^o \text{ erfc}(o)$$

$$= a_o + A_o$$

so that $\quad A_o = (C_o - a_o)$ $\hspace{3cm}$ (2)

For odd terms of the series of eqn. (1),

$$o = a_n \cdot h_n(o) + A_n \cdot i^n \text{ erfc}(o)$$

$$= A_n \cdot i^n \text{ erfc}(o)$$

so that, $\quad A_n = o \quad ; \quad n = 1,3,5 \ldots$ $\hspace{2cm}$ (3)

And for even terms of the series,

$$o = a_n \cdot h_n(o) + A_n \cdot i^n \text{ erfc}(o)$$

$$= \frac{n!}{(n/2)!} \cdot a_n + \frac{A_n}{2^n \cdot \Gamma(\frac{n}{2} + 1)}$$

so that, $\quad A_n = -2^n \cdot n! \cdot a_n \quad ; \quad n = 2,4, \ldots$ $\hspace{2cm}$ (4)

Thus,

$$C_1(x,t) = a_0 + (C_0-a_0) \cdot \text{erfc}\left(\frac{x}{2\sqrt{D_1 t}}\right) + \sum_{n=1}^{\infty} (D_1 t)^{n/2} \cdot a_n \cdot h_n\left(\frac{x}{2\sqrt{D_1 t}}\right)$$

$$- \sum_{n=2}^{2,\infty} (D_1 t)^{n/2} \cdot a_n \cdot 2^n \cdot n! \cdot i^n \, \text{erfc}\left(\frac{x}{2\sqrt{D_1 t}}\right) \qquad (5)$$

$$C_1(X_0(t),t) = a_0 + (C_0-a_0) \cdot \text{erfc}(\delta) + \sum_{n=1}^{\infty} (D_1 t)^{n/2} \cdot h_n(\delta) \cdot a_n$$

$$- \sum_{n=2}^{2,\infty} (D_1 t)^{n/2} \cdot 2^n \cdot n! \cdot i^n \, \text{erfc}(\delta) \cdot a_n \qquad (6)$$

where $\delta = \sqrt{B}/2\sqrt{D_1}$.

Using the relations,

$$\frac{d}{dx} h_n(x) = 2n \, h_{n-1}(x)$$

$$\frac{d}{dx} i^n \, \text{erfc}(x) = -i^{n-1} \, \text{erfc}(x),$$

the expression for $D_1 \dfrac{\partial C_1}{\partial x}$ can be written as,

$$D_1 \frac{\partial C_1}{\partial x} = D_1 \left[-(C_0-a_0) \cdot \frac{2}{\sqrt{\pi}} \cdot \frac{e^{-x^2/4D_1 t}}{2\sqrt{D_1 t}} + \sum_{n=1}^{\infty} (D_1 t)^{n/2} \cdot \frac{2n}{2\sqrt{D_1 t}} \cdot \right.$$

$$\left. h_{n-1}\left(\frac{x}{2\sqrt{D_1 t}}\right) + \sum_{n=2}^{2,\infty} (D_1 t)^{n/2} \cdot \frac{2^n \cdot n! \cdot a_n}{2\sqrt{D_1 t}} \cdot i^{n-1} \, \text{erfc}\left(\frac{n}{2\sqrt{D_1 t}}\right) \right]$$

$$= \frac{\sqrt{D_1}}{2\sqrt{t}} \left[-\frac{2}{\sqrt{\pi}} \cdot (C_0-a_0) \cdot e^{-x^2/4D_1 t} + \sum_{n=1}^{\infty} (D_1 t)^{n/2} \cdot 2n \cdot a_n \cdot \right.$$

$$\left. h_{n-1}\left(\frac{x}{2\sqrt{D_1 t}}\right) + \sum_{n=2}^{2,\infty} (D_1 t)^{n/2} \cdot 2^n \cdot n! \cdot a_n \cdot i^{n-1} \, \text{erfc}\left(\frac{x}{2\sqrt{D_1 t}}\right) \right]$$

Now since $\dfrac{dX_o(t)}{dt} \cdot C_1(x,t) = \dfrac{\sqrt{B}}{2\sqrt{t}} \cdot C_1(x,t) = \dfrac{\sqrt{D_1}}{2\sqrt{t}} \cdot \delta \cdot C_1(x,t)$,

the expression for the L.H.S. of impurity conservation condition (2.5), can be expressed as,

$$\left[D_1 \frac{\partial C_1}{\partial x} + \frac{dX_o(t)}{dt} C_1\right]_{x=X_o(t)} = \frac{\sqrt{D_1}}{2\sqrt{t}} \left[2\delta\, a_o + (C_o - a_o) \cdot \{2\,\delta \cdot \mathrm{erfc}(\delta) - \right.$$

$$\frac{2e^{-\delta^2}}{\sqrt{\pi}} + \sum_{n=1}^{\infty} (D_1 t)^{n/2} \cdot a_n \{2n \cdot h_{n-1}(\delta) + 2\delta \cdot h_n(\delta)$$

$$+ \sum_{n=2}^{2,\infty} (D_1 t)^{n/2} \cdot a_n \cdot 2^n \cdot n! \; \{i^{n-1}\, \mathrm{erfc}(\delta)$$

$$- 2\delta \cdot i^n\, \mathrm{erfc}(\delta)\}]$$

Since,

$$h_{n+1}(x) = 2x \cdot h_n(x) + 2n \cdot h_{n-1}(x)$$

and

$$2(n+1)\, i^{n+1}\, \mathrm{erfc}(x) = i^{n-1}\, \mathrm{erfc}(x) - 2x i^n\, \mathrm{erfc}(x)$$

We have,

$$\left[D_1 \frac{\partial C_1}{\partial x} + \frac{dX_o}{dt} C_1\right]_{x=X_o(t)} = \frac{\sqrt{D_1}}{2\sqrt{t}} \left[2\delta \cdot a_o + (C_o - a_o) \cdot \{2\delta \cdot \mathrm{erfc}(\delta) \right.$$

$$- \frac{2e^{-\delta^2}}{\sqrt{\pi}}\} + \sum_{n=1}^{\infty} (D_1 t)^{n/2} \cdot a_n \cdot h_{n+1}(\delta)$$

$$+ \sum_{n=2}^{2,\infty} (D_1 t)^{n/2} \cdot a_n \cdot 2^{n+1}(n+1)! \cdot i^{n+1}\, \mathrm{erfc}(\delta)] \qquad (7)$$

APPENDIX II

Transforming the dependent variable $C_2(z,t)$ in eqn. (2.2a), to $C(z,t) = C_2(z,t) + C_B$, the resulting diffusion equation and boundary/initial conditions are,

$$D_2 \frac{\partial^2 C}{\partial z^2} + \frac{r\sqrt{B}}{2\sqrt{t}} \frac{\partial C}{\partial z} = \frac{\partial C}{\partial t} \tag{1}$$

$$C(z,o) = C(\infty,t) = 0 \tag{2}$$

$$[\frac{\partial C}{\partial z} - \alpha C]_{z=o} = -m.\alpha.C_1(X_o(t),t) - \alpha C_B \tag{3}$$

The solution to eqns. (1) - (3) can be obtained by using Duhamel's theorem and is given as,

$$C(z,t) = \frac{\partial}{\partial t} \int_o^t \{-\alpha C_B - m.\alpha.C_1(X_o(\lambda), \lambda)\}.N(z,t-\lambda)d\lambda \tag{4}$$

where $N(z,t)$ is the solution to eqn. (1) with $C(z,t)$ replaced by $N(z,t)$ for the following boundary/initial conditions.

$$N(z,o) = N(\infty,t) = 0 \tag{2a}$$

$$[\frac{\partial N}{\partial z} - \alpha N]_{z=o} = 1 \tag{3a}$$

Now if a transformation of $\Psi = \frac{\partial N}{\partial z} - \alpha N$ is carried out in eqn. (1), with $C(z,t)$ replaced by $N(z,t)$, the resulting diffusion eqn. in Ψ and boundary/initial conditions are,

$$D_2 \frac{\partial^2 \Psi}{\partial z^2} + \frac{r\sqrt{B}}{2\sqrt{t}} \frac{\partial \Psi}{\partial z} = \frac{\partial \Psi}{\partial t} \tag{5}$$

$$\Psi(z,o) = \Psi(\infty,t) = 0 \tag{6}$$

$$\Psi(o,t) = 1 \tag{7}$$

Solution to eqns. (5) - (7) is,

$$\Psi(z,t) = \frac{erfc(\frac{z+r\sqrt{Bt}}{2\sqrt{D_2 t}})}{erfc(\frac{r\sqrt{Bt}}{2\sqrt{D_2}})} = \beta \cdot erfc(\frac{z+r\sqrt{Bt}}{2\sqrt{D_2}t}) \tag{8}$$

where

$$\beta = \frac{1}{erfc(\frac{r\sqrt{B}}{2\sqrt{D_2}t})}$$

Thus,

$$\frac{\partial N}{\partial z} - \alpha N = \Psi = \beta \cdot erfc(\frac{z+r\sqrt{Bt}}{2\sqrt{D_2}t}) \tag{9}$$

General   solution to eqn. (9) is,

$$N(z,t) = K_1 \cdot e^{\alpha z} + e^{\alpha z} \int_o^z \beta \ erfc(\frac{z'+r\sqrt{Bt}}{2\sqrt{D_2}t}) \cdot e^{-\alpha z'} \cdot dz'$$

where K_1 is an arbitrary constant. Since $N \to o$ as $z \to \infty$, it is evident that $K_1 = 0$. Thus,

$$N(z,t) = \beta \cdot e^{\alpha z} \int_o^z e^{-\alpha z'} \ erfc(\frac{z'+ r\sqrt{Bt}}{2\sqrt{D_2}t}) \cdot dz'$$

$$= -\frac{\beta}{\alpha} \cdot [erfc(\frac{z+r\sqrt{Bt}}{2\sqrt{D_2}t}) - e^{\alpha(z+r\sqrt{Bt})+\alpha^2 D_2 t} \cdot erfc(\frac{z+r\sqrt{Bt}}{2\sqrt{D_2}t}$$

$$+ \alpha\sqrt{D_2}t)]$$

$$= -\frac{g(z,t)}{\alpha} \tag{10}$$

where,

$$g(z,t) = \beta[\text{erfc}(\frac{z+r\sqrt{Bt}}{2\sqrt{D_2}t}) - e^{\alpha(z+r\sqrt{Bt})+\alpha^2 D_2 t} \cdot \text{erfc}(\frac{z+r\sqrt{Bt}}{2\sqrt{D_2}t} + \alpha\sqrt{D_2}t)]$$

(11)

The expression for $C_2(z,t)$ now can be written as,

$$C_2(z,t) = -C_B + \frac{\partial}{\partial t} \int_0^t \{C_B + m \cdot C_1(X_o(\lambda),\lambda)\} \cdot g(z,t-\lambda)d\lambda$$

Substituting for $C_1(X_o, \lambda)$, we have,

$$C_2(z,t) = -C_B + \frac{\partial}{\partial t} \int_0^t [C_B + m\{a_o + (C_o-a_o)\text{erfc}(\delta)\}$$

$$+ \sum_{n=1}^{\infty} m D_1^{n/2} a_n h_n(\delta) \lambda^{n/2}$$

$$- \sum_{n=2}^{2,\infty} m D_1^{n/2} 2^n \cdot n! \cdot a_n \cdot i^n \text{ erfc}(\delta) \lambda^{n/2}] \cdot g(z,t-\lambda)d\lambda$$

$$= -C_B + [C_B + m \cdot a_o + (C_o-a_o) \cdot \text{erfc}(\delta)] \cdot g(z,t)$$

$$+ \sum_{n=1}^{\infty} m \cdot D_1^{n/2} \cdot a_n \cdot h_n(\delta) \cdot \frac{\partial}{\partial t} \lambda^{n/2} \cdot g(z,t-\lambda)d\lambda$$

$$- \sum_{n=1}^{2,\alpha} m \cdot D_1^{n/2} \cdot 2^n \cdot n! \cdot a_n \cdot t^n \text{ erfc}(\delta) \cdot \frac{\partial}{\partial t} \int_0^t \lambda^{n/2} \cdot g(z,t-\lambda)d\lambda$$

(12)

Now since,

$$\frac{\partial g(z,t)}{\partial z}\Big|_{z=0} = S(t) = [-\alpha \cdot \beta \cdot e^{\alpha(z+r\sqrt{Bt})+\alpha^2 D_2 t} \cdot \text{erfc}(\frac{z+r\sqrt{Bt}}{2\sqrt{D_2}t} + \alpha\sqrt{D_2}t)]_{z=0}$$

$$= -\alpha \cdot \beta \cdot e^{r\alpha\sqrt{Bt}+\alpha^2 D_2 t} \cdot \text{erfc}(\frac{r\sqrt{B}}{2\sqrt{D_2}} + \alpha\sqrt{D_2}t)$$

and

$$g(o,t) = \beta \cdot erfc(\frac{r\sqrt{B}}{2\sqrt{D_2}}) - \beta \cdot e^{r\alpha\sqrt{B}t+\alpha^2 D_2 t} \cdot erfc(\frac{r\sqrt{B}}{2\sqrt{D_2}} + \alpha\sqrt{D_2}t)$$

$$= 1 + \frac{S(t)}{\alpha}$$

the R.H.S. of impurity conservation condition (2.5) can be written as,

$$[D_2 \frac{\partial C_2}{\partial z} + \frac{r\sqrt{B}}{2\sqrt{t}} C_2]_{z=o} = -\frac{r\sqrt{B}}{2\sqrt{t}} C_B + [C_B + m\{a_o + (C_o - a_o) erfc(\delta)\}] \cdot$$

$$[D_2 \cdot S(t) + \frac{r\sqrt{B}}{2\sqrt{t}} (1 + \frac{S(t)}{\alpha})]$$

$$+ \sum_{n=1}^{\infty} m D_1^{n/2} a_n h_n(\delta)[D_2 \cdot \frac{\partial}{\partial t} \int_o^t \lambda^{n/2} \cdot \frac{\partial g}{\partial z}|_{z=o} \cdot d\lambda$$

$$+ \frac{r\sqrt{B}}{2\sqrt{t}} \cdot \frac{\partial}{\partial t} \int_o^t \lambda^{n/2} \cdot g(o, t-\lambda) d\lambda]$$

$$- \sum_{n=2}^{2,\infty} m D_1^{n/2} 2^n \cdot n! \cdot a_n i^n erfc(\ ) \cdot [D_2 \cdot \frac{\partial}{\partial t} \int_o^t \lambda^{n/2} \frac{\partial g}{\partial z}|_{z=o} \cdot d\lambda$$

$$+ \frac{r\sqrt{B}}{2\sqrt{t}} \frac{\partial}{\partial t} \int_o^t \lambda^{n/2} \cdot g(o, t-\lambda) d\lambda$$

$$= \frac{1}{2\sqrt{t}} [-r\sqrt{B} \cdot C_B + [C_B + m\{a_o + (C_o - a_o) erfc(\delta)\}] \cdot [(2D_2\sqrt{t} +$$

$$\frac{r\sqrt{B}}{\alpha}) \cdot S(t) + r\sqrt{B}]$$

$$+ \sum_{n=1}^{\infty} m D_1^{n/2} a_n h_n(\delta) \cdot [(2D_2\sqrt{t} + \frac{r\sqrt{B}}{\alpha}) \cdot \frac{\partial}{\partial t} \int_o^t \lambda^{n/2} \cdot S(t-\lambda) d\lambda$$
$$+ r\sqrt{B} t^{n/2}]$$

$$- \sum_{n=2}^{2,\infty} m D_1^{n/2} \cdot 2^n \cdot n! \cdot a_n \cdot i^n erfc(\delta) [(2D_2\sqrt{t} + \frac{r\sqrt{B}}{\alpha}) \frac{\partial}{\partial t} \int_o^t \lambda^{n/2} \cdot$$

$$S(t-\lambda) d\lambda + r\sqrt{B} \cdot t^{n/2}]] \tag{13}$$

APPENDIX III

Using eqns. (2.12) and (2.14), the impurity conservation condition of eqn. (2.5) can be written as,

$$2\delta \cdot a_0 + (C_0 - a_0) \cdot \{2\delta \cdot \text{erfc}(\delta) - \frac{2e^{-\delta^2}}{\sqrt{\pi}}\} + \sum_{n=1}^{\infty} [D_1^{n/2} \cdot h_{n+1}(\delta)] a_n \cdot t^{n/2}$$

$$- \sum_{n=2}^{2,\infty} [D_1^{n/2} \cdot 2^{n+1} \cdot (n+1)! \cdot i^{n+1} \, \text{erfc}(\delta)] a_n \cdot t^{n/2}$$

$$= -2r \cdot \delta \cdot C_B + [C_B + m \{a_0 + (C_0 - a_0) \text{erfc}(\delta)\}] \cdot [S(t) \cdot Q(t) + 2r \cdot \delta t]^{n/2}$$

$$+ \sum_{n=1}^{\infty} (m \cdot D_1^{n/2} \cdot h_n(\delta) \cdot a_n) \cdot \{Q(t) \frac{\partial}{\partial t} \int_0^t \lambda^{n/2} \cdot S(t-\lambda) d\lambda + 2r \cdot \delta \cdot t^{n/2}$$

$$- \sum_{n=2}^{2,\infty} (m \cdot D_1^{n/2} \cdot 2^n \cdot n! \cdot i^n \, \text{erfc}(\delta) \cdot a_n) \cdot Q(t) \cdot \frac{\partial}{\partial t} \int_0^t \lambda^{n/2} \cdot S(t-\lambda) \cdot d\lambda$$

$$+ 2r \cdot \delta \cdot t^{n/2} \quad\quad (1)$$

where $Q(t) = \frac{1}{\sqrt{D_1}} (2D_2\sqrt{t} + \frac{r\sqrt{B}}{\alpha}) = 2\mu\sqrt{D_2} t + \frac{2r\delta}{\alpha}$

$$\mu = \sqrt{D_2}/\sqrt{D_1}$$

and $S(t)$ is as defined in Appendix II.

The R.H.S. of eqn. (1) is rather complicated and it is difficult to determine the value of a_n's for a general case. Some special cases, however, are considered below.

Case I : $\delta \approx 0$

For this case, the odd terms of the series on both the

sides become zero and even terms cancel each other on their respective sides. The L.H.S. then reduces to a constant $(C_0 - a_0)$. Comparing the constants on both the sides in eqn.(1), then leads to

$$C_0 - a_0 = 0 \tag{2}$$

or

$$a_0 = C_0$$

$$p(t) = mC_1(X_0(t), t) = mC_0 \tag{2a}$$

Case II : $\alpha\sqrt{D_2}\, t \gg 1$

For $\alpha\sqrt{D_2}\, t \gg 1$, $\quad S(t) = -\dfrac{\beta \cdot e^{-r^2 B/4D_2}}{\sqrt{\pi} \cdot D_2 \cdot t}$

and

$$\frac{\partial}{\partial t} \int_0^t \lambda^{n/2} \cdot S(t-\lambda) \cdot d\lambda = -\frac{\beta \cdot e^{-r^2 B | 4D_2}}{\pi\sqrt{D_2}} \cdot \frac{\Gamma\left(\frac{n+2}{2}\right)}{\Gamma\left(\frac{n+1}{2}\right)} \cdot t^{\frac{n-1}{2}}$$

Furthermore, approximating $\dfrac{r\sqrt{B}\,t}{\alpha\sqrt{D_2}\,t} \approx 0$ in eqn. (1) and comparing the coefficients of like powers of 't' on both sides of eqn. (1), one gets,

$$2 \cdot \delta \cdot a_0 + (C_0 - a_0) \cdot \left\{2\delta \cdot \text{erfc}(\delta) - \frac{2e^{-\delta^2}}{\sqrt{\pi}}\right\} = 2r \cdot \delta \cdot C_B + \{C_B + m[a_0$$

$$+ (C_0 - a_0) \cdot \text{erfc}(\delta)]\} \cdot \left\{2r\delta - \frac{2}{\sqrt{\pi}}\, \mu \cdot \beta \cdot e^{-r^2 B/4D_2}\right\} \tag{3}$$

$$a_n \cdot \left[D_1^{n/2} \cdot h_{n+1}(\delta)\right] = a_n\left[m \cdot D_1^{n/2} \cdot h_n(\delta)\, \{\, r\sqrt{B} - \frac{2}{\sqrt{\pi}}\, \sqrt{D_2} \cdot \beta \cdot e^{-r^2 B/4D_2} \cdot\right.$$

$$\left.\frac{\Gamma\left(\frac{n+2}{2}\right)}{\Gamma\left(\frac{n+1}{2}\right)}\,\}\right], \quad n = 1, 3, 5, \ldots \tag{4}$$

and,

$$a_n \cdot D_1^{n/2}[h_{n+1}(\delta) - 2^{n+1} \cdot (n+1)! \cdot i^{n+1} \text{ erfc}(\delta)] = D_1^{n/2} \cdot a_n \{h_n(\delta)$$

$$- 2^n \cdot n! \cdot i^n \text{ erfc}(\delta)\} \cdot \{r\sqrt{B} - \frac{2}{\sqrt{\pi}} \sqrt{D_2} \cdot \beta \cdot e^{r^2 B/4D_2} \frac{\Gamma(\frac{n+2}{2})}{\Gamma(\frac{n+1}{2})}\} \, ,$$

$$n = 2,4,6, \ldots \qquad (5)$$

From eqn. (4) and (5) it is clear that $a_n = 0$ for all $n \geq 1$. From eqn. (3), the value of a_0 and hence the expression for $a_0 + (C_0 - a_0)$ erfc(δ) is derived to be,

$$A = m[a_0 + (C_0 - a_0) \cdot \text{erfc}(\delta)] =$$

$$\frac{m[C_0(e^{-\delta^2}/\sqrt{\pi}) - (\mu \cdot \beta/\sqrt{\pi}) \cdot e^{-r^2 B/4D_2} \cdot \text{erf }(\delta) \cdot C_B]}{(e^{-\delta^2}/\sqrt{\pi}) + \delta \cdot \text{erf }(\delta) + m \cdot r \cdot \delta \cdot \text{erf }(\delta) \cdot F(r,B,D_2)} \qquad (6)$$

where,

$$F(r,B,D_2) = -1 + \frac{1}{\sqrt{\pi}(r\sqrt{B}/2\sqrt{D_2}) \cdot e^{r^2 B/4D_2} \cdot \text{erfc}(r\sqrt{B}/2\sqrt{D_2})}$$

$$(6a)$$

Also, for $\alpha\sqrt{D_2}t \gg 1$,

$$g(z,t) = \beta \cdot [\text{erfc}(\frac{z+r\sqrt{Bt}}{2\sqrt{D_2}t}) - \frac{1}{\sqrt{\pi} \cdot \alpha\sqrt{D_2}t}] \qquad (7)$$

$$p(t) = mC_1(X_0(t),t) = A \qquad (7a)$$

Case III : $\alpha\sqrt{D_2}\,t \gg \dfrac{r\sqrt{B}}{2\sqrt{D_2}}$

With this approximation, S(t), Q(t) are written as,

$$S(t) \approx -\alpha\cdot\beta\cdot e^{\alpha^2 D_2 t}\cdot erfc(\alpha\sqrt{D_2}\,t);\quad Q(t) \approx 2\mu\sqrt{D_2}\,t \quad \text{and}$$

$$[S(t)\ Q(t)+2r\delta\,] \approx S(t)\cdot Q(t)$$

and

$$\frac{\partial}{\partial t}\int_0^t \lambda^{n/2}\cdot S(t-\lambda)\,d\lambda = \int_0^t \lambda^{n/2}\cdot S_1(t-\lambda)\,d\lambda - \alpha\beta t^{n/2} \qquad (8)$$

where

$$S_1(t) = \frac{\partial}{\partial t}S(t) = \alpha^2\cdot D_2\cdot\beta\left[\frac{1}{\sqrt{\pi D_2 t}} + \frac{S(t)}{\beta}\right] \qquad (9)$$

Substituting eqn. (9) in eqn. (8),

$$\frac{\partial}{\partial t}\int_0^t \lambda^{n/2}\cdot S(t-\lambda)\,d\lambda = \alpha^2 D_2 \int_0^t \lambda^{n/2}\cdot S(t-\lambda)\cdot d\lambda + \alpha^2\beta\sqrt{D_2}\cdot$$

$$\frac{\Gamma\left(\frac{n+2}{2}\right)}{\Gamma\left(\frac{n+3}{2}\right)}\cdot t^{\frac{n+1}{2}} \ -\alpha\beta t^{n/2} \qquad (10)$$

Substituting for S(t), Q(t) and the definite integral of eqn. (10), in R.H.S. of eqn. (1), the R.H.S. can be written as,

$$R.H.S. = -2r\cdot\delta\cdot C_B+[C_B+m\,\{\,a_0+(C_0-a_0)\ erfc(\delta)\}]\cdot[2\mu\cdot D_2^{1/2}\cdot\sqrt{t}\cdot S(t)]$$

$$+ \sum_{n=1}^{\infty} m\cdot D_1^{n/2}\cdot h_n(\delta)\cdot a_n\cdot I(t) - \sum_{n=2}^{2,\ \infty} m\cdot D_1^{n/2}\cdot 2^n\cdot n!\cdot$$

$$i^n\ erfc(\delta)\cdot a_n\cdot I(t) \qquad (11)$$

where,

$$I(t) = Q(t) \cdot \frac{\partial}{\partial t} \int_0^t \lambda^{n/2} \cdot S(t-\lambda) d\lambda + 2r \ \delta t^{n/2}$$

$$= 2\mu\alpha^2 \ D_2^{3/2} \cdot \sqrt{t} \int_0^t \lambda^{n/2} \cdot S(t-\lambda) d\lambda + 2\mu\alpha^2\beta D_2 \cdot \frac{\Gamma(\frac{n+2}{2})}{\Gamma(\frac{n+3}{2})} \cdot t^{\frac{n+2}{2}}$$

$$- 2\mu\alpha\beta \ \sqrt{D_2} \cdot t^{\frac{n+1}{2}} + 2r\delta \cdot t^{n/2} \tag{12}$$

The L.H.S. of eqn. (1) remains unchanged in the situation considered. Letting $t \to o^+$, on both sides of eqn. (1), with its RHS replaced by eqn. (11), one gets,

$$2\delta \ a_o + (C_o - a_o) \cdot [2\delta \cdot \text{erfc}(\delta) - \frac{2e^{-\delta^2}}{\sqrt{\pi}} = -2r \cdot \delta \cdot C_B \tag{13}$$

From eqn. (13), first the expression for a_o, thence the same for A as defined in eqn. (6), is derived as,

$$A = m \cdot \frac{C_o(e^{-\delta^2}/\sqrt{\pi} - r \cdot \delta \cdot \text{erfc}(\delta) \ C_B}{(e^{-\delta^2}/\sqrt{\pi}) + \delta \cdot \text{erf}(\delta)} \tag{14}$$

Substituting eqn. (13), (14) in eqn. (1) with RHS replaced by eqn. (11), the eqn. (1) can be written as,

$$\sum_{n=1}^{\infty} D_1^{n/2} \ h_{n+1}(\delta) \cdot a_n \cdot t^{n/2} - \sum_{n=2}^{2,\infty} [D_1^{n/2} \cdot 2^{n+1} \cdot (n+1)! \cdot i^{n+1} \cdot$$

$$\text{erfc}(\delta) \ ] a_n t^{n/2}$$

$$= 2A \cdot \mu\sqrt{D_2} t \cdot S(t) + \sum_{n=1}^{\infty} m \ D_1^{n/2} \ h_n(\delta) \ a_n \cdot I(t)$$

$$- \sum_{n=2}^{2,\infty} m \ D_1^{n/2} \cdot 2^n \cdot n! \cdot i^n \ \text{erfc}(\delta) \cdot a_n \cdot I(t) \tag{15}$$

The value of a_n's may now be determined by successively differentiating both the sides w.r.t. $\sqrt{t}$ and letting $t \to o$. It can be seen that the series terms on RHS of eqn. (15) will always tend to zero as $t \to o$ after each differentiation. The coefficients a_n's are given by,

$$m \, D_1^{n/2} \, h_n(\delta) \, a_n = \frac{m \cdot h_n(\delta)}{h_{n+1}(\delta)} \cdot 2A\mu\beta \cdot n \cdot (-1)^{n+1} \cdot (\alpha\sqrt{D_2})^n$$

$$\text{for } n = 1,3,5, \ldots$$

$$m \, D_1^{n/2} \, [h_n(\delta) - 2^n \cdot n! \cdot i^n \, \mathrm{erfc}(\delta)]$$

$$= \frac{[h_n(\delta) - 2^n \cdot n! \cdot i^n \, \mathrm{erfc}(\delta)] \cdot m}{[h_{n+1}(\delta) - 2^{n+1} \cdot (n+1)! \cdot i^{n+1} \, \mathrm{erfc}(\delta)]} \cdot 2A\mu\beta \cdot n \cdot (-1)^{n+1}$$

$$(\alpha\sqrt{D_2})^n \; ; \text{ for } n = 2,4,6, \ldots \qquad (16)$$

Since typically, $\delta > 1$, so that $2^n \cdot n! \cdot i^n \, \mathrm{erfc}(\delta) \ll h_n(\delta)$, the expression for a_n can be written as,

$$m \, D_1^{n/2} \, h_n(\delta) \, a_n = \frac{h_n(\delta)}{h_{n+1}(\delta)} \cdot 2m \, A\mu\beta \cdot n \cdot (-1)^{n+1} \, (\alpha\sqrt{D_2})^n \qquad (17)$$

$$\text{for } n = 1,2,3, \ldots$$

Thus,

$$p(t) = m \, C_1(X_o(t),t) = A + \sum_{n=1}^{\infty} \frac{h_n(\delta)}{h_{n+1}(\delta)} \cdot 2mA\mu\beta \cdot n \cdot (-1)^n \cdot$$

$$(\alpha\sqrt{D_2})^n \cdot t^{n/2} \qquad (18)$$

APPENDIX   IV

(A)   Etchant for Gold :

      Potassium Iodide   - 4 gm

      Iodine   - 1 gm

      Deionized water -- 40 c.c.

The potassium iodide and iodine are dissolved in water at room temperature and stored for later use.

(B)   Etchant for Chromium :

The etchant consists of two parts : (i) 100 gm. NaOH dissolved in 200 c.c. deionized water and (ii) 100 gm. $K_3Fe(CN)_6$ dissolved in 300 c.c. deionized water. The two solutions are prepared and stored separately. Just before use, these are mixed in the ratio of 1:3 .

APPENDIX   V

Impurity distribution in silicon, for the case of diffusion in non-oxidising ambient is given by,

$$C_2(x) = C_o[\text{erfc}(\frac{x}{2\sqrt{D_2}t}) - e^{\alpha x + \alpha^2 D_2 t} \cdot \text{erfc}(\frac{x}{2\sqrt{D_2}t} + \alpha\sqrt{D_2}t)]$$

(1)

At $x = x_1$ and $x = x_2$, the eqn. (1) may be written as,

$$C_2(x_1) = C_o[\text{erfc}(\frac{x_1}{2\sqrt{D_2}t}) - e^{\alpha x_1 + \alpha^2 D_2 t} \cdot \text{erfc}(\frac{x_1}{2\sqrt{D_2}t} + \alpha\sqrt{D_2}t)]$$

(2)

$$C_2(x_2) = C_o[\text{erfc}(\frac{x_2}{2\sqrt{D_2}t}) - e^{\alpha x_2 + \alpha^2 D_2 t} \cdot \text{erfc}(\frac{x_2}{2\sqrt{D_2}t} + \alpha\sqrt{D_2}t)]$$ (3)

In eqns. (2) and (3), C_o and D_2 are unknown. Eqns. (2) and (3) may be simultaneously solved for C_o and D_2 in the following manner.

From eqns. (2) and (3),

$$\text{erfc}(\frac{x_1}{2\sqrt{D_2}t}) - e^{\alpha x_2 + \alpha^2 D_2 t} \cdot \text{erfc}(\frac{x_1}{2\sqrt{D_2}t} + \alpha\sqrt{D_2}t) - \frac{C_2(x_1)}{C_2(x_2)} \cdot [\text{erfc}(\frac{x_2}{2\sqrt{D_2}t})$$

$$- e^{\alpha x_1 + \alpha^2 D_2 t} \cdot \text{erfc}(\frac{x_2}{2\sqrt{D_2}t} + \alpha\sqrt{D_2}t)] = 0$$

(4)

Since $C_2(x_1)$, x_1, $C_2(x_2)$, x_2 and α are known, the eqn.(4) can be numerically solved for D_2 by Newton-Raphson method. With D_2 known, the value of C_o can be determined by substituting for D_2 in either eqn. (2) or eqn. (3).

The same method as described above, has been applied to calculate the value of diffusion parameters A, D_2 in case of diffusion in oxidising/chloro-oxidising ambient. In this case,

$$C_2(z) = A \cdot \text{erfc}\left(\frac{z + r\sqrt{Bt}}{2\sqrt{D_2 t}}\right) \tag{5}$$

In eqn. (5) only A and D_2 are unknown. By considering the impurity concentration at two points, z_1, z_2, the values of A and D_2 can be determined in a similar manner as described above.

APPENDIX VI

The diffusion equation for excess self-interstitials $(C_I - C_I^{eq})$ can be written as,

$$D_I \frac{\partial^2 (\Delta C_I)}{\partial x^2} = \frac{\partial (\Delta C_I)}{\partial t} \qquad (1)$$

$$\Delta C_I(\infty, t) = \Delta C_I(x, 0) = 0$$

$$-D_I \frac{\partial (\Delta C_I)}{\partial x} + k_{ICl} (\Delta C_I) = At^{-1/2} - k_{ICl} C_I^{eq} \qquad (2)$$

where $\quad k_{ICl} = (k_{Cl} C_{Cl} + k_I)$

Taking Laplace Transform of eqn. (1) w.r.t. 't' and writing $\mathcal{L}[\Delta C(x,t)] = \Delta \overline{C}(x,s)$, and using the initial conditions given in eqn. (2),

$$D_I \frac{\partial^2 \Delta \overline{C_I}}{\partial x^2} - s \cdot \Delta \overline{C}_I = 0$$

so that,

$$\Delta \overline{C}_I(x,s) = A_1 e^{\sqrt{(\frac{s}{D_I})} x} + A_2 e^{\sqrt{(\frac{s}{D_I})} x} \qquad (3)$$

Taking Laplace Transform of the boundary conditions in eqn. (2),

$$\Delta \overline{C}_I(\infty, s) = 0 \qquad (2a)$$

and

$$-D_I \frac{\partial \Delta \overline{C}_I}{\partial x} + k_{ICl} \cdot \Delta \overline{C}_I = A_I \sqrt{\pi}/\sqrt{s} - k_{ICl} \frac{C_I^{eq}}{s} \qquad (2b)$$

Using (2a) in (3) leads to $A_1 = 0$. Substituting for $\overline{C}_I$ in (2b) from eqn. (3),

$$[-D_I \, A_2 \, [- \sqrt{(\tfrac{s}{D_I})}] \, e^{-\sqrt{\tfrac{s}{D_I}} \, x} + A_2 \, k_{ICl} \, e^{-\sqrt{\tfrac{s}{D_I}} \, x}]_{x=0} = A_I \, \sqrt{\tfrac{\pi}{s}} - k_{ICl} \, \frac{C_I^{eq}}{s}$$

or

$$A_2 \, [\sqrt{sD_I} + k_{ICl}] = \frac{A_I \sqrt{\pi}}{\sqrt{s}} - \frac{k_{ICl} C_I^{eq}}{s}$$

$$A_2 = [\frac{A_I \sqrt{\pi}}{\sqrt{D_I} \, (\sqrt{s} + \tfrac{k_{ICl}}{\sqrt{D_I}}) \cdot \sqrt{s}} - \frac{k_{ICl} \, C_I^{eq}}{\sqrt{D_I} \cdot s \cdot (\sqrt{s} + \tfrac{k_{ICl}}{\sqrt{D_I}})}]$$

Thus,

$$\Delta\overline{C}_I = A_I \, \sqrt{\tfrac{\pi}{D_I}} \, \frac{e^{-x\sqrt{s}/\sqrt{D_I}}}{\sqrt{s}(\sqrt{s} + \tfrac{k_{ICl}}{\sqrt{D_I}})} - \frac{k_{ICl} \, C_I^{eq}}{\sqrt{D_I}} \, \frac{e^{-x\sqrt{s}/\sqrt{D_I}}}{s(\sqrt{s} + \tfrac{k_{ICl}}{\sqrt{D_I}})}$$

Taking inverse Laplace,

$$\Delta C_I(x,t) = A_I \, \sqrt{\tfrac{\pi}{D_I}} \, [e^{t'_n + 2x_n\sqrt{t'_n}} \, \text{erfc}(x_n + \sqrt{t'_n})] -$$

$$\frac{k_{ICl} \, C_I^{eq}}{\sqrt{D_I}} \, [\frac{\sqrt{D_I}}{k_{ICl}} \, \text{erfc}(x_n) - \frac{\sqrt{D_I}}{k_{ICl}} \, e^{t'_n + 2x_n\sqrt{t'_n}} \, \text{erfc}(x_n + \sqrt{t'_n})]$$

where $x_n = x/2\sqrt{D_I t}$; $\qquad t'_n = k_{ICl}^2/D_I$

For $x_n = 0$, (near the surface)

$$\Delta C_I(0,t) = A_I \, \sqrt{\tfrac{\pi}{D_I}} \, e^{t'_n} \, \text{erfc}(\sqrt{t'_n}) - C_I^{eq} \, [1 - e^{t'_n} \, \text{erfc}(\sqrt{t'_n})] \qquad (4)$$

REFERENCES   Chapter 1

[1]   R.B. Fair, 'Concentration Profiles of Diffused Dopants
        in Silicon', in Impurity Doping Processes in Silicon,
        Materials Processing Theory and Practices, vol. 2, ed.
        by F.F.Y. Wang, North Holland Press, p. 317 (1981) and
        references there-in.

[2]   A.J.F. Willoughby, 'Double Diffusion Processes in
        Silicon', ibid, p.1 (1981).

[3]   J.D. Meindl, K.C. Saraswat, J.D. Plummer, in Semicon-
        ductor Silicon 1977, ed. by H.R. Huff and E. Sirtl,
        Electrochem. Soc., V77-2, p. 894 (1977).

[4]   W. Frank, A. Seeger, U. Gosele, in 'Defects in Semi-
        conductors', ed. by J. Narayan, T.Y. Tan, p. 31 (North-
        Holland, New York, 1981).

[5]   U. Gosele, W. Frank, ibid p. 55 (1981) and references
        there-in.

[6]   S.M. Hu, ibid, p. 333 (1981) and references there-in.

[7]   R.W. Dutton et al., in Semiconductor Silicon 1977,
        ed. by H.R. Huff and E. Sirtl , Electrochem. Soc.,
        vol. 77-2, p. 910 (1977).

[8]   S.M. Hu, in 'Atomic Diffusion in Semiconductors', ed. by
        D. Shaw, p. 318 (1973).

[9]   K.H. Nicholas, Solid St. Electron., 9, p. 35 (1966).

[10]   R.N. Ghoshtagore, Phy. Rev. Lett., 25, p. 856 (1970).

[11]   G. Masetti, S. Solmi, G. Soncini, Solid St. Electron., 16, p. 1419 (1973).

[12]   G. Masetti, S. Solmi, G. Soncini, Phil. Mag., 33, p. 613 (1976).

[13]   K. Taniguchi, K. Kurosawa, M. Koshiwagi, J. Electrochem. Soc., 127, p. 2243 (1980).

[14]   D.A. Antoniadis, A.M. Lin, R.W. Dutton, App. Phys. Lett., 33, p. 1030 (1978).

[15]   A.M. Lin, D.A. Antoniadis, R.W. Dutton, J. Electrochem. Soc., 128, p. 1131 (1981).

[16]   S.M. Hu, App: Phys. Lett., 27, p. 165 (1975).

[17]   R. Francis, P.S. Dobson, J. App. Phys., 50, p. 280 (1979).

[18]   R.B. Fair, J. Electrochem. Soc., 128, p. 1360 (1981).

[19]   A.M. Lin et al., J. Electrochem. Soc., 128, p. 1121 (1981).

[20]   T.Y. Tan and U. Gosele, App. Phys. Lett., 39, p. 86 (1981).

[21]   S.M. Hu, ibid, 43, p. 449 (1983).

[22]   Y. Nabeta et al., J. Electrochem. Soc., 123, p. 1416 (1976).

[23]   P.S. Dobson, Phil. Mag., 24, p. 567 (1971).

REFERENCES   CHAPTER II

[1]   A.S. Grove et al., J.App. Phys., 35, p. 2695 (1964).

[2]   D.A. Antoniadis, M. Rodini, R.W. Dutton, J. Electro-
       chem. Soc. 126, p.1939 (1979) and ref. (10) there-in.

[3]   R.N. Ghoshtagore, Solid St. Electron., 15, p. 1113(1972).

[4]   W.G. Allen, K.V. Anand, Solid St. Electron., p.397(1971).

[5]   F.M. Smits, R.C. Miller, Phys.Rev., 104,p.1242 (1956).

[6]   W.H. Chen and W.S. Chen, J.Electrochem.Soc., 114,
       p.1297 (1967).

[7]   R.N. Ghoshtagore, Solid St.Electron., 21, p.1239(1978).

[8]   H.S. Carslaw, J.C. Jaeger, 'Conduction of Heat in Solids',
       2nd ed., Oxford Univ. Press (1959).

[9]   J. Crank, 'Mathematics of Diffusion', Clearendon Press
       (1956).

[10]   M. Abramovitz, I.A. Stegun, 'Handbook of Mathematical
       Functions', Dover Publication, Inc., New York (1965).

REFERENCES   CHAPTER III

[1]   R.B. Fair, 'Concentration Profiles of Diffused Dopants in
       Silicon', in Impurity Doping Processes in Silicon, ed.by
       F.F.Y. Wang, Materials Processing Theory and Practices,
       vol.2, North Holland Pub.Co., pp.349-370 (1981).

[2]   T. Kato, et al., Jap.J.App.Phys., 11, p.1066 (1972).

[3]   S.N. Ghosh Dastidar, Solid State Technology, 18, n11,
       p.37 (1975).

[4]   W. Kern, P.A. Putoinen, RCA Review, p.187, June (1970).

[5]   W.A. Pliskin, R.P. Gnall, J.Electrochem.Soc.,111,p.872
       (1964).

[6]   J.M. Eldridge, P. Balk, Tr. of the Metallurgical Soc.
       of AIME, 242, p.539 (1968).

[7]   I. Franz, W. Langheinrich, Solid St.Electron., 11,
       p.987 (1968).

[8]   H. Maes, W. Vandervorst and R.J. Van Overstracten,
       'Impurity Profiles of Implanted Ions in Silicon', in
       Impurity Doping Processes in Silicon, Materials Process-
       ing Theory and Practices, vol.2, ed. F.F.Y. Wang, North
       Holland Publishing Co., pp. 534-631 (1981).

[9]   F.M. Smits, Bell System Tech.J., 37, p.711 (1958).

[10]   (i) L.J. Vander Pauw, Philips Research Reports, 13,
            p.1 (1958).

       (ii) L.J. Vander Pauw, Philips Tech.Rev., 20, p.220
            (1958-59).

[11] M.V. Sullivan, J.H. Eigler, J.Electrochem. Soc., 104, p. 226 (1957).

[12] M. Wright Jenkins, J. Electrochem. Soc., vol. 124, p. 757 (1977).

[13] G. Eranna, D. Kakati, Solid St. Electron., 25, p.611 (1982).

[14] H.D. Barber et al., J. Electrochem. Soc., 123, p.1404 (1976).

[15] G.C. Jain et al., J. Electrochem. Soc., 126, p.89 (1979).

[16] N.D. Arora et al., Solid St. Electron., 25, p.965 (1982).

[17] H. Ryssel et al., J.Phys. E: Sci. Instr., 6,p.492(1973).

[18] D.A. Antoniadis et al., J. Electrochem. Soc., 125, p.813 (1978).

[19] R.N. Ghoshtagore, Solid St. Electron., vol.15, p.1113 (1972).

[20] (i) R.N. Ghoshtagore, Solid St. Electron., vol. 17, p. 1065 (1974).

  (ii) (ii) R.N. Ghoshtagore, Solid St. Electron., vol. 21, p. 1239 (1978).

REFERENCES   CHAPTER IV

[1]   A.S. Grove et al., J.App. Phys., 35, p. 2695 (1964)

[2]   C.T. Sah, H. Sello, D.A. Tremere, J.Phys.Chem. of
        Solids, 11, p. 288 (1959)

[3]   R.N. Ghoshtagore, Solid St.Electron., 18, p.399 (1975)

[4]   J.M. Eldridge and P. Balk, Trans. Metallurgical Soc. of
        AIME, 242, p. 539 (1968)

[5]   R.B. Allen, H. Bernstein, A.D. Kurtz, J.App.Phys., 31,
        p. 1334 (1960).

[6]   R.M. Burger, R.P. Donovan, 'Fundamentals of Silicon
        Integrated Device Technology', vol.I, Prentice-Hall Inc.
        Englewood Cliffs, N.J. (1968)

[7]   G. Masetti, S. Solmi, G. Soncini, Phil. Mag. 33, p.613
        (1976)

[8]   G. Masetti, S. Solmi, G. Soncini, Solid St. Electron.
        16, p.1419 (1973).

[9]   P.S. Dobson, Phil. Mag., 26, p. 1301 (1972).

[10]   P.S. Dobson, Phil. Mag., 24, p. 567 (1971).

[11]   R.B. Fair, 'Concentration Profiles of Diffused Dopants in
        Silicon', in Impurity Doping Processes in Silicon, ed.
        F.F.Y. Wang, Materials Processing Theory and Practices,
        vol. 2, North Holland Press, pp. 318-436 (1981) and
        reference there-in.

[12]   R.B. Fair, J.C.C. Tsai, J. Electrochem. Soc., 124,
        p. 1107 (1977).

[13] R.N. Ghoshtagore, Solid St. Electron., 15, p. 1113 (1972).

[14] J.S. Makris, B.J. Masters, J. Electrochem. Soc. 120, p. 1252 (1973)

[15] S. Matsumoto et al., Jap. J.App. Phys. 13, p.1899(1974)

[16] D.A. Antoniadis et al., App. Phys. Lett., 33, p.1030 (1978)

[17] D.A. Antoniadis et al., J.Electrochem.Soc., 125, p. 813 (1978)

[18] S.M. Hu, 'Diffusion in Silicon and Germanium', in Atomic Diffusion in Semiconductors, ed. D. Shaw, Plenum Press, pp. 217-220, p.228 (1973).

[19] A.F.W. Willoughby, 'Double Diffusion Processes in Silicon', in Impurity Doping Processes in Silicon ed. F.F.Y. Wang, Materials Processing Theory and Practices, vol. 2, North Holland Press, p.1 (1981) and references therein.

[20] U. Gosele, W. Frank, 'Point Defects, Diffusion Mechanisms and Shrinkage and Growth of Extend Defects in Silicon',in Defects in Semiconductors, ed. J. Narayan, T.Y. Tan, Mat. Res. Soc. Symp. Proc. vol.2, North Holland Press, p. 55 (1981) and references there-in

[21] S.M. Hu, J.App. Phys. 45, p. 1567 (1974)

[22] W. Frank, A. Seeger, U. Gosele, 'From the Mystery to the Understanding of the Self-Interstitials in Silicon', in Defects in Semiconductors, ed.J. Narayan, T.Y. Tan, Mat.Res.Soc.Symp.Proc. vol.2, North Holland Press,p.31 (1981) and references there-in.

[23]   G.R. Booker, W.J. Tunstall, Phil.Mag., 13, p.71 (1966).

[24](a)R.J. Jaccodine, C.M. Crum, App.Phys.Lett., V8,p.29(1966)
    (b)O.L.Krivanek,D.M. Maher,App.Phys. Lett., 32,p.451(1978)

[25]   S.M. Hu, 'Oxygen, Oxidation Stacking Faults and Related
       Phenomena in Silicon', in Defects in Semiconductors,
       Materials Research Soc.Symp.Proc. vol.II, ed.J.Narayan,
       T.Y. Tan,p.333(1981) and references there-in

[26]   D.A. Antoniadis,I. Moscowitz, J.App.Phys., 53, p. 6788
       (1982)

[27]   S.M. Hu, J. Vac.Sc.Technology, 14, p.17 (1977)

[28]   A.M. Lin et al., J.Electrochem.Soc., 128,p.1131(1981)

[29]   K. Taniguchi et al.,J. Electrochem.Soc., 127, p.2243
       (1980)

[30]   K. Taniguchi, D. Antoniadis, App.Phys.Lett., 42,p.961
       (1983)

[31]   W.A. Tiller, J.Electrochem.Soc., 127, p.619, 625 (1980)

[32]   W.A. Tiller, J.Electrochem.Soc., 128, p.689 (1981)

[33]   S.P. Murarka, Phys.Rev.,B16, p.2849 (1977)

[34]   B. Leroy, J.App.Phys., 50, p.7996 (1979)

[35]   A.M. Lin et al., J.Electrochem. Soc., 128, p.1121(1981)

[36]   T.Y. Tan, U. Gosele, App.Phys.Lett., 39, p.86 (1981)

[37]   S.M. Hu, App.Phys.Lett., 43, p. 449 (1983)

[38]   R.B. Fair, J.Electrochem.Soc., 125, p.2050 (1978)

[39]   W.G. Allen, K.V. Anand, Solid St.Electron., 14,p.397
       (1971)

[40]   G. Masetti et al., ibid, 19, p. 545 (1976)

[41]   W.G. Allen, ibid, 16, p.709 (1973)

[42]   W.K. Burton et al., Phil.Trans.Roy.Soc., A243, p.299
        (1950)

[43]   R. Francis, P.S. Dobson, J.App.Phys., 50, p.280 (1979)

[44]   S.M. Hu, App.Phys.Lett., p.165 (1975)

[45]   E.J. Janssens, G.J. Declerck, J.Electrochem.Soc., 125,
        p.1696 (1978)

[46]   D.L. Heald et al., J.Electrochem. Soc., 123, p.302(1976)

[47]   C.M. Osburn, ibid, 121, p.809 (1974)

[48]   H. Shiraki, Jap.J.App.Phys., 15, p.1 (1976)

[49]   T. Hattori, Solid St.Technology, p.83, July (1982)

[50](a)R.J. Kriegler et al., J.App.Phys., 45, p.341 (1974)
     (b)Y.J.Vander Meullen et al., J.Electrochem.Soc.,122,p.284
        (1975)

[51]   B.E. Deal et al., J.Electrochem.Soc., 125,p.2024(1978)

[52]   J.W. Rouse et al., ibid, 131, p. 887 (1984)

[53]   H. Frenzel, P. Balk, J. Vac. Sc. Technology, 16, p.1454
        (1979)

[54]   B.R. Singh, P. Balk, J.Electrochem. Soc., 126, p.1288
        (1979)

[55]   D.W. Hess, B.E. Deal, ibid, 124, p. 735 (1977)

[56]   B.R. Singh, P. Balk, J.Electrochem.Soc., 125, p. 453
        (1978)

[57]   C.L. Claeys et al., Semiconductor Silicon, 1977 ed. by
        H.R. Huff and E. Sirtl (The Electrochem. Soc.,
        Princeton, 1977), p. 773, (1977).

[58]   H. Shiraki, Jap.J.App.Phys., 14, p. 747 (1975)

[59]   T. Hattori, J.Electrochem. Soc., 123, p. 945 (1976)

[60]   Y. Nabeta et al., ibid, 123, p.1417 (1976)

[61]   S.P. Murarka, Phys.Rev. B21, p. 692 (1980)

[62]   R.B. Fair, J.Electrochem.Soc., 128, p.1360 (1978)
        and references there-in

[63]   J.R. Manning, Diffusion Kinetics for Atoms in Crystals,
        Van Nostrand Co.Inc. (1968)

[64]   B. Tuck, Introduction to Diffusion in Semiconductors,
        IEE Monographs Series 16 (1974)